National Library of Canada

Acquisitions and Bibliographic Services Branch

395 Wellington Street
Ottawa, Ontario
K1A 0N4

Bibliothèque nationale du Canada

Direction des acquisitions et des services bibliographiques

395, rue Wellington
Ottawa (Ontario)
K1A 0N4

Your file Votre référence

Our file Notre référence

NOTICE

The quality of this microform is heavily dependent upon the quality of the original thesis submitted for microfilming. Every effort has been made to ensure the highest quality of reproduction possible.

If pages are missing, contact the university which granted the degree.

Some pages may have indistinct print especially if the original pages were typed with a poor typewriter ribbon or if the university sent us an inferior photocopy.

AVIS

La qualité de cette microforme dépend grandement de la qualité de la thèse soumise au microfilmage. Nous avons tout fait pour assurer une qualité supérieure de reproduction.

S'il manque des pages, veuillez communiquer avec l'université qui a conféré le grade.

La qualité d'impression de certaines pages peut laisser à désirer, surtout si les pages originales ont été dactylographiées à l'aide d'un ruban usé ou si l'université nous a fait parvenir une photocopie de qualité inférieure.

Canada

APPLIED TIME SERIES ANALYSIS FOR FORECASTING PROCESS CYCLE TIMES AND PROCESS YIELDS IN THE SEMICONDUCTOR MANUFACTURING INDUSTRY

by

Walid B.H. Meliane

A thesis submitted to the school of Graduate Studies
in partial fullfilment of the requirements for the degree of

Master of Applied Science

in the
Department of Chemical Engineering
University of Ottawa
Ottawa, Canada

October 1st, 1995

ISBN 0-612-04948-5

UNIVERSITÉ D'OTTAWA
UNIVERSITY OF OTTAWA

Abstract

Complementary metal oxide semiconductor (CMOS) integrated circuits (ICs) are the dominant technology in the semiconductor industry. CMOS fabrication consists of several manufacturing steps or stages (e.g. deposition, oxidation, implant and metallization). Batches of silicon wafers proceed as batches through the different stages where they are progressively transformed to finally emerge as ICs. Meeting delivery date is important to ensure customer satisfaction and maintain momentum between manufacturing divisions. Two major concerns are to produce the right quantity of ICs in the expected period of time. Yield and cycle time are two critical parameters used to assess process performance. The main objectives of this work were to obtain reliable forecasts of yields and cycle times and to monitor the process for detection of upsets.

We explored the use of time series models such as ARIMA, transfer function and intervention models. A simultaneous outlier treatment and forecasting strategy was developed which combined the joint estimation of model parameters and outlier effects procedure with some new control charts. This method is particularly suited for highly correlated processes that are frequently subjected to large outliers. Choice of time basis was an important issue in this work (i.e., week of emergence from or entrance to the process). For ARIMA modeling, cycle time series were found to follow a highly correlated AR(1) process whereas yield series were just white noise. Five-step ahead ARIMA forecasts were often inaccurate due to the presence of frequent and large outliers. One step-ahead ARIMA forecasts were quite satisfactory. Transfer function models relating yield data to the process capacity data were built. Transfer function models for overall process cycle times were constructed using as inputs cycle times for various stages in the process. Five step-ahead forecasts were highly improved using these transfer functions. Overall, better results were obtained using the week at which the lot enters the process as the time basis for data analysis.

A mes parents et Dorsaf

Acknowledgements

I would like to thank Dr. David McLean of the University of Ottawa and N. Burn of Northern Telecom for providing me with the right amount of guidance and independance throughout this thesis. I really enjoyed working with them in this exciting area of research. I wish them all the best in the years to come. My most sincere words of appreciation to S. Rajguru of Northern Telecom for supporting this project.

TABLE OF CONTENTS

List of Tables

List of Figures

Chapter One

INTRODUCTION

The 1980's have been the transition period that enabled the world to progressively pass into the information age. This happened due to the discovery of new ways to create integrated circuits (ICs). Metal oxide semiconductor (MOS) ICs have become the dominant technology in the semiconductor industry and continue to be the fastest growing segment of the industry. The use of MOS technology enabled the production of devices with millions of transistors on a single IC chip. As a consequence, new markets such as memories, microprocessors, electronic watches, electronic telephones, and FAX machines were developed at low costs.

The three major types of MOS devices are P-channel, N-channel, and complementary MOS (CMOS). The latter uses both P-channel and N-channel techniques permitting the production of transistors with high functional density, low power density and high speed. CMOS fabrication consists of several manufacturing steps or stages which may be grouped into procedures according to their occurrence in the process sequence flow. Each of these procedures is conducted at a different location in the

fabrication plant. The raw material entering the process consists of silicon wafers. These wafers proceed as batches through the different procedures where they are progressively transformed to finally emerge as ICs. Two critical variables may be used to assess the performance of the manufacturing process: yield and cycle time. These variables are directly related to the quantity and rate of production and may be determined for each stage and procedure, as well as for the overall process.

1.1 Problem Definition

Northern Telecom Electronics (Corkstown) is a manufacturing division of Northern Telecom (Canada) that is responsible for the supply of MOS devices, particularly CMOS transistors. Other divisions use these transistors to manufacture a wide variety of electronic devices. If Northern Telecom Electronics does not manufacture and keep in inventory enough units of its product to meet the demand of other divisions, repercussions on the productivity of the overall firm are felt, leading to lost sales and lower profits. On the other hand, keeping an inventory is costly. If the inventory of ICs is too large, the firm will have higher carrying costs and lower profits. The firm can maximize profits by producing the right quantity of CMOS devices in the expected length of time.

Unfortunately, the future rate of production can never be known with certainty, so decisions about production and inventory levels must be based on forecasts of yields and cycle times. In this way, if the yield is predicted to drop or the cycle time to increase, appropriate decisions, such as processing more wafers, may be more quickly taken to correct for the upset prior to its occurrence.

1.2 Approach

Forecasts can be formed in many different ways. The method chosen depends on the purpose and importance of the forecasts as well as the costs of the alternative forecasting methods. Some statistical forecasting methods involve developing stochastic

models that may be used to extrapolate past patterns generated by a stochastic process into the future. A very effective method to develop such stochastic models is through the use of time series modeling. A time series is defined as a set of data generated at discrete, equispaced, intervals of time by a stochastic process.

ARIMA Models

Models derived from this technique are often referred to as autoregressive integrated moving average (ARIMA) models, and are represented in their general form by

$$\phi(B)\nabla^d \tilde{Z}_t = \theta(B)a_t \tag{1.1}$$

where $\tilde{Z}_t$ stands for the deviation of the time series from its mean μ (i.e., $\tilde{Z}_t = Z_t - \mu$) and a_t is a white noise sequence whose elements are identically independently distributed as a Normal probability density function with mean zero and variance σ_a^2, $N(0,\sigma_a^2)$. The autoregressive operator of order p, $\phi(B)$, and the moving average operator of order q, $\theta(B)$, are respectively given by

$$\phi(B) = (1 - \phi_1 B - \phi_2 B^2 - \ldots - \phi_p B^p) \tag{1.2}$$

$$\theta(B) = (1 - \theta_1 B - \theta_2 B^2 - \ldots - \theta_q B^q) \tag{1.3}$$

The term ∇^d represents the differencing operator of order d that may be expressed in terms of the backshift operator B as

$$\nabla^d = (1 - B)^d \tag{1.4}$$

where

$$BZ_t = Z_{t-1} \tag{1.5}$$

The differencing operator, ∇, is used when the series $\tilde{Z}_t$ is nonstationary, that is, the observations do not have a constant mean value but rather tend to drift away from the mean level. Usually, only a single differencing is required to obtain a stationary series. Physically this corresponds to modeling the change in the series rather than the series itself. A stationary series has a mean, variance and autocorrelation function that are essentially constant through time. The autocorrelation function is one way of measuring

how the observations within a single series of data are related to each other and provides a convenient way to identify a suitable form of ARIMA model.

These ARIMA models are popular for their ability to represent a wide range of processes by a parsimoniously parameterized model. Moreover, a well established iterative model building procedure has been developed by Box and Jenkins (1970). This iterative modeling approach consists of three stages: identification, estimation, and diagnostic checking. The autocorrelation function (ACF) and the partial autocorrelation function (PACF) provide direct information on the order of the moving average operator and the autoregressive operator, respectively. The ACF measures the correlation of the observations within a time series at various lags while the PACF is a relative measure of the importance of adding terms in a lagged regression of a stationary time series (Liu and Hanssens, 1991). The estimates of the ARMA parameters are often obtained by maximizing a likelihood function. This function may be reasonably approximated by a *conditional likelihood* function as discussed in Box and Jenkins(1970). A more *exact likelihood* function, as shown in Hillmer and Tiao (1979), may be used whenever a moving average term is present. These two methods differ in that the *conditional likelihood* algorithm assumes that the white noise terms $a_p=...=a_{p-q+1}=0$ while the *exact likelihood* algorithm computes estimates for these values. For diagnostic checking we plot the ACF and the PACF for the residuals to make sure that they behave as a serially independent time series with a mean value of zero and constant variance.

Transfer Function (TF) Models

Since ARIMA models are univariate models (i.e., they represent an algebraic statement telling how observations on a variable are statistically related to past observations on the same variable) their forecasts are based only on past values of the variable being forecast. When two or more related series are under study, we may want to relate the observed value of one series to its own past values, and also to the past and present values of the other time series. In this case, the univariate ARIMA models may be

extended to represent dynamic relationships between the series and hence to estimate transfer functions.

The general form of the multiple-input, single-output transfer function model, assuming that the input variables ($X_{1t},...,X_{mt}$) and output variables (Y_t) are all stationary series, can be expressed as

$$Y_t = C + \nu_1(B) X_{1t} + ... + \nu_m(B) X_{mt} + N_t \tag{1.6}$$

where C is a constant, N_t is the disturbance term following an ARIMA(p,d,q) model and $\nu_i(B)$ is the transfer function relating the input series X_{it} to the output series Y_t. This transfer function may also be represented as follows

$$\nu_i(B) = \frac{\omega_i(B)}{\delta_i(B)} B^b \tag{1.7}$$

where

$$\omega_i(B) = (1 + \omega_{i1} B + ... + \omega_{is} B^s) \tag{1.8}$$

$$\delta_i(B) = (1 - \delta_{i1} B - ... - \delta_{ir} B^r) \tag{1.9}$$

The value b represents the number of sampling intervals of delay in the process response (i.e., the dead time). The parameters of the numerator polynomial $\omega(B)$ describe the initial effects of the input as well as any effects that follow no specific pattern. The denominator polynomial $\delta(B)$ characterizes the decay pattern of initial effects in the response. The operators $\omega(B)$ and $\delta(B)$ consist normally of only a few terms (0, 1 or 2).

As in the case of ARIMA model building, there are three stages for transfer function modeling: identification, estimation, and diagnostic checking. The most critical stage in the transfer function modeling is the identification stage which may be carried out using two different methods. One procedure, introduced by Box and Jenkins (1970), utilizes a cross correlation function and a filtering technique known as prewhitening. This procedure has been termed the CCF method. The second procedure is the linear transfer function (LTF) method which follows an approach proposed by Liu and Hanssens (1982). The LTF approach is appealing because it can be easily explained and simplifies the

identification stage by reducing the number of steps necessary to obtain the required information. The estimation step is the same as for the modeling of ARIMA models. The check for correlation in the residual series is still important in the modeling of a transfer function model. However, due to our assumption of independence between the explanatory variables and the disturbance, it is also of importance to check the cross correlation function between these different time series. Another essential test is to check for outliers in the data set. Once an adequate transfer function model is determined we may use it to predict future values of the time series.

Interventions

Time series are often affected by various external events such as technological changes called interventions. Traditionally a two-sample t-test was carried out to detect a change in the mean level of a series caused by an intervention. However this method is very inefficient since it is applicable only if the intervention is a step change and, as shown by Box and Tiao (1975), it is not appropriate when the data is serially correlated. A method for analyzing data in the presence of known external events is proposed by Box and Tiao (1975). In this approach, termed Intervention Analysis, the time series is represented by two distinct components: a set of interventions on the series, I_{it} and an underlying disturbance term, N_t. For the case of k interventions, the general form of the intervention model is

$$Y_t = C + \frac{\omega_1(B)}{\delta_1(B)} I_{1t} + \ldots + \frac{\omega_k(B)}{\delta_k(B)} I_{kt} + N_t \qquad (1.10)$$

where I_{it} is a binary indicator vector (that is a vector assuming the values 0 or 1) that defines the period of the intervention and N_t is a disturbance following an ARIMA model. The term $\omega_i(B)/\delta_i(B)$, as in the transfer function model, is a characterization of the effect(s) of the intervention (I_{it}) on the output-series variable (Y_t). The procedure used to model intervention models is quite similar to the one used in transfer function modeling. For transfer functions, models are identified for both the noise term and the explanatory variables; for intervention models, we need to identify a model for the disturbance while

we postulate models for the rest (Liu and Hudak, 1991). The intervention model may then be used for forecasting.

Outliers

Time series are often subjected to unexpected events which cause the observed data to differ significantly from their normal behaviour. Such data are called outliers. There are four main types of outliers: additional outlier (AO), innovational outlier (IO), temporary change outlier (TC) and level shift outlier (LS). Since outliers can seriously alter the estimates of the model parameters in a time series, it is important that they be identified and account for properly. Chen *et al.*(1992) developed an iterative procedure for joint estimation of model parameters and outlier effects. Once the occurrence and the impact of an outlier are properly identified and estimated, intervention analysis may be used to account for the outliers in further modeling and forecasting.

Forecasting

When forecasting, we are interested in future values of a time series denoted by Z_{t+l}, where $l>1$. Sampling time t is called the forecast origin, and l is called the forecast lead time. The minimum mean square error forecast (MMSE), $\hat{Z}_t(l)$, of Z_{t+l} at origin t, for lead time l, is the conditional expectation of Z_{t+l} given all previous observations on variable Z up to time t, that is,

$$\hat{Z}_t(l) = E[Z_{t+l} \mid Z_t, Z_{t-1}, \ldots] \tag{1.11}$$

The MMSE forecast, $\hat{Z}_t(l)$ may be regarded as a function of l for fixed t and will be called the forecast function for origin t. The MMSE forecast can be recursively computed using

$$\begin{aligned}\hat{Z}_t(l) = C + \phi_1 \hat{Z}_t(l-1) + \ldots + \phi_p \hat{Z}_t(l-p) \\ + E[a_{t+l}] - \theta E[a_{t+l-1}] - \ldots - \theta_q E[a_{t+l-q}]\end{aligned} \tag{1.12}$$

where

$$\begin{aligned} \hat{Z}_t(l) &= Z_{t+l} \quad \text{if } l \le 0 \\ E[a_{t+l}] &= a_{t+l} \quad \text{if } l \le 0 \\ E[a_{t+l}] &= 0 \quad \text{if } l > 0 \end{aligned} \tag{1.13}$$

Frequently, using information coming from associated series X_{it} , X_{it-1},... (i=1,2,...) may considerably improve forecasts of a times series Y_t, Y_{t-1} ,.... This is especially true if changes in Y tend to be anticipated by changes in X_t , in which case economists call X_t a "leading indicator" for Y. Suppose an adequate transfer function model for a single explanatory variable is

$$Y_t = \frac{\omega(B)}{\delta(B)} X_t + \frac{\theta(B)}{\gamma(B)} a_t \tag{1.14}$$

where $\gamma(B)=\phi(B)\nabla^d$. Equation (1.14) may also be expressed as

$$\gamma(B)\delta(B)Y_t = \gamma(B)\omega(B)X_t + \delta(B)\theta(B)a_t \tag{1.15}$$

which may be written as

$$\delta^*(B)Y_t = \omega^*(B)X_t + \theta^*(B)a_t \tag{1.16}$$

As for ARIMA forecasts, the MMSE $\hat{Y}_t(l)$ of Y_{t+l} at origin t is given by the conditional expectation of Y_{t+l} at time t (Box and Jenkins, 1970). Writing $p^*=p+d$, we have for the lead-l forecast

$$\begin{aligned} \hat{Y}_t(l) = {} & \delta^*_1 E[Y_{t+l-1}] + \ldots + \delta^*_{p^*+r} E[Y_{t+l-p^*-r}] + \\ & \omega^*_0 E[X_{t+l-b}] - \ldots - \omega^*_{p^*+s} E[X_{t+l-b-p^*-s}] + \\ & E[a_{t+l}] - \theta^*_1 E[a_{t+l}] - \ldots - \theta^*_{q+r} E[a_{t+l-q-r}] \end{aligned} \tag{1.17}$$

where

$$\begin{aligned} E[Y_{t+l}] &= Y_{t+l} \quad \text{if } l \le 0 \\ \hat{Y}_t(l) &\quad \text{if } l > 0 \\ E[X_{t+l}] &= X_{t+l} \quad \text{if } l \le 0 \\ \hat{X}_t(l) &\quad \text{if } l > 0 \\ E[a_{t+l}] &= a_{t+l} \quad \text{if } l \le 0 \\ 0 &\quad \text{if } l > 0 \end{aligned} \tag{1.18}$$

For accurate forecasting, the process has to be in a state of statistical control. The process is only subjected to "common-cause" disturbances, that is, disturbances that occur under normal operation and do not require any special control action. Special causes are defined as those that produce a significant shift in the level or variability of the controlled output variable. Traditionally, departures from a state of statistical control are detected through the use of control charts (e.g., Shewhart, CUSUM and EWMA charts). These charts monitor variation in process outputs (usually those directly related to product quality, e.g. cycle times and yields) to enable the identification and the removal of special causes. These techniques assume that the process is generating independent and identically distributed (iid) random variables. This assumption is frequently invalid in the manufacturing industry due to some inertia effects, e.g. tanks and reactors. Typically, time series models are used to construct control charts that account for serial correlation in the observations (Alwan and Roberts, 1988).

1.3 Objectives

A major concern in the fabrication of ICs is to produce the right quantity of high-quality transistors in the expected period of time. The prime goal of this work is to predict future cycle time and yield values. In order to accurately predict those process variables we need to determine the best forecasting model. Time series modeling will yield a better understanding of the series under study which in turn may be used to know more about the process. The modeling stage is a critical one since it is the basis of all subsequent work.

The derived time series models will then be used to obtain reliable forecasts. These forecasts will help us improve the process since they permit corrective action(s) prior the upset(s) occurrence. Even if the forecasts predict good fab yields or cycle times, we will still want to understand the reason(s) why this is happening in order to maintain the same conditions.

Moreover, variability of the process cycle times and process yields should be minimized to reduce operating costs and to more easily meet delivery times. Thus, another important objective will be to monitor the process for detection of sources of variability. The empirically derived models can be used as the basis for monitoring procedures to signal when upsets occur. Such a monitoring technique should be more sensitive than using standard control charts. Once the main sources of variability have been detected, people in charge of the process area will be informed for further analysis, i.e. experimental analysis. This knowledge should help us improve the process.

All the above information may be combined together to set up a strategy to simultaneously monitor, control and forecast critical process variables. This method should allow for continuous process improvement. An important issue throughout this work will be to choose a suitable time basis for data analysis and business planning.

The specific objectives of this thesis may then be summarized as follows:

1. to determine a suitable time basis for data analysis
2. to obtain reliable forecasts for the process cycle times and process yields using the above models;
3. to develop a monitoring procedure for detection of upsets using the previously derived ARIMA models;
4. to set up a strategy for simultaneous outlier treatment and forecasting using all the above information.

1.4 Scope of Work and Methods

Two types of forecasting models will be used in this work. First, available observations on the overall fab yields and cycle times will be modeled as ARIMA time series. Then, ARIMA forecasts for the overall process variables are computed using the MMSE forecasting method. The effect(s) of the process capacity on the process cycle times and fab yields will be investigated. We will identify the main procedures that control the overall performance of the process variables. Afterwards, ARIMA models for the

process capacity and the procedure variables will be determined. These models will be used to find adequate transfer functions for the overall process variables. Transfer function forecasts are determined using the MMSE forecasting method. Then, a comparison between the ARIMA and the transfer function forecasts will be carried out to determine the most suitable forecasting model. Also, it will be important to monitor the process for detection of upsets. This will be achieved by constructing "new" control charts that make use of the previous time series models. Finally, all the above modeling, forecasting and monitoringresults will be used to set up a simultaneous control and forecasting strategy.

Chapter Two

PROCESS DESCRIPTION

Silicon's oxidation properties make it the primary semiconductor material for integrated circuit (IC) manufacturing. Silicon, an element like gold, zinc, or uranium, is used because of its unique properties. It is very plentiful since it is basically extracted from sand. Also silicon is a semiconductor, which means that it is neither a good conductor of electricity nor a good insulator, but can be regulated in the amount of its conductivity. As shown in Figure 2.1., the basic elements of a MOS transistor are the source, gate, and drain. In the MOS-insulated gate structures, the gate may be thought of as one electrode of a parallel-plate capacitor with a dielectric, usually SiO_2, separating it from the other electrode substrate. If the source of the N-channel transistor is grounded and a sufficient positive voltage, with respect to substrate potential, is applied to the gate, a conducting current sheet is formed under the gate dielectric at the surface of the substrate. The region between the source and drain is referred to as the channel region. The gate voltage at which inversion is just completed is called the threshold voltage. At gate voltages lower than the threshold voltage the surface is not inverted, and hence the transistor is cut off, and no current flows from the drain to the source.

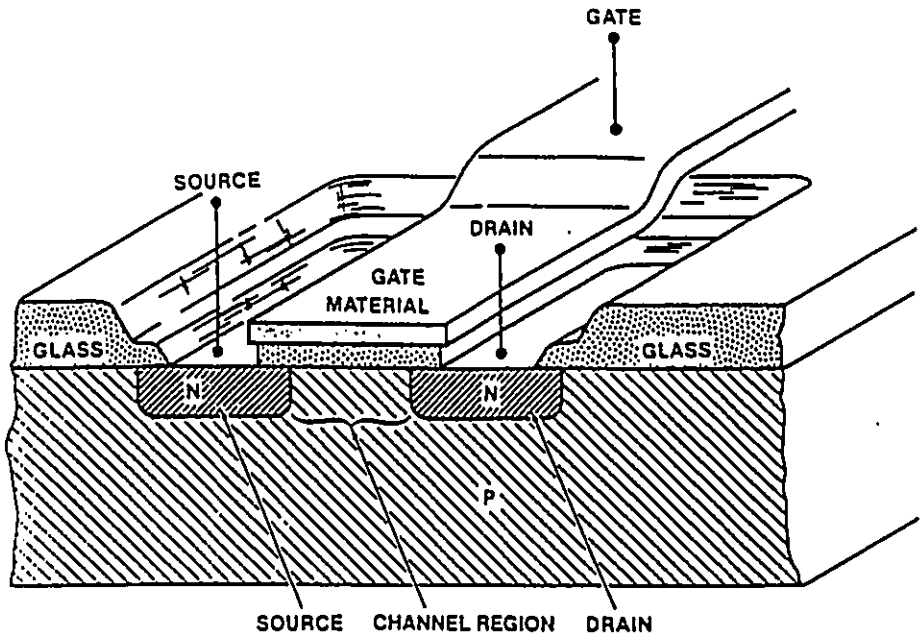

Figure 2.1 Basic Elements of a MOS Transistor

2.1 Processing Steps Involved in Wafer Fabrication

There are many processing variations, adopted by different manufacturers, for achieving specific MOS transistor structures. However, the processes used by each company usually contain the same fundamental stages. Typically, wafer fabrication involves a series of photolithography (PE) steps, between which are various cycles of oxidation, chemical vapor deposition (CVD), diffusion, ion implantation, etching and stripping (see Figure 2.2). When processing wafers in fabrication, these processing steps are combined into a certain order or work flow (see Appendix A). The main steps for fabricating a silicon-gate CMOS circuit are briefly discussed here.

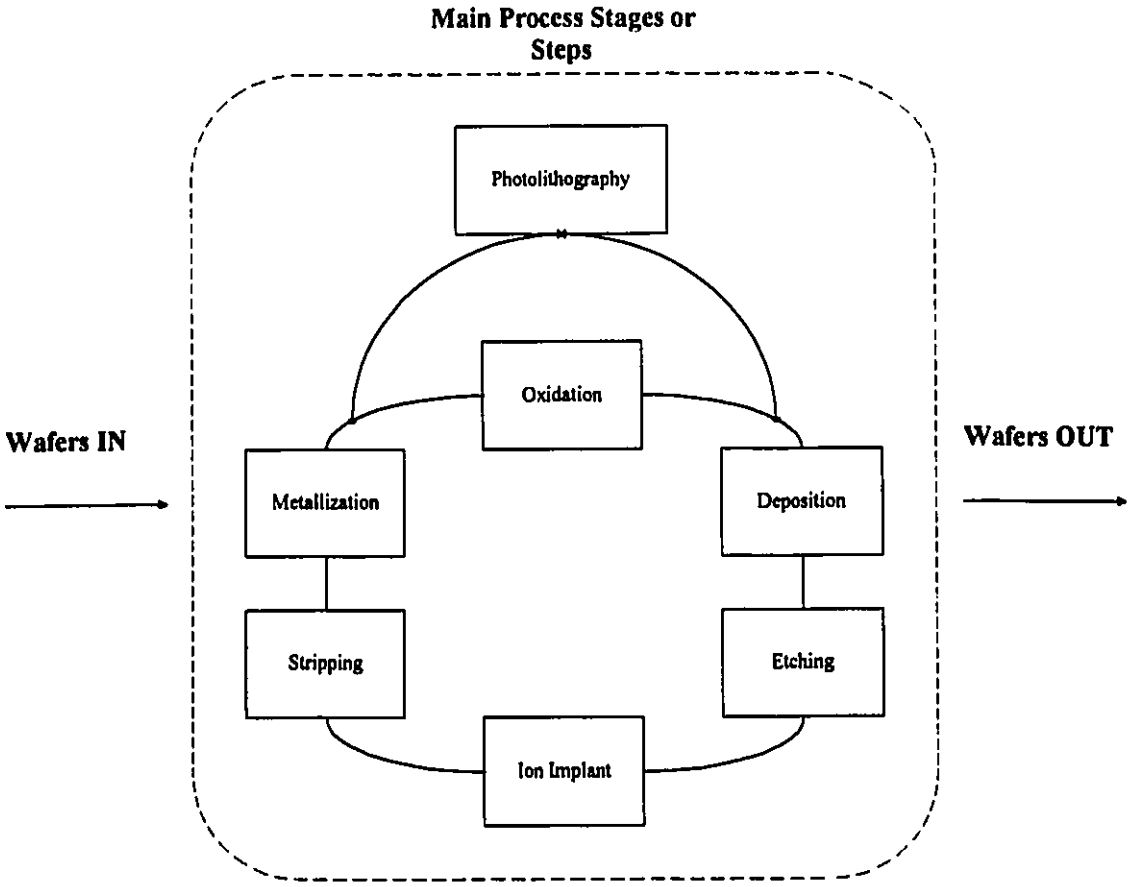

Figure 2.2 Schematic Diagram of a CMOS Process.

Oxidation

Oxidation is the process where an oxide layer is grown on the silicon surface principally to either mask the silicon from chemical action or to act as an electrical insulator. When silicon is exposed to an oxidizing atmosphere, such as oxygen, the following reaction takes place,

$$Si + O_2 \rightarrow SiO_2$$

It is a thermal process normally performed in the temperature range between 600^0C and 1200^0C. The oxidizing species may be dry oxygen, wet oxygen (i.e., saturated with water vapor) at a temperature usually between 85^0C and 95^0C, or steam. Oxidation is used as a stepping stone to most other processing steps. Sometimes oxidation is used only as a tool for

the masking operation. It becomes a vehicle for isolating certain sections of the wafer (through masking) so that later diffusions and oxidations can be performed in selected spots of the wafer. In other processes, the oxide is used as a part of the electrical circuit itself, or it can be used for both of these purposes. The major goal of oxidation is to achieve a clean, uniform thickness of oxide on the surface of each wafer. A number of factors control how thick the oxide layer will be. The amount of oxygen introduced to the surface, the temperature at which the surface is set, and the length of time the wafers are left in the furnace all have an effect on the thickness that is produced.

Diffusion

Diffusion is the net transport of a substance from one region to another within a single phase. Diffusion is a basic physical property of matter resulting from the Brownian motion of atoms. In semiconductor fabrication it is the transport of atoms in a lattice, governed by Fick's Law. Diffusion is a method of introducing dopant atoms into the silicon, usually through "windows" etched in an oxide masking layer. The operation allows dopants to enter those areas of the semiconductor wafer surface that are not masked with SiO_2, imparting important electrical characteristics. Dopants are divided in two categories: N and P. N dopants are negative in charge while P dopants are positive in charge. N dopants include phosphorus, antimony and arsenic while P dopants include boron, gallium and aluminum. Diffusion is accomplished in a high temperature furnace, typically in the range of 900^0C to 1200^0C. The dopant is driven into the wafer by the heat from the furnace. The depth (and width) of the diffusion is controlled by the time the wafer is in the furnace, and by the temperature of the furnace.

Ion Implant

Ion implantation is a means of introducing controlled amounts of dopants into semiconductor material. This technology uses electrically accelerated dopant ions, with energy ions of 20-200keV, to bombard target semiconductor materials. Specific dopant ions can be

selected by using an analyzing mass-separation magnet that bends ion paths in accordance with their atomic weights. The primary benefit of ion implantation is that the dopant ion beam can easily be scanned over a large area, and the dopant penetration depth is controlled by the ion energy. Therefore, in some respects, it can be considered as an adjunct to diffusion, and it is commonly used as an alternate means of accomplishing a pre-deposition. Moreover, ion implantation offers features that cannot be duplicated by normal diffusion processes. Ion implantation can dope through an oxide, something that is not ordinarily done by diffusion. This capability allows the threshold voltage of MOS transistors to be adjusted after the gate oxide is grown. Another way that ion implantation is different from diffusion is that the wafers are processed at relatively low temperatures, up to 125^0C.

Chemical Vapor Deposition

Chemical vapor deposition (CVD) processes for semiconductors originated with the application of epitaxial thin films on silicon. This application revolutionized semiconductor device performance and paved the way for forming a variety of films in the fabrication of ICs. Silicon dioxide (SiO_2), silicon nitride (Si_3N_4) and polycrystalline silicon films are commonly deposited using CVD methods. CVD reactions can be initiated by the application of thermal energy, glow discharges (plasma or electronic radiation and radio frequency RF plasma). For the CVD reactions commonly used in depositing SiO_2, Si_3N_4, and polysilicon, the reaction is generally maintained by thermal energy supplied by conventional resistance heating. Plasma is being increasingly used as an energy source, and RF is limited almost entirely to epitaxial depositions, where it used primarily as a thermal energy source to heat the susceptors that hold the wafers. There are two basic methods used for CVD depositions: atmospheric pressure (APCVD) and low pressure (LPCVD). However the use of low pressure, hot-wall systems, for the CVD of SiO_2, Si_3N_4, and polysilicon offers a number of advantages. Studies have shown that capital, labor, energy, and gas costs per wafer processed are significantly less than when APCVD is used. Using LPCVD, the wafers can be closely spaced and positioned vertically in a configuration similar to that for thermal oxidations since at low pressure (0.1 to

1.0 Torr) the deposition is limited by reaction kinetics, and thus the process proceeds properly even with close wafer spacing. The temperature uniformity that can be maintained using the resistance-heating method yields excellent uniformity in film thickness.

Metallization

Metallization is the process where thin metallic lines are formed on a silicon die to electrically interconnect the various elements comprising a semiconductor device. Since the metal, as deposited, covers the entire surface of the wafer, interconnections between devices are formed by etching away all metal that is not to be used. Applications for metallization in ICs can be separated into three primary groups: ohmic contacts, gate and interconnect metal, and top metal. For an ohmic contact, the metal must directly contact the silicon surface and be alloyed so that a metal/silicon region is formed. Aluminum has been the metal of choice for ohmic contacts primarily due to the ease of patterning. In addition to circuit speed, the gate metal affects flat band voltage (V_{fb}) of a MOS structure. V_{fb} contributes to V_t, which is the voltage needed at the gate metal to achieve conduction between source and drain. Doped polysilicon has been the normal gate metal for MOS devices. Top-level metal provides a connection from the circuit to the outside world. Generally deposited and patterned during the final stages of processing, it is usually a current carrier and it usually thick. Aluminum is normally used as a top metal due to ease of deposition and patterning. The metal deposition process is done in a vacuum chamber. The earliest widely used technique for vacuum deposition of metals for ICs was the filament evaporation system. However, the use of e-beam heating as a means of evaporating metal for ICs came into general use when it was found to provide sodium-free deposition of aluminum on MOS wafers.

Photolithography

In semiconductor manufacturing, photolithography is used to transfer very small patterns that define precisely dimensioned areas in a photo-sensitive acid-resistant material, referred to as photoresist that covers the wafer surface. The basic photolithography process

involves application of photoresist to the wafer masking, exposing the resist with the desired pattern, and developing the resist, which chemically removes the unwanted portions. This leaves the wafer surface exposed only in areas where surface treatment at the next step is required. A bake step hardens the resist for subsequent processing, which may be an etch to remove material, an ion implant, or even a metal deposition. Upon completion of the above stages, the wafers travel back into the diffusion area for another slightly different cycle of deposition, diffusion and oxide growth. They then return to photolithography for the next mask step, and so on until all steps of the process are complete.

Etching

Etching is a process where material is removed from the silicon substrate or from film deposited or grown thereon. When a mask is used to protect specific areas of the substrate surface, the goal of etching is to precisely remove the exposed material. The mask material may be photoresist or some other material, such as nitride, that is not attacked by the etch environment. Etching can be conducted using either wet chemicals or dry processes. The major drawback of wet etching is that it is unable to adequately define very small dimensions with high pattern density. These problems are solved when radio frequency (RF) plasmas are used to etch microelectronic devices. It is then possible to reproduce the image of a mask with a high degree of integrity.

Stripping

In IC wafer fabrication the necessity for extreme cleanliness cannot be overstated. Wafer cleaning is performed to enhance cleanliness by removing impurities, such as adsorbed chemical species and particulate matter, from the wafer surface. Photoresist stripping from silicon dioxide is done using wet chemical systems, H_2SO_4-based systems such as the Piranha or the $(NH_3)S_2O_8$ systems. Since aluminum reacts with oxidizing acids rules systems, phenol-based organic acid photoresist strippers have been used with aluminum.

2.2 Process Diversity and Complexity

There are several families of MOS (metal oxide semi-conductor) devices. These devices are generally described in terms of the actual fabrication technology. The major families of MOS devices are P-channel MOS, N-channel MOS and CMOS (complementary MOS). BiCMOS (bipolar complementary MOS), the integration of bipolar devices into circuit designs that are primarily CMOS, is becoming more popular. The P-channel and N-channel designations refer to the polarity of the current carrier in the channel. In a N-channel device, dopants are negatively charged (e.g., phosphorus) whereas in a P-channel device dopants have a positive charge (e.g., boron). CMOS has both P-MOS and N-MOS transistors fabricated on the same circuit.

The NT manufacturing division in Ottawa (Corkstown) runs both CMOS and BiCMOS processes. In the subsequent work, we will be only interested in the CMOS process. The latter can be broken down into four process technologies, as shown in Figure 2.3. In each process-technology, a batch of wafers proceeds through nine different procedures where they are progressively transformed to finally emerge as integrated circuits with millions

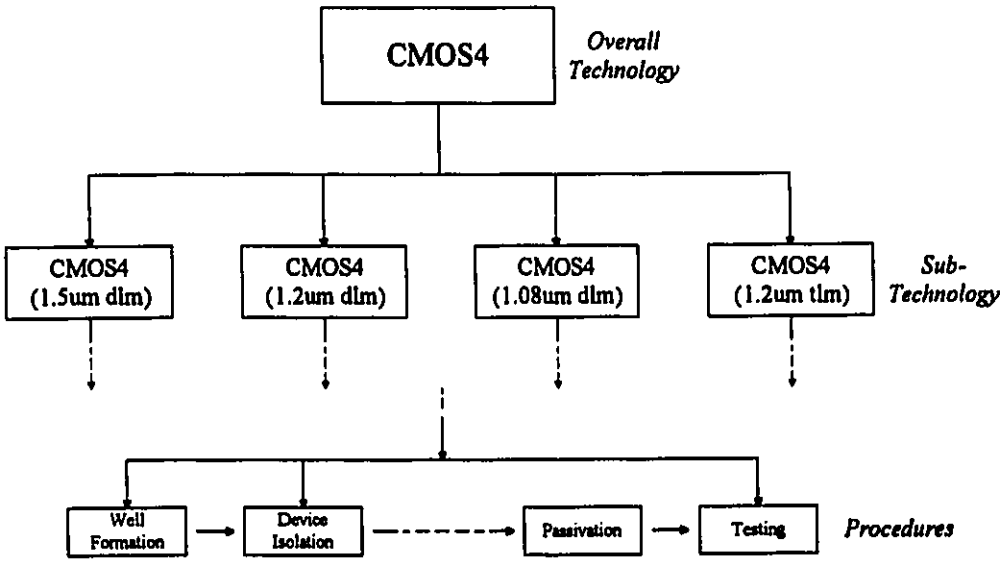

Figure 2.3 Process Diagram of the Overall CMOS Process

of transistors. Each process-technology produces different CMOS devices. Manufactured CMOS transistors can have either two or three layers of metallization. These layers can have 1.08μm or 1.2μm thickness. In this way, a CMOS (1.08μm dlm) represents a CMOS process-technology having two layers of metallization of 1.08μm thickness.

The overall CMOS process contains up to 15 photomask levels and the BiCMOS has up to 26 levels. The overall CMOS manufacturing process contains about 100 stages and the BiCMOS process contains up to 130 stages. Each of these processes includes several other options such as analog capacitors and EPROMs (Electronically Programmable Read-Only Memory). Typically, the facility runs about 100 different product codes (designs) at the same time and over 200 in a single year.

Several other technical factors contribute to the complexity of this process. These factors include the presence of experimental lots on top of the regular production lots. Experimental wafers may be stocked for further design for an appreciable amount of time and often have different paths from the standard production lots. These experimental lots usually consist of a smaller number of wafers. Therefore, the number of wafers within a lot is not constant through time. In order to stay competitive, the process flow is continuously revised and improved by the addition of new stages and the deletion of old stages. The overall CMOS manufacturing process is continuously evolving which adds more complexity to the process. Moreover, a non constant number of production lots is processed through time and each production lot do not always contain the same number of wafers. On top of the production and the experimental lots, some split lots and scrap lots exist in the overall CMOS manufacturing process.

2.3 Split Lots and Scrap Lots

As shown in Figure 2.4, two types of special lots exist within the overall CMOS process: split lots and scrap lots.

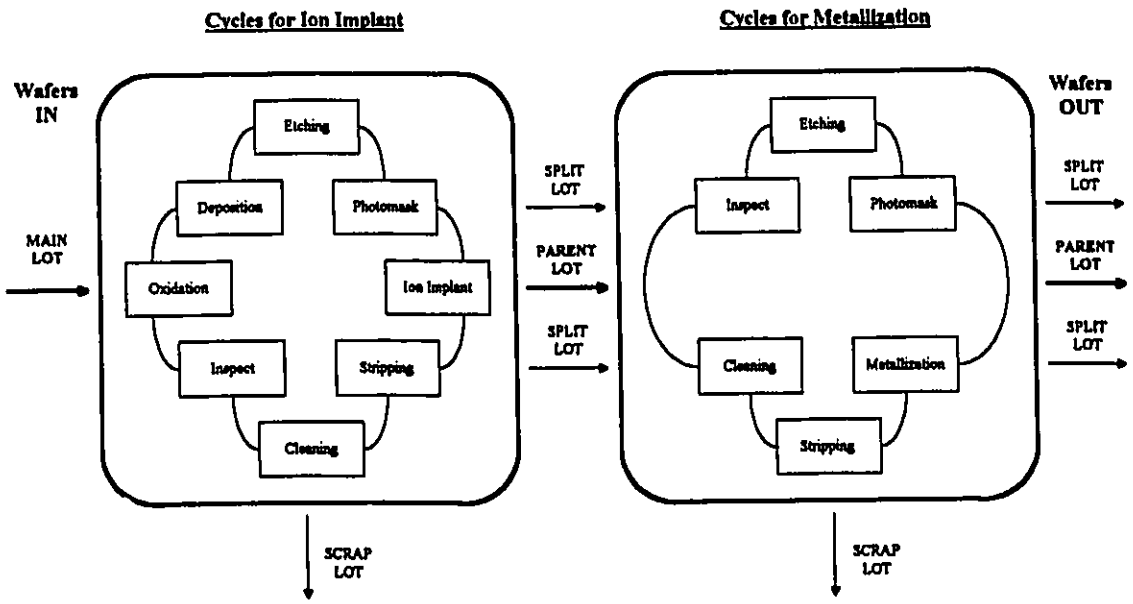

Figure 2.4 Diagram of a Process Sequence Flow for a Technology

At any point in the process, an entire lot may be completely scrapped and disposed for waste treatment. This happens whenever all the wafers within a lot do not meet requirements and cannot be recovered. These lots are referred to as scrap lots. Scrap lots have, as expected, a zero yield value. Also, depending on the stage at which it is scrapped, its cycle time will be lower than the one associated with normal lots. However, it is sometimes possible to recover a lot, or at least some of the wafers within it that do not meet standards, through rework.

In such a case, that lot is split within the process into two or more lots: a parent lot and one or more split lots. Usually, these split lots do not emerge at the same time. The delay between the emergence of the parent lot and the emergence of the split lots may be of several weeks. This happens whenever the split is stocked for further design or new tests.

2.4 Choice of time basis

Current Time Basis

As discussed in the Introduction, the week at which a lot emerges from the process (i.e. out-date) is currently used as the time basis for data analysis and business planning in the manufacturing division. Figure 2.5 and 2.6. show sequential plots of the cycle time and yield variables, respectively, for the overall CMOS process when the out-date is used as the time basis for data collection. Time series plots of the cycle time and yield variables for the four technologies may be found in the Appendix B. Due to the proprietary nature of the data coded values (based on a linear transformation) of the yields and cycle times have been used throughout this thesis.

Effects of Split Lots and Scrap Lots

As discussed earlier, the overall CMOS process contains scrap lots and split lots. A scrap lot by definition, does not make it through the entire process flow. Its yield is then equal to zero, whereas its cycle time is always lower than the one associated with a normal lot. Including scrap lots in the calculation of cycle time data will cause it to be underestimated.

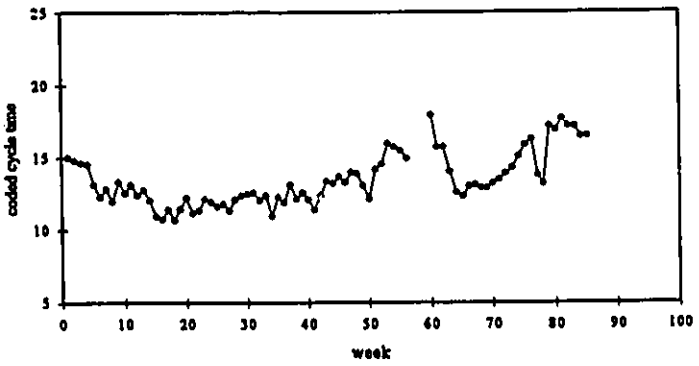

Figure 2.5 Time Series Plot of the Out-date Cycle Time Data for the Overall Process.

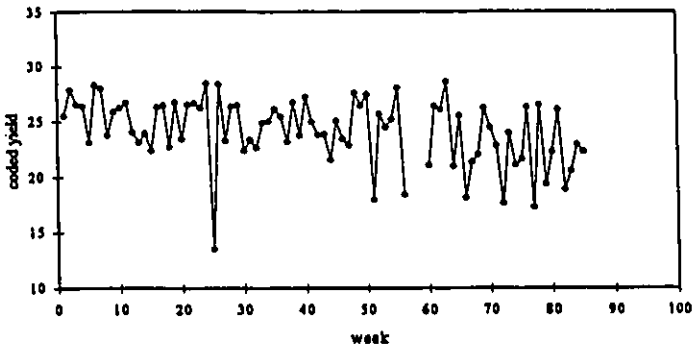

Figure 2.6 **Time Series Plot of the Out-date Yield Data for the Overall Process.**

To avoid this, the current practice is to neglect scrap lots in the calculation of cycle time. However, this policy still results in a bias in the cycle time since scrap lots are not accounted for. The collected cycle time is underestimated. Indeed, any lot that is scrapped within the process has to be replaced in order to meet delivery.

Also, a main lot may be split at any time in the process into two or more split lots. Currently, the cycle time associated with any split lot is the sum of its previous cycle time (before it was split) and its remaining cycle time. For example, a main lot starting with N_M number of wafers may be split at one point in the process into k split lots of N_{SPi} (i = 2,...,k) wafers. Let Ct_M be the cycle time of the main lot (before the split) and Ct_{SPi} (i = 1,2,..,k) be the remaining cycle times of the split lots (after the split). Then the resulting cycle time Ct_{RSPi} (i=1,2,..,k) associated with a split lot is given by,

$$Ct_{RSPi} = Ct_M + Ct_{SPi} \qquad (i = 1,2,\ldots,k) \qquad (2.1)$$

On the other hand, yield values associated with split lots are calculated based uniquely on the number of wafers in and out of the remaining procedures, after the split occurs. Using the same nomenclature, the resulting out-date yield associated with a split lot is given by

$$Yd_{RSPi} = Yd_{SPi} \qquad (i = 1,2,\ldots,k) \qquad (2.2)$$

Unlike cycle time, yield values of split lots do not depend on their "past history" in the main lot. Moreover, split lots do not usually come out at the same period of time. Because data

collection is based on the out-date time basis, each split lot is treated as an independent entity. Thus, an extra observation is added to the collected out-date data each time a splitting occurs in the process.

Alternative Time Basis

As discussed above, process variables based on the out-date time basis are misleading. They do not represent the "true" process behavior. Cycle times are underestimated because of the presence of scrap lots and an extra observation is introduced into the process each time a splitting occurs. One way to overcome these problems is by using the week of entrance of the lot into the process as the time basis.

Split lots were then joined to their main lot to give a single data point. Assuming a main lot is splitted into k lots, the resulting cycle time value is now given by

$$Ct_{RSP} = Ct_M + \max\left[Ct_{SP1}, Ct_{SP2}, \ldots, Ct_{SPi}\right] \tag{2.3}$$

The cycle time is now correctly accounting for split lots since integrated circuits (ICs) are delivered only when the entire initial batch of wafers has been successfully transformed into ICs. Thus the last split lot has to emerge from the process before the initial main batch of wafers is packaged for delivery.

The yield for split lots was calculated by recombining them with their main lot using the number of wafers in each split lot as a weighting factor such that,

$$Yd_{RSP} = \frac{\sum_{i=1}^{k} N_{SPi}\ Ct_{SPi}}{\sum_{i=1}^{k} N_{SPi}} \tag{2.4}$$

This way more weight was given to the yields for splits with a large number of wafers.

As seen before, the out-date cycle time does not represent the "true" process behavior since scrap lots are neglected. In terms of business planning, any lot that is scrapped within the process has to be replaced in order to meet delivery. So, a scrap lot should be reported as a delay in the production. The time that a scrap lot spent in the process before being scrapped, Ct_{SC}, should be considered as a penalty to the process. The resulting cycle time of a scrap lot

was consequently calculated as the sum of the average cycle time of all unscrapped lots entering the same week, $\overline{Ct}_{USC}$, and the cycle time of the scrap lot, Ct_{SC}, that is,

$$Ct_{RSC} = \overline{Ct}_{USC} + Ct_{SC} \tag{2.5}$$

On the other hand, the yield of a scrap lot was set to zero by definition. Figures 2.7 and 2.8, show time series plots of the in-date cycle time and in-date yield for the overall CMOS process. Plots of the cycle times and yields for the different technologies are found in Appendix B.

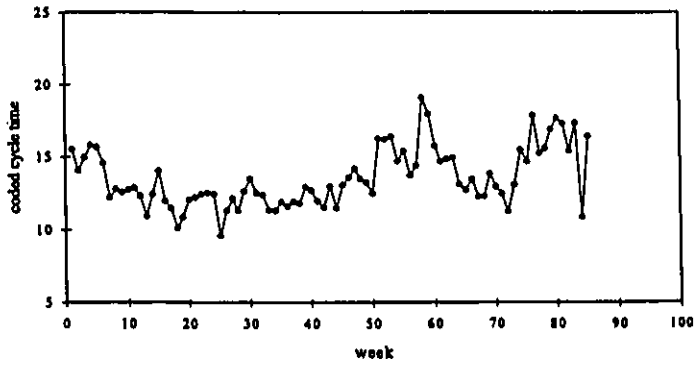

Figure 2.7 **Time Series Plot of the In-date Cycle Time Data for the Overall Process.**

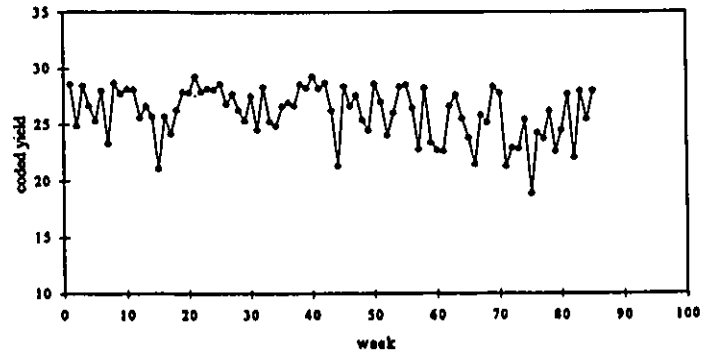

Plot of the Coded In-date Yield for the Overall CMOS4 Process

Figure 2.8 **Time Series Plot of the In-date Cycle Time Data for the Overall Process.**

2.5 Current Method for Control and "Forecasting"

Control

Presently, NT is attempting to control overall cycle times using the Predictable Delivery Method (PDM) shown in Figure 2.9. In this method, the location of each lot is evaluated with respect to the remaining amount of processing. The median, mean, and standard deviation of the 'run' and 'wait' times at every stage is calculated and then compared to some target lead times. If the lot is ahead of the predicted lead time, more wait time is applied on the next stage(s) whereas less wait time is associated with a lot that is behind of schedule.

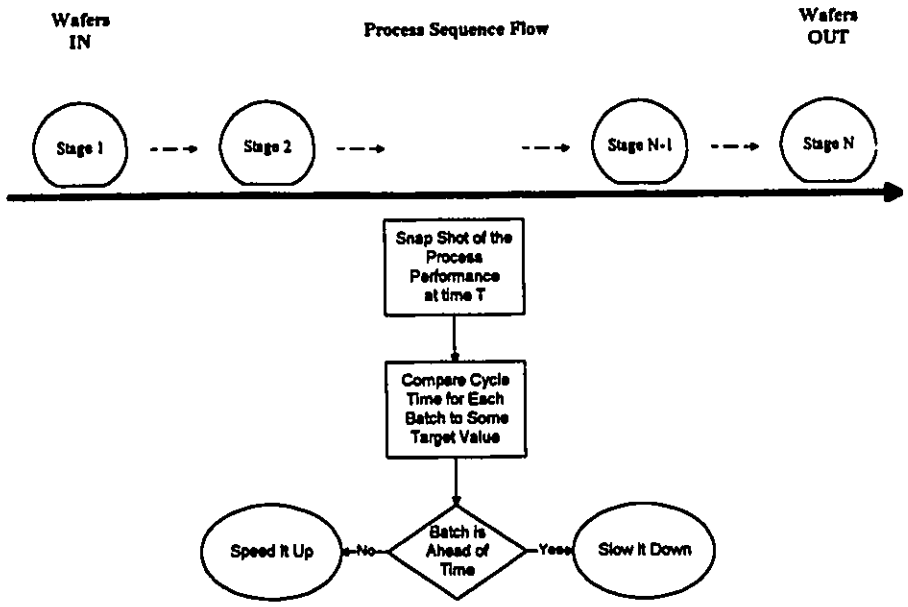

Figure 2.9 Predictable Delivery Method

Although it is implied by its name, the PDM is not a "prediction" method. Its aim is to make the process perform according to some set cycle time criteria instead of trying to forecast future cycle time values. Moreover, the PDM is an *ad hoc* control procedure; the extent of the manipulations are arbitrary. The overall process is subjected to some regular external events,

including control actions of the PDM, which are responsible for some of the correlation in the process. However, control actions of the PDM do not take into consideration the correlation in the cycle times. This could result in inflating process variability through overcontrol. This problem was not addressed in this work.

Forecasting

Currently, there is no formal forecasting procedure. If forecasts are required the standard procedure is to simply use the mean of some previous data, usually four points. This procedure has some limitations since it does not account for the correlation existing in the process nor does it consider potential significant drifts in the process. As a result, business planning and production personnel had a need for a systematic and reliable prediction tool.

In order to perform effective control and forecasting it is necessary to represent the process by a mathematical model that accounts for all past information. Time series analysis is an effective method to build such mathematical models (e.g. ARIMA models and transfer function models).

Chapter Three

FORECASTING CYCLE TIMES AND YIELDS WITH ARIMA MODELS

3.1 Introduction

The primary objective of this thesis was to produce reliable forecasts of process cycle times and process yields. Since these variables are directly related to quality and rate of production, they are essential for good business planning, process control and monitoring process performance. In this chapter, ARIMA models are constructed for the overall process and the individual process technologies. An implicit requirement for the development of unbiased ARIMA models is that the data represent the true underlying process behavior and not be inflicted with outliers. Unfortunately, the data for the

processes under investigation here contained numerous outliers. The effects of such outliers are discussed and an analysis of procedures to deal with them is presented. As a result, outlier detection methods and intervention models (Cheng and Liu, 1993) were used for building the ARIMA models for this system. This represents a new approach for modeling yields and cycle times. The resulting ARIMA models were then used to obtain forecasts for the yields and cycle times.

As discussed in Chapter 2, cycle times and yields can be calculated based on either the in-date or the out-date. A preliminary comparison between these two time bases was done in Section 2.4. Further comparison between the in-date and the out-date time basis is also conducted in this chapter.

3.2 Background and Literature Survey

3.2.1 Introduction

The use at time t of available observations from a time series to forecast its value at some future time $t+l$ can provide a basis for business planning, production planning and production control. A time series is a set of observations generated sequentially in time by a process. The latter is said to be deterministic if it can be exactly defined by a mathematical expression. Conversely, a stochastic process is one that follows probabilistic laws, which is generally the case in the manufacturing industry. The models for time series that are needed to achieve optimal forecasts are stochastic models.

A special class of stochastic models for describing time series models, which has received a great deal of attention, are the so-called stationary models, which assume that the data fluctuate about a constant mean value, μ,

$$\mu = E[\, Z_t \,] \tag{3.1}$$

with constant variance, σ_z^2,

$$\sigma_z^2 = E\left[Z_t - \mu\right]^2 \tag{3.2}$$

The simplest stochastic stationary model for describing time series, which has been used as the basis for traditional SPC techniques, is the white noise model, which can mathematically be expressed as,

$$Z_t = \mu + a_t \tag{3.3}$$

where the a_t's are independent identically distributed random "shocks" with mean zero and constant variance, σ_a^2. However, the assumption that the adjacent observations are independent and identically distributed is very rarely applicable in the continuous manufacturing industry where process measurements are taken over short period of time. These data are referred to as being autocorrelated.

The statistical dependence in the data is expressed by the correlation and autocorrelation between successive observations. The autocorrelation measures the correlation of the observations within a time series at various lags. For any positive integer l, the lag l autocorrelation is the correlation between Z_{t+l} and Z_t,

$$\rho_l = \frac{E[(Z_t - \mu)(Z_{t+l} - \mu)]}{\sqrt{E[(Z_t - \mu)^2]E[(Z_{t+l} - \mu)^2]}} \tag{3.4}$$

It is a dimensionless number that can take values only between -1 and 1. The autocorrelation function, ACF, is the sequence of autocorrelations for lags 0, 1, 2, ...

A stationary process can be defined by its mean, variance, and autocorrelation, which are essentially constant through time.

For a bivariate stochastic process constituted of two series (X_t, Y_t), the stationarity assumption implies that the bivariate process is uniquely characterized by its means μ_X, μ_Y and its covariance matrix. The latter is defined by the usual covariances

$$\begin{gathered}\gamma_{XX}(l) = E[(X_t - \mu_X)(X_{t+l} - \mu_X)] = E[(X_t - \mu_X)(X_{t-l} - \mu_X)] \\ \gamma_{YY}(l) = E[(Y_t - \mu_Y)(Y_{t+l} - \mu_Y)] = E[(Y_t - \mu_Y)(Y_{t-l} - \mu_Y)] \\ \gamma_{XY}(l) = E[(X_t - \mu_X)(Y_{t+l} - \mu_Y)] = E[(Y_t - \mu_Y)(X_{t-l} - \mu_Y)] = \gamma_{XY}(-l)\end{gathered} \tag{3.5}$$

where $\gamma_{XX}(l)$ and $\gamma_{YY}(l)$ are the autocovariance coefficients of the X and Y series. Note that the lag l cross covariance coefficient between X and Y is not the same as for Y and X. Then, the lag l cross correlation between Y_t and X_t is given by the dimensionless quantity

$$\rho_{XY}(l) = \frac{\gamma_{XY}(l)}{\sigma_X \sigma_Y} \tag{3.6}$$

which represents the correlation between Y_t and X_{t-k}. For positive values of l, the lag l cross correlation between Y_t and X_t is a measure of how the series X_t is a leading indicator for Y_t, while the lag k cross correlation between X_t and Y_t is a measure of how the series Y_t is a leading indicator for X_t (Hudak and Liu, 1992).

The analysis of experimental data that have been observed at equispaced points in time leads to new and unique problems in statistical modeling and inference. The correlation introduced by the sampling of adjacent time points can severely restrict the applicability of many conventional statistical methods that depend on the assumption that the observations are independent and identically distributed. A systematic approach to address these correlations is commonly called *time series analysis*.

There are two approaches to time series analysis: the *time domain approach* and the *frequency domain approach*. The frequency domain approach assumes that the time series is best regarded as a sum or linear superposition of sine and cosine functions of different frequencies. On the other hand, the time domain approach assumes that correlation in adjacent time series values is best explained in terms of a regression of the current value on past values. This assertion depends on the Wold decomposition which asserts that the current point can be predicted as the sum of a linear combination of the past values of a noise series and a deterministic component orthogonal to that linear combination (Wold, 1938). In this work, we only use the time domain approach.

Time series analysis deals only with data measured at equally spaced, discrete time intervals. Modern time series analyses and applications are usually model based. The objective is to find a good model that describes how the observations in a single time series are related to each other. There are many different types of models used for time series analysis.

3.2.2 ARIMA Models

Introduction

One popular class of models are the Box-Jenkins ARIMA (Autoregressive Integrated Moving Average) models. These models have the ability to represent a wide range of processes with a parsimonious model. They can also be extended to permit modeling in the presence of external events or interventions (Tiao, 1981). Moreover, a well established procedure for modeling has been developed by Box and Jenkins (1970).

An autoregressive moving average (ARMA) model has the form

$$Z_t - \phi_1 Z_{t-1} - \phi_2 Z_{t-2} - \ldots - \phi_p Z_{t-p} = C + a_t - \theta_1 a_{t-1} - \theta_2 a_{t-2} - \ldots - \theta_q a_{t-q} \tag{3.7}$$

where C is a constant and $\{a_t\}$ is a sequence of random errors that are independently and identically distributed as a normal distribution, $N(0,\sigma_a^2)$. Such sequences are often called "white noise". The above equation can be rewritten as

$$(1 - \phi_1 B - \phi_2 B^2 - \ldots - \phi_p B^p) Z_t = C + (1 - \theta_1 B - \theta_2 B^2 - \ldots - \theta_q B^q) a_t \tag{3.8}$$

where B is the backshift operator defined by $B^b Z_t = Z_{t-b}$. Equation 3.8 can be further abbreviated by writing it as

$$\phi(B) Z_t = C + \theta(B) a_t \tag{3.9}$$

where

$$\begin{aligned} \phi(B) &= (1 - \phi_1 B - \phi_2 B^2 - \ldots - \phi_p B^p) \\ \theta(B) &= (1 - \theta_1 B - \theta_2 B^2 - \ldots - \theta_q B^q) \end{aligned} \tag{3.10}$$

This is known as an ARMA(p,q) model. The value p denotes the order of the autoregressive operator $\phi(B)$, and q denotes the order of the moving average operator $\theta(B)$. The model can also be expressed as

$$Z_t = \mu + \frac{\theta(B)}{\phi(B)} a_t \tag{3.11}$$

where $\mu = C/(1 - \phi_1 - \phi_2 - \ldots - \phi_p)$ is the mean of the stationary time series.

If the series does not return quickly to a single overall mean, usually a new series with a constant mean is created. Then the autoregressive portion of the ARMA(p,q) model must include an operator to induce stationary. This is most frequently accomplished through a differencing operator of the form $\nabla^S=(1-B)^d$, where d denotes the degree of differencing. That is, instead of modeling the nonstationary series Z_t, we model the series

$$(1-B)Z_t = Z_t - Z_{t-1} \tag{3.12}$$

Physically this corresponds to modeling some change in the series rather than the series itself. Although, only a single differencing is usually required, situations may arise where the operator need to be repeated. The model then becomes an autoregressive integrated moving average model, ARIMA(p,d,q), of the form

$$\phi(B)(1-B)^d Z_t = C + \theta(B)a_t \tag{3.13}$$

or equivalently

$$\nabla^d Z_t = \mu + \frac{\theta(B)}{\phi(B)}a_t \tag{3.14}$$

The mean of a time series may be treated as a deterministic component of the series. To focus on the stochastic behavior of the series the data may be expressed in terms of deviations from the mean. That is, define a new time series $\tilde{Z}_t$

$$\tilde{Z}_t = Z_t - \mu \tag{3.15}$$

which represents the deviation of the process from some origin, or from its mean, if the process is stationary. The new series $\tilde{Z}_t$ will behave exactly as the old series Z_t, or $\nabla^d Z_t$ if the series is nonstationary, except that the mean of the $\tilde{Z}_t$ series will equal precisely zero rather than μ. Let $\tilde{Z}_t$ be the deviation of an observed time series from some origin, then the general ARIMA model may be expressed as

$$\nabla^d \tilde{Z}_t = \frac{\theta(B)}{\phi(B)}a_t \tag{3.16}$$

Building such a model is best achieved by a three-stage iterative procedure based on identification, estimation and diagnostic checking (Box and Jenkins, 1970).

Identification

In this step, characteristics of the autocorrelation function (ACF) and partial autocorrelation function (PACF) are examined to identify pattern characteristics of a specific model. The task is then to determine the most suitable values of p, d, and q for the ARIMA(p,d,q) model. The autocorrelation function is a sequence of autocorrelations from lag l through a specified lag order. The ACF of a stationary series shows a rapid decay to zero. If a series is nonstationary, then its ACF will be high for a number of lags; and decreases slowly to zero. Stationarity may be induced by suitable differencing. The degree of differencing, d, necessary to achieve stationarity is reached when the autocorrelation function of $\nabla^d Z_t$ dies out rapidly to zero.

After evaluating the value of d, the next task is to find the orders p and q of the differenced stationary series. The ACF and the PACF are the two main tools used to identify p and q. They measure the statistical relationship between observations in a single data series. The ACF provides direct information on the order of the moving average operator, $\theta(q)$, if p=0. The PACF is a relative measure of the importance of adding terms in a lagged regression of a stationary time series. That is, the sample PACF can be obtained by sequentially fitting

$$\begin{aligned} Z_t &= \phi_{11} Z_{t-1} + a_t \\ Z_t &= \phi_{21} Z_{t-1} + \phi_{22} Z_{t-2} + a_t \\ &\vdots \quad \vdots \quad \vdots \qquad\qquad \vdots \\ Z_t &= \phi_{l1} Z_{t-1} + \phi_{l2} Z_{t-2} + \ldots + \phi_{ll} Z_{t-l} + a_t \end{aligned} \tag{3.17}$$

and retaining the estimate of the last term of each fit, $\phi_{11}, \phi_{22}, \ldots, \phi_{ll}$. The estimate of ϕ_{ll} has a value between -1 and 1, and can be interpreted as the relationship between the ordered pairs (Z_t , Z_{t+l}) taking into account the effect due to $Z_{t-1}, Z_{t-2}, \ldots, Z_{t-l+1}$. Thus the set of estimates of $\phi_{11}, \phi_{22}, \ldots, \phi_{ll}$ is referred to as the sample PACF of the series Z_t.

From the definition of the PACF, this latter provides direct information on the order of autoregressive operator, $\phi(p)$, provided q=0. A more precise representation of the behavior of pure autoregressive (AR) or moving average (MA) processes is given in Table 3.1. Thus, for pure AR and MA models, the PACF and ACF provide relatively simple and effective tools to determine d, p and q.

Table 3.1 Behavior of Pure AR and MA Processes

	ACF	PACF
MA(q)	"Cuts off" after lag q	"Dies out" in an exponential or sinusoidal fashion
AR(p)	"Dies out" in an exponential or sinusoidal fashion	"Cuts off" after lag p

When the orders p and q are not zero, then the identification of the model can be more difficult if only sample ACF and PACF of a series are available for use.

Tsay and Tiao (1984) introduced a unified approach for the identification of both the mixed stationary and nonstationary models. They construct and display a table of values, see Figure 3.1, called the extended autocorrelation function (EACF), to suggest

SIMPLIFIED EXTENDED ACF TABLE (5% LEVEL)

(Q-->)	0	1	2	3	4	5	6	7	8	9	10	11	12
(P= 0)	X	X	X	X	X	X	X	X	X	0	0	0	0
(P= 1)	X	0	0	0	0	0	0	0	0	0	0	0	0
(P= 2)	X	X	0	0	0	0	X	0	0	0	0	0	0
(P= 3)	X	0	0	0	0	0	X	0	0	0	0	0	0
(P= 4)	X	0	0	0	0	0	0	0	0	0	0	0	0
(P= 5)	X	X	0	0	0	0	0	0	0	0	0	0	0
(P= 6)	X	0	0	0	X	0	0	0	0	0	0	0	0

Figure 3.1 Simplified Table of the Extended Autocorrelation Function

the maximum orders of p and q. The tables of values can be summarized in a condensed form by replacing those values that are within two standard errors of zero by 'o' (to indicate not different from zero), and by 'x' otherwise. The maximum values of p and q can then be determined by finding a position (p_0, q_0) in the table so that most values in the table are 'o' for the (i,j) coordinates in the triangular region where $i = p_0 + k$, and $j = q_0 + k$, $k = 0,1,2,...$ In the case shown below, p_0=1 and q_0=0 which suggests fitting an ARMA(1,1).

Estimation.

Once the model is specified, efficient estimates of the model parameters should be obtained. The general stationary ARMA(p,q) model, given by equation 3.16, may also be written as

$$a_t = C + Z_t - \phi_1 Z_{t-1} - \phi_2 Z_{t-2} - \ldots - \phi_p Z_{t-p} + \theta_1 a_{t-1} + \theta_2 a_{t-2} + \ldots + \theta_q a_{q-1} \qquad (3.18)$$

As discussed in Box and Jenkins (1970), fitting the parameters ϕ and θ is equivalent to fitting the above model to the Z_ts. Assuming a time series with n observations $Z_1, Z_2, \ldots, Z_n$, one needs to choose some starting values (Z^*, a^*), prior to the beginning of the Z_t series, to calculate a_t. Note that Z^* has p elements while a^* has q elements. Thus, for any values of the parameters (ϕ, θ), a set of values $a_t(\phi, \theta | Z^*, a^*, Z)$ with $t = 1, 2, \ldots, n$ can be calculated, conditioned on the choice of the starting values (Z^*, a^*). Typically, the starting values are chosen equal to their expected values, i.e. the elements of Z^* and a^* will all be zero. Assuming that the a_t s are normally distributed with mean zero and variance σ_a^2, the *conditional* log likelihood is given by

$$l^*(\phi,\theta,\sigma_a) = -n \ln \sigma_a - \frac{S^*(\phi,\theta)}{2\sigma_a^2} \qquad (3.19)$$

where $S^*(\phi,\theta)$ is the *conditional* sum of squares function,

$$S^*(\phi,\theta) = \sum_{t=1}^{n} a_t^2(\phi,\theta | Z^*, a^*, Z) \qquad (3.20)$$

Typically, maximum likelihood estimates are obtained by minimizing the above *conditional* sum of squares function based on n-p observations, i.e. $Z_1, \ldots, Z_p$ are regarded as fixed.

Hillmer and Tiao (1979), derived an approximation to the likelihood function that incorporates a more *exact* likelihood function. This method also calculates the likelihood function on the basis of the stochastic structure of *n-p* observations. However, the two approaches differ in that the *conditional* algorithm assumes $a_p = ... = a_{p-q+1} = 0$ while the *exact* likelihood algorithm computes estimates for these values. Hence, this *exact* approach is "exact" for MA parameters only. The *conditional* and *exact* algorithms do not affect the estimates of a pure AR process. While the objective function to be minimized is the sum of squared residuals in the *conditional* method, it is the sum of squared residuals plus an adjustment term in the *exact* method (Hillmer and Tiao, 1979).

Diagnostic checks.

After the parameters have been estimated, the fitted model should be subjected to diagnostic checks and tests for model adequacy. The most important test of statistical adequacy of an ARIMA model involves checking the assumption that the errors or random shocks, a_t, are independently and normally distributed. The basic analytical tool at the diagnostic check stage is the residual ACF. If the residuals approximate white noise, then all autocorrelation coefficients should not be significantly different from zero. The ARIMA model should be reformulated if diagnostic checks show this assumption is not true.

Another check on the residuals is through a "portmanteau" lack of fit test, the *Q*-statistic (Jung-Box, 1978). For an ARIMA(*p*,*d*,*q*) process this test is given

$$Q = n\sum_{k=1}^{l}\rho_k^2 \tag{3.21}$$

where *n* is the number of observations used to fit the model. This value represents a scaled sum of squares of the computed ACF values. It is possible to show (Box and Pierce, 1970) that Q approximately follows a χ^2 distribution with (*l-p-q*) degrees of freedom. Thus, a "portmanteau" test of the hypothesis of model adequacy, may be made

by referring an observed value of Q to a table of the percentage points of χ^2 (Box and Jenkins, 1970).

An observation $\tilde{Z}_t$ generated by an ARIMA process may be expressed in three explicit forms. The most popular is the difference equation form where an observed value is written in terms of the present and past values of shock,

$$\tilde{Z}_t = \phi_1 \tilde{Z}_{t-1} + \phi_2 \tilde{Z}_{t-2} + \ldots \phi_p \tilde{Z}_{t-p} - \theta_1 a_{t-1} - \theta_2 a_{t-2} - \ldots - \theta_q a_{t-q} + a_t \quad (3.22)$$

Another form is in terms of the present and past values of the series and the current shock (noise) to the system,

$$\pi(B)\tilde{Z}_t = a_t \quad (3.23)$$

where

$$\pi(B) = 1 - \pi_1 B - \pi_2 B^2 - \ldots \quad (3.24)$$

The coefficients of the linear polynomial $\pi(B)$ satisfy the relationship $\pi(B)=\phi(B)/\theta(B)$. The coefficients of $\pi(B)$ indicate the relative importance of past observations in predicting the future and how the current value of the series may be derived from past values and the current shock. The π weights may also be used in forecasting future values. The third form is an infinite weighted sum of current and previous shocks $\{a_t\}$, also known as the random-shock form,

$$\tilde{Z}_t = \psi(B) a_t \quad (3.25)$$

where

$$\psi(B) = 1 + \psi_1 B + \psi_2 B^2 + \ldots \quad (3.26)$$

The coefficient of the linear polynomial $\psi(B)$ are such that $\psi(B)=\theta(B)/\phi(B)$. The coefficients of $\psi(B)$ indicate how the current value of the series may be derived from the noise series. The ψ weights are used in the calculation of the variance of the error in forecasted values and may also used in the updating of forecasts (Box and Jenkins, 1970).

Forecasting

The ultimate application of ARIMA modeling is to forecast future values of a time series. Let t be the current time period. When forecasting we are interested in predicting some future value of a time series, $\tilde{Z}_{t+l}$, where $l > 0$. The forecast origin is t, and l is called the forecast lead time. The minimum mean square error (MMSE) forecast at origin t, designated as $\hat{Z}_t(l)$, is the conditional expectation of $\tilde{Z}_{t+l}$, at time t (Box and Jenkins, 1970). That is, $\hat{Z}_t(l)$ is the mathematical expectation of $\tilde{Z}_{t+l}$ given previous observations up to time t

$$\hat{Z}_t(l) = E[Z_{t+l} / Z_t, Z_{t-1}, \dots] = E_t[Z_{t+l}] \tag{3.27}$$

The simplest and most elegant way to produce forecasts from an ARIMA model is to express the model in the difference equation form. The MMSE forecast at time t, $\hat{Z}_t(l)$, can be recursively computed using

$$\hat{Z}_t(l) = \phi_1 \hat{Z}_t(l-1) + \dots + \phi_p \hat{Z}_t(l-p) - E_t[a_{t+l}] - \theta_1 E_t[a_{t+l-1}] - \dots - \theta_q E_t[a_{t+l-q}] \tag{3.28}$$

where

$$\begin{aligned} &\hat{Z}_t(l) = Z_{t+l} && \text{if } l \le 0 \\ &E[a_{t+l}] = a_{t+l} && \text{if } l \le 0 \\ &E[a_{t+l}] = 0 && \text{if } l > 0 \end{aligned} \tag{3.29}$$

The resulting MMSE forecast $\hat{Z}_t(l)$ becomes then

$$\hat{Z}_t(l) = \phi_1 \hat{Z}_t(l-1) + \dots + \phi_{l-1} \hat{Z}_t(1) + \phi_l Z_t + \dots + \phi_p Z_{t-p} - \theta_l a_t - \dots - \theta_q a_{t-q} \tag{3.30}$$

While MMSE forecasts are most conveniently calculated from the difference-equation form, in creating confidence intervals for these forecasts it is more convenient to start with the random-shock form. The MMSE forecast $\hat{Z}_t(l)$ is obtained by taking conditional expectations on equation 3.25

$$\hat{Z}_t(l) = \psi_l a_t + \psi_{l+1} a_{t-1} + \psi_{l+2} a_{t-2} + \dots \tag{3.31}$$

Subtracting equations 3.25 and 3.31, gives the forecast error for lead time l, $e_t(l)$, which is defined as the difference between an observed $\tilde{Z}_t$ and its forecast $\hat{Z}_t(l)$,

$$e_t(l) = Z_t - \hat{Z}_t(l) \tag{3.32}$$

Assuming that the white noise sequence for the model has a variance σ^2_a, this forecast error is normaily distributed with zero mean and variance $V(e_t(l))$ given by

$$V(\hat{e}_t(l)) = \sigma_a^2(1 + \psi^2_1 + \psi^2_2 + \ldots + \psi^2_{l-1}) \tag{3.33}$$

As seen before, the random-shock form of an ARIMA model may be very useful in updating forecasts. We can express the forecasts $\hat{Z}_{t+1}(l)$ and $\hat{Z}_t(l+1)$, of the future observation $\tilde{Z}_{t+l+1}$, made at origins $t+1$ and t, as

$$\hat{Z}_t(l+1) = \psi_{l+1}a_t + \psi_{l+2}a_{t-1} + \ldots \tag{3.34}$$

$$\hat{Z}_{t+1}(l) = \psi_l a_{t+1} + \psi_{l+1}a_t + \psi_{l+2}a_{t-1} + \ldots \tag{3.35}$$

On subtraction of equations 3.34 and 3.35, it follows that

$$\hat{Z}_{t+1}(l) = \hat{Z}_t(l+1) + \psi_l a_{t+1} \tag{3.36}$$

Then, when $\tilde{Z}_{t+1}$ becomes available, the white noise coefficient $a_{t+1}=Z_{t+1}-Z_t(l)$ is calculated and proportional updates are used to obtain forecasts at origin $t+1$ from the above equation.

3.2.3 Intervention Analysis

Various external events, such as political, economic, technical or technological changes can affect a time series. Assuming that the occurrence and the timing of these interventions are known, deterministic inputs can be used in time series models to represent these identified events. Incorporating such interventions into a time series model should improve parameter estimates and forecasts.

A method, suggested by Box and Jenkins (1975), to analyze a time series in the presence of external known events is intervention (or impact) analysis. In this approach, a series involving a single intervention is represented by a stochastic and a deterministic component

$$Y_t = C + \frac{\omega(B)\,B^b}{\delta(B)} I_t + N_t \tag{3.37}$$

where N_t represents the underlying series and $\omega(B)B^b/\delta(B)I_t$ represents the effect(s) of the intervention.

Process variables might be affected by an infinite variety of interventions. The two most common types of interventions may be represented by the pulse and the step functions. A pulse function, $P_t(T)$, is an indicator variable that represents an intervention that occurs for one time period T only, such that

$$P_t(T) = \begin{cases} 1 & \text{for } t = T \\ 0 & \text{otherwise} \end{cases} \tag{3.38}$$

On the other hand, a step function is an indicator variable that represents an intervention that remains in effect beginning from a particular time period. It is usually represented as $S_t(T)$, where T is the time that the intervention begins,

$$S_t(T) = \begin{cases} 1 & \text{for } T_1 \le T \le T_2 \\ 0 & \text{otherwise} \end{cases} \tag{3.39}$$

Note that $S_t(T)$ and $P_t(T)$ are directly related according to

$$(1 - B)\,S_t(T) = P_t(T) \tag{3.40}$$

The rational operator $\omega(B)B^b/\delta(B)$ characterizes the impact of the intervention on the time series. More specifically, the parameters of the numerator polynomial $\omega(B)$ describe the impact of the intervention whereas the denominator operator $\delta(B)$ characterizes the decay pattern of the impact(s) to be reflected in time series. In practice, $\delta(B)$ can be expressed either as $\delta(B) = 1$ if the intervention does not have any residual effect or as $\delta(B) = 1 - \delta B$, if a decay pattern is present. The parameter δ is directly proportional to the length of the residual effect.

The first step in building an intervention model is to determine an initial expression for the disturbance series N_t. One way to identify an ARIMA model for N_t in an intervention model is to determine an initial ARIMA model for Y_t. However, as discussed by Guttman and Tiao (1978) and Chang and Tiao (1983), interventions can drastically change the autocorrelation patterns in a time series. Since interventions can seriously bias the resting ARIMA, only data before and after the intervention (depending on which part provides the most information) should be used to specify an initial model for Y_t, and therefore N_t. Another alternative is to use a proxy AR(1) model for N_t, as discussed later in Chapter 4.

Once a preliminary model for the disturbance is identified, the optimal intervention model is found by an iterative search consisting of a sequence of estimation, diagnostic checking and model reformulation steps. Using the estimated preliminary model for N_t, the linear intervention weights are evaluated by some ordinary nonlinear least-squares method. The pattern of these weights are then compared to some theoretical patterns to determine a form for the rational intervention operator $\omega(B)B^b/\delta(B)$. Next, an estimate of the resulting disturbance is then generated in the usual way

$$\hat{N}_t = Y_t - \hat{C} - \frac{\hat{\omega}(B)\,B^{\hat{b}}}{\hat{\delta}(B)} I_t \tag{3.41}$$

The ACF, PACF and EACF of the estimated disturbance series are then studied to identify a new ARIMA model for N_t. The residual series of the resulting intervention model

$$\hat{a}_t = Y_t - \hat{Y}_t \tag{3.42}$$

are then examined to check model adequacy. The model is reformulated, if necessary, and the above steps are repeated until an adequate transfer function model is obtained.

3.2.4 Outlier Detection and Treatment

Introduction

In the previous Section, we considered intervention models with the external events or interventions represented by deterministic binary (0 or 1) input variables. However, these events are often not explicitly to the analyst. Such unknown events cause these unusual or unexpected observations called outliers. A number of benefits may be gained from detecting outliers in a time series. First, it may lead to a better understanding of the series under study since a search into the history of the time series to find a plausible explanation of a detected event may uncover new cause and effect relationship. While an ARIMA model is designed to grasp the homogeneous memory pattern of a time series, the presence of outliers may seriously bias the fitting of such a time series model. Thus, better modeling and estimation is achieved if outliers are detected and treated appropriately. The overall forecasting performance of a model can be highly improved by adjusting for the presence of outliers.

Outliers as Interventions

Typically, intervention analysis is used to adjust for the effect of an outlier once its occurrence and its form are correctly identified. Detected outliers are then included in the adjusted model as intervention components. Consider a time series Z_t, expressed in terms of deviation variables $\tilde{Z}_t$, whose behavior is described by an ARMA(p,q),

$$\tilde{Z}_t = \frac{\theta(B)}{\nabla^d \phi(B)} a_t \tag{3.43}$$

where $\phi(B)$ and $\theta(B)$ are the AR operator of order p and the MA operator of order q, respectively. Note that $\tilde{Z}_t$ is assumed to be stationary after suitable differencing. A time series contaminated with non-repetitive events may be represented by the following intervention model

$$Y_t = \tilde{Z}_t + \frac{\omega(B)}{\delta(B)} P_t(T) \tag{3.44}$$

where $P_t(T)$ is a deterministic binary pulse variable indicating the occurrence of an outlier while $\omega(B)$ and $\delta(B)$ are the usual transfer function operators. The indicator function $P_t(T)$ may be expressed as

$$P_t(T) = \begin{cases} 1 & for\ t = T \\ 0 & otherwise \end{cases} \tag{3.45}$$

where T is the possibly unknown location of the outlier. Note that if T is known the analysis reduces to the intervention analysis.

Main Types of Outliers

Depending on the form of the rational transfer function $\omega(B)/\delta(B)$, four types of outliers may be distinguished: additive outlier (AO), innovational outlier(IO), level shift (LS) and temporary change(TC). The simplest type of outlier is the AO which may be represented by the following operator

$$\frac{\omega(B)}{\delta(B)} = \omega_{AO} \tag{3.46}$$

This type of outlier produces an immediate and unique effect of magnitude ω_{AO} at time T, that is only one observation of the overall series is affected by an AO. In this case, the intervention model given by equation 3.37 becomes

$$\begin{aligned} Y_t &= Z_t + \omega_{AO} P_t(T) \\ &= \frac{\theta(B)}{\phi(B)} a_t + \omega_{AO} P_t(T)) \end{aligned} \tag{3.47}$$

An innovational outlier (IO) affects all values observed after its occurrence. Its effect is "proliferated" according to the ARIMA model of the process. An IO may be represented by

$$\frac{\omega(B)}{\delta(B)} = \omega_{IO} \frac{\theta(B)}{\phi(B)} \tag{3.48}$$

Substituting the above equation in the general equation of an intervention model gives,

$$\begin{aligned} Y_t &= Z_t + \omega_{IO}\frac{\theta(B)}{\phi(B)}P_t(T) \\ &= \omega_{IO}\frac{\theta(B)}{\phi(B)}(a_t + P_t(T)) \end{aligned} \tag{3.49}$$

Notice that, while an AO modifies one observation, Z_T, an IO changes one shock term, a_T.

The third main type of outlier is the level shift (LS). A LS is an event that alters a series at a given time and thus it produces a permanent perturbation in the series. It has the following form

$$\frac{\omega(B)}{\delta(B)} = \frac{\omega_{LS}}{1-B} \tag{3.50}$$

or, equivalently

$$\frac{\omega(B)}{\delta(B)}P_t(T) = \omega_{LS}S_t(T) \tag{3.51}$$

where $S_t(T)$ is a step function as defined by equation 3.39. Comparing equations 3.44 and 3.48, it can be noticed that the only difference between an AO and a LS is that the latter affects permanently all observed values starting from $t = T$ ($S_t(T)$), whereas in the case of an AO only one observation is altered at time $t = T$ ($P_t(T)$).

The last main type of outlier is the temporary change (TC). A TC is an event having such an initial impact and whose effect decays exponentially according to some dampening factor, say d (Liu and Hudak, 1992). Such an outlier may be represented by

$$\frac{\omega(B)}{\delta(B)} = \frac{1}{1-\delta} \tag{3.52}$$

where δ is the called "dampening" factor since it is designed to model the pace of the dynamic dampening effect. Chen and Liu (1992) suggested to use the value $\delta = 0.7$.

Detection and Estimation Procedure.

A common approach to deal with outliers in a time series is to detect the occurrence, the timing and the types of outliers, and then use intervention models (Box and Tiao, 1975) to adjust for their effects. This approach involves iterations between stages of outlier detection and estimation of an intervention model. A number of methods have been suggested by Hillmer *et al.* (1983), Tsay (1988) and Chang *et al.* (1988). However, these methods do not perform well when outliers are relatively close to each other. In such a case, some outliers may not be identified due to a masking effect. This may often lead to biased estimates of model parameter. A procedure less vulnerable to the spurious and masking effects during outlier detection was suggested by Chen and Liu (1992). This iterative method produces joint estimates of model parameters and outlier effects through a series of outlier detection and adjustment steps.

As discussed by Box and Jenkins (1976), an ARIMA model may be represented as

$$\pi(B) Z_t = a_t \tag{3.53}$$

where

$$\pi(B) = \frac{\phi(B)}{\theta(B)} = 1 - \pi_1 B - \pi_2 B^2 - \ldots \tag{3.54}$$

Similarly, the estimated residuals, $\hat{e}_t$, that may be contaminated with outliers are obtained by filtering Y_t through the $\pi(B)$ operator

$$\hat{e}_t = \pi(B) Y_t \tag{3.55}$$

Substituting the definition of the four types of outliers, discussed above, gives

$$\begin{aligned}
\hat{e}_t &= \omega_{AO} \pi(B) P_t(T) + a_t \\
\hat{e}_t &= \omega_{IO} P_t(T) + a_t \\
\hat{e}_t &= \omega_{LS} \frac{\pi(B)}{(1-B)} P_t(T) + a_t \\
\hat{e}_t &= \omega_{TC} \frac{\pi(B)}{(1-\delta B)} \pi(B) P_t(T) + a_t
\end{aligned} \tag{3.56}$$

The above equations may be more generally re-expressed as

$$\hat{e}_t = \omega x_{it} + a_t \qquad where \quad \omega_i = \begin{cases} \omega_{AO}, & i = 1 \\ \omega_{IO}, & i = 2 \\ \omega_{LS}, & i = 3 \\ \omega_{TC}, & i = 4 \end{cases} \tag{3.57}$$

In the above equation, the series x_{it} assumes the value 0 for $t \leq$ T; the value 1 for t = T; and for T+k (k = 1, 2, ..., n-T) the value for x_{it}'s are

$$\begin{aligned} &i = 1 \quad (AO): && -\pi_k \\ &i = 2 \quad (IO): && 0 \\ &i = 3 \quad (LS): && 1 - \sum_{j=1}^{k} \pi_j \\ &i = 4 \quad (TC): && \delta^k - \sum_{j=1}^{k-1} \delta^{k-j} \pi_j - \pi_k \end{aligned} \tag{3.58}$$

The least squares estimate for the effect of a single outlier may be represented as

$$\begin{aligned} \hat{\omega}_{AO}(T) &= \frac{\sum_{t=T}^{n} \hat{e}_T x_{1t}}{n} \\ \hat{\omega}_{IO}(T) &= \hat{e}_T \\ \hat{\omega}_{LS}(T) &= \frac{\sum_{t=T}^{n} \hat{e}_T x_{3t}}{\sum_{t=T}^{n} x_{3t}^2} \\ \hat{\omega}_{TC}(T) &= \frac{\sum_{t=T}^{n} \hat{e}_T x_{4t}}{\sum_{t=T}^{n} x_{4t}^2} \end{aligned} \tag{3.59}$$

Chang *et al.* (1988) suggested using the maximum value of the standardized statistics of the outlier effect as an alternative for outlier detection. These statistics follow a normal distribution and are defined by

$$
\begin{aligned}
\hat{\tau}_{AO}(T) &= \frac{\hat{\omega}_{LS}(T)}{\hat{\sigma}_a}\left(\sum_{t=T}^{n}\hat{e}_t x_{1t}^2\right)^{1/2} \\
\hat{\tau}_{IO}(T) &= \frac{\hat{\omega}_{IO}(T)}{\hat{\sigma}_a} \\
\hat{\tau}_{LS}(T) &= \frac{\hat{\omega}_{LS}(T)}{\hat{\sigma}_a}\left(\sum_{t=T}^{n}\hat{e}_t x_{3t}^2\right)^{1/2} \\
\hat{\tau}_{TC}(T) &= \frac{\hat{\omega}_{TC}(T)}{\hat{\sigma}_a}\left(\sum_{t=T}^{n}\hat{e}_t x_{4t}^2\right)^{1/2}
\end{aligned}
\tag{3.60}
$$

where σ_a is the median absolute deviation (MAD) of the residual standard deviation, which is defined as

$$\hat{\sigma}_a = 1.483\, median\left\{\left|\hat{e}_t - \tilde{e}\right|\right\} \tag{3.61}$$

The term $\tilde{e}$ represents the median of the estimated residuals (Andrews *et al.*, 1972). The above test statistics (equation 3.60) are used to determine whether an observation was altered or not by an outlier. More specifically, the values obtained from these test statistics are compared with some pre-specified critical value. An outlier is decided to be present if the critical value is exceeded. The critical value for such tests is dependent on the underlying ARIMA model and the sample. Usually, the value of 3.0 is chosen, where there is a probability of 0.003 that the critical value is exceeded due to chance alone. This value gives reasonable sensitivity to outliers (Chen and Liu, 1992).

The iterative procedure, for joint outlier detection and model parameter estimation, consists of three main stages: initial parameter estimation and outlier detection; joint estimation of outlier effects and model parameters; detection of outliers based on the final parameter estimates. In stage 1, the aim is to calculate the maximum likelihood estimates of the model parameters based on the original series (for the first iteration) or the adjusted series (thereafter). Based on these preliminary estimates of the model parameter, all the potential outliers are detected using the tests statistics given by equation 3.60. All the information collected in stage 1 is then used to find joint estimates of the model

parameters and outlier effects. In stage 3, these results provide a basis for outlier identification and the estimation of their effects. The above three stages are repeated until all spurious observations are removed. This procedure provides an adjusted Y_t series, i.e. free of outliers.

3.3 Results and Discussion

In what follows, univariate ARIMA forecasts are produced using cycle time and yield data for the overall process as well as for the individual technologies. The cycle times and yields were weekly averages. As mentioned in Section 2.1, these values were coded, based on a linear transformation, due to the proprietary nature of the data. This transformation did not affect the overall nature of the results, only their absolute values. Data was collected over a period of 85 weeks, giving cycle time and yield series with 85 observations. However, ARIMA models were constructed based on only 72 data points. The reason was that many external events, e.g. shift and management changes which could change the process, happened after that time period. The remaining 13 observations were still used to determine the accuracy of the forecasts obtained.

3.3.1 Overall Process

Process Cycle Time Data

Figure 3.2 is a plot of the in-date cycle time data for the overall process. The data seem to wander around a constant mean. However, we must withhold judgment about stationarity of the mean until we examine the sample autocorrelation. The ACF and the PACF for the in-date cycle time data are given in Figure 3.3. Considering the estimated ACF in Figure 3.3a, we see that the first five autocorrelations are significantly different from zero at about the 5% level, i.e. only the first five spikes in the ACF extend beyond the control limits. Those limits are placed about two standards errors above and below

zero using Barlett's approximation (Pankratz, 1991 p.36). The autocorrelations decay rather quickly to zero. We conclude that the mean of the in-date cycle time series is probably stationary. An AR model seems appropriate since the ACF decays rapidly toward zero rather than cutting off sharply to zero. The estimated PACF in Figure (3.3b) suggests an AR(1) since it cuts off to zero after lag 1.

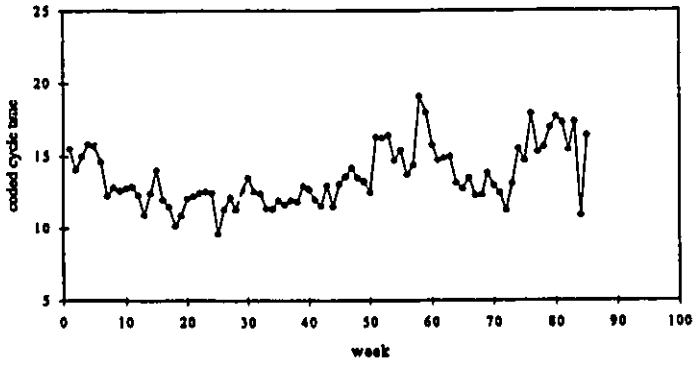

Figure 3.2 Plot of the Coded In-date Cycle Time for the Overall Process

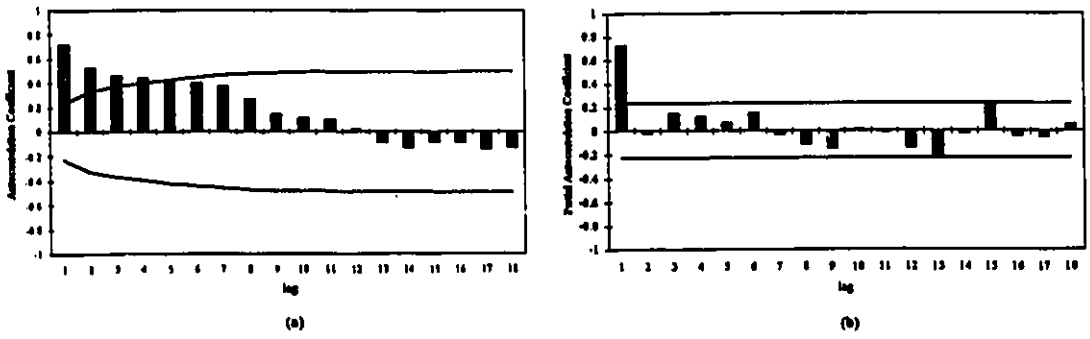

Figure 3.3 Autocorrelation Function and Partial Autocorrelation Function of the Coded In-date Cycle Time for the Overall Process

This model is confirmed by a simplified extended autocorrelation function, EACF, which is displayed in Table 3.2. A triangular region of '0' values appears to emanate from the vertex where p=1 and q=0.

Table 3.2 Simplified EACF of the Coded In-date Cycle Time for the Overall Process

(Q-->)	0	1	2	3	4	5	6	7	8	9	10	11	12
(P= 0)	X	X	X	X	O	O	O	O	O	O	O	O	O
(P= 1)	O	O	O	O	O	O	O	O	O	O	O	O	O
(P= 2)	O	O	O	O	O	O	O	O	O	O	O	O	O
(P= 3)	X	O	O	O	O	O	O	O	O	O	O	O	O
(P= 4)	X	X	O	O	O	O	O	O	O	O	O	O	O
(P= 5)	X	O	O	X	O	O	O	O	O	O	O	O	O
(P= 6)	X	X	X	O	X	O	O	O	O	O	O	O	O

A tentative model to represent the in-date cycle time data for the overall CMOS process is written as

$$Z_t = C + \phi Z_{t-1} + a_t \tag{3.62}$$

Table 3.3 displays the "traditional" maximum likelihood estimates of the above model (Box and Jenkins, 1970), using the SCA paragraph (routine) *ESTIM*. The model seems to satisfy the stationary requirement since $|\phi_1| < 1.0$. The in-date cycle time data is quite highly correlated with a $\phi_1 = 0.73$.

Table 3.3 ARIMA Estimation Results of the Coded In-date Cycle Time for the Overall Process

PARAMETER	VARIABLE	NUM./	FACTOR	ORDER	CONS-	VALUE	STD	T
LABEL	NAME	DENOM.			TRAINT		ERROR	VALUE
1 CNST		CNST	1	0	NONE	3.27	1.00	3.27
2		AR	1	1	NONE	0.73	0.08	9.10

TOTAL SUM OF SQUARES	.21364E+03
TOTAL NUMBER OF OBSERVATIONS	72
RESIDUAL SUM OF SQUARES	.98350E+02
R-SQUARE	.543
EFFECTIVE NUMBER OF OBSERVATIONS	71
RESIDUAL VARIANCE ESTIMATE	.13899E+01
RESIDUAL STANDARD ERROR	.13764E+01

The estimate of the autoregressive parameter, ϕ_1, is significantly different from zero since its t-value is greater than three. Also the estimated constant C=3.27 which gives the estimated mean $\mu = C/(1-\phi) = 3.27/(1-0.73) = 12.11$. To determine if these models are statistically adequate, we test the residuals $\hat{a}_t$ for independence. The residuals are estimates of the random errors which are assumed to be statistically independent.

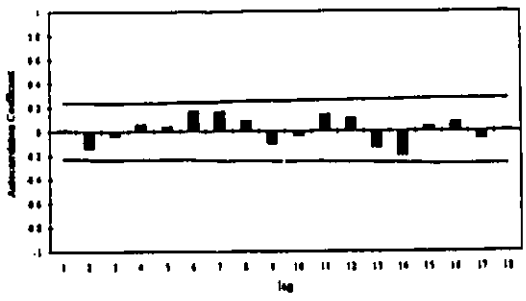

Figure 3.4 **Autocorrelation Function of the In-date Cycle Time Residuals from the Fitted AR(1) Model for the Overall Process**

The sample ACF of the residuals are used to test independence, as shown in Figure 3.4. The model seems adequate since the ACF of the residuals is randomly distributed and insignificant at the 5% level. The model for the in-date cycle time for the overall process is,

$$Z_t = 3.27 + 0.73\, Z_{t-1} + a_t \tag{3.63}$$

From the R^2 value, we see that the above model explains only 54.3% of the variability in the data for the overall process. A portmanteau lack of fit test, as discussed in Section 3.2.2, was also carried out. For the above model, Q = 16.7. Comparison with a $\chi^2_{17,0.005}$ = 27.59 reveals no significant lack of fit.

The same three stage procedure was carried out for the out-date cycle time data shown in Figure 3.5. Note that the out-date cycle time series contains three missing data points at t = 57, 58 and 59. Typically, missing observations are replaced by taking the average value of the adjacent observations. The out-date cycle time data seem to be highly positively correlated. The sample ACF given in Figure 3.6a does not decay rapidly to zero perhaps suggesting a nonstationary process. However, since the estimated PACF cuts off after lag 1, as shown in Figure 3.6b, an AR(1) model is suggested. The EACF displayed in Table 3.4. supports the choice of an AR(1) model since the vertex gives p=1 and q=0. In any case, the AR(1) model is always a good initial guess since the value of ϕ_0 should give us a better indication about the stationarity of the series, (i.e. if $\phi_0 \approx 1.0$ then the data is nonstationarity).

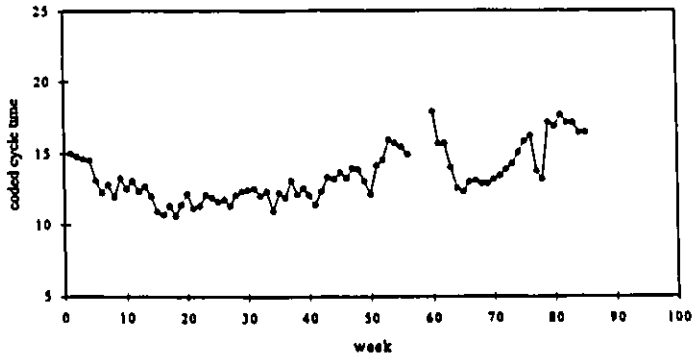

Figure 3.5 **Plot of the Coded Out-date Cycle Time for the Overall Process**

Table 3.4 **Simplified EACF of the Coded Out-date Cycle Time for the Overall Process**

(Q-->)	0	1	2	3	4	5	6	7	8	9	10	11	12
(P= 0)	X	X	X	X	O	O	O	O	O	O	O	O	O
(P= 1)	O	O	O	O	O	O	O	O	O	O	O	O	O
(P= 2)	X	O	O	O	O	O	O	O	O	O	O	O	O
(P= 3)	O	X	O	O	O	O	O	O	O	O	O	O	O
(P= 4)	X	O	O	O	O	O	O	O	O	O	O	O	O
(P= 5)	X	O	O	O	O	O	O	O	O	O	O	O	O
(P= 6)	X	X	O	O	O	O	O	O	O	O	O	O	O

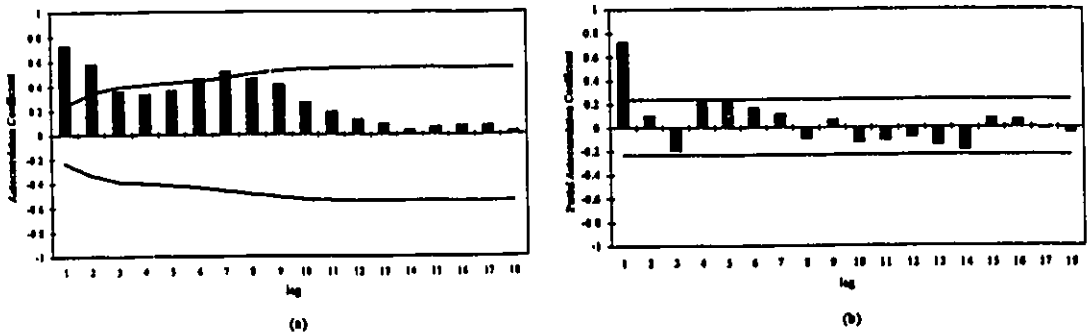

Figure 3.6 **Autocorrelation Function and Partial Autocorrelation Function of the Coded Out-date Cycle Time for the Overall Process**

Table 3.5a. shows the "traditional" estimation results. The estimated constant C_0=1.67 which gives the estimated mean $\mu_0=C_0/(1-\phi_0)=1.67/(1-0.86)=11.92$. The ϕ_0 parameter is significant and satisfies the stationarity criterion $|\phi_0|<1.0$. However, the out-date cycle time series is very highly correlated, $\phi_0 = 0.86$. Also, the mean of the series is only marginally significant since the associated t-value is only 2.36. The above model explains 75.1% of the variation within the data. Based on the preceding analysis, it is possible that alternative model to fit the data is the random-walk process,

$$Z_t = Z_{t-1} + a_t \tag{3.64}$$

Estimation results are shown in Table 3.5b. Both models display no lack of fit. However, the AR(1) model produces a smaller standard error of the residuals. The AR(1) model was then preferred. Figure 3.7 shows the ACF of the residuals from fitting the AR(1) model. No evidence of lack of fit is seen.

Table 3.5 **ARIMA Estimation Results of the Coded Out-date Cycle Data for the Overall Process**
(a) ARIMA(1,0,0) or AR(1)
(b) ARIMA(0,1,0) or Random Walk

(a)

PARAMETER LABEL	VARIABLE NAME	NUM./ DENOM.	FACTOR	ORDER	CONS-TRAINT	VALUE	STD ERROR	T VALUE
1 CNST		CNST	1	0	NONE	1.571	0.7080	2.36
2	CTOVALO	AR	1	1	NONE	.8586	.0588	14.59

TOTAL SUM OF SQUARES	.577238E+03
TOTAL NUMBER OF OBSERVATIONS	72
RESIDUAL SUM OF SQUARES	.141660E+03
R-SQUARE	.751
EFFECTIVE NUMBER OF OBSERVATIONS	71
RESIDUAL VARIANCE ESTIMATE	.219190E+01
RESIDUAL STANDARD ERROR	.990818E+01

(b)

PARAMETER LABEL	VARIABLE NAME	NUM./ DENOM.	FACTOR	ORDER	CONS-TRAINT	VALUE	STD ERROR	T VALUE

TOTAL NUMBER OF OBSERVATIONS	72
EFFECTIVE NUMBER OF OBSERVATIONS	71
RESIDUAL STANDARD ERROR	102250E+01

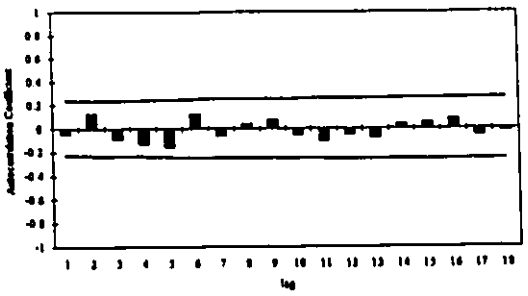

Figure 3.7 **Autocorrelation Function of the Out-date Cycle Time Residuals from the Fitted AR(1) Model for the Overall Process**

Both the in-date and the out-date cycle time data seem to follow an AR(1) model. Based on these fits we can check for outliers to complete the diagnostic check. Table 3.6a. reveals one innovational (IO) outlier at $t = 25$ and two temporary change (TC) outliers at $t = 51$ and 58 for the in-date cycle time. No outliers were detected for the out-date cycle time as shown in Table 3.6b. Thus, these outliers should be incorporated within a model to estimate potential outlier effects jointly with the underlying ARIMA model to check whether the outliers detected are real.

Table 3.6 **Outlier Detection of the Coded Cycle Data for the Overall Process Using (a) In-date Time Basis (b) Out-date Time Basis.**

(a)

```
-----------------------------------------
INITIAL RESIDUAL STANDARD ERROR =   1.3764
TIME     ESTIMATE   T-VALUE    TYPE
   58      16.12      4.98       TC
   51      11.67      4.03       TC
   25      -9.49     -3.54       IO
ADJUSTED RESIDUAL STANDARD ERROR =  1.0374
```

(b)

```
-----------------------------------------
INITIAL RESIDUAL STANDARD ERROR =   0.9921
TIME     ESTIMATE   T-VALUE    TYPE
       NO OUTLIER
ADJUSTED RESIDUAL STANDARD ERROR =  0.9921
```

The iterative procedure incorporated in the *OESTIM* paragraph of the SCA system for the joint estimation of model parameters and outlier effects proposed by Chen and Liu (1990), as discussed in Section 3.2.4, was used for this purpose.

The resulting intervention model for the in-date cycle time data is given in Table 3.7. This model includes detected outliers B25SER=$P_t^{(25)}$, B51SER=$P_t^{(51)}$ and B58SER=$P_t^{(58)}$ as intervention components. Of note is the decrease in the value of ϕ_1, 0.73 to 0.56, when the outliers were taken into account. This reflects the bias introduced in the estimate of ϕ_1 when outliers are not accounted for. This also indicates that the inherent process data are not as highly correlated as initially estimated in Table 3.1. Moreover, the residual standard error of the intervention model is smaller than the one for the original ARIMA model; the residual standard error decreased from 11.38 to 11.04. This confirms that the intervention model fits the data better than the original ARIMA model. The usual diagnostic checks do not indicate any anomalies: the intervention model satisfies the portmanteau test with Q = 15.6 compared with a $\chi^2_{17,0.005} = 27.59$, and the ACF of the residuals, shown in Figure 3.8, has no significant values.

Table 3.7 ARIMA Joint Detection-Estimation Results of the Coded In-date Cycle Time for the Overall Process

PARAMETER	LABEL	VARIABLE NAME	NUM./ DENOM.	FACTOR	ORDER	CONS-TRAINT	VALUE	STD ERROR	T VALUE
1	CNST		CNST	1	0	NONE	12.53	.2635	47.55
2		B25SER	NUM.	1	0	NONE	-2.6724	0.7570	-3.53
3	PH1	B25SER	DENM	1	1	EQ 01	.5618	.0852	6.59
4		B51SER	NUM.	1	0	NONE	4.1690	0.8272	5.04
5		B51SER	DENM	1	1	NONE	.8630	.0722	11.96
6		B58SER	NUM.	1	0	NONE	16.0264	2.7349	5.86
7		B58SER	DENM	1	1	NONE	.7012	.1173	5.98
***	PH1	CTOVALI	D-AR	1	1	EQ 01	.5618	.0852	6.59

TOTAL NUMBER OF OBSERVATIONS. 72
EFFECTIVE NUMBER OF OBSERVATIONS. 71
RESIDUAL STANDARD ERROR . . . . . 104433E+01

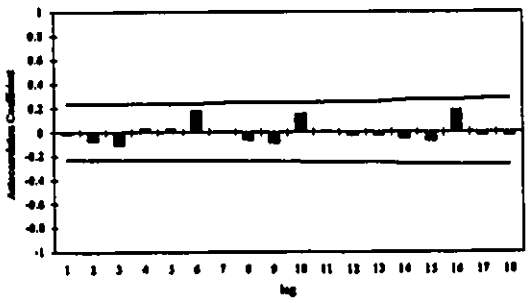

Figure 3.8 Autocorrelation Function of the In-date Cycle Time Residuals from the Above Fitted Intervention Model for the Overall Process.

The underlying AR(1) model for the in-date cycle time series is given by

$$Z_t = 12.53 + \frac{1}{(1-0.56B)} Z_{t-1} + a_t \qquad (3.65)$$

This case provides a good example to show how neglecting outliers can prevent accurate identification of the underlying process model. The joint detection-estimation procedure was used in identification and estimation of all subsequent models.

The model for the out-date cycle time was a very highly correlated AR(1) process that was close to being non-stationary. The fitted model is

$$Z_t = 11.92 + \frac{1}{(1-0.86B)} Z_{t-1} + a_t \qquad (3.66)$$

We can also notice that the in-date cycle time series has a larger mean value than the out-date cycle time, 12.53 vs 11.92. This is due to the fact that in-date cycle time data incorporate scrap lots as penalties to the process whereas in the out-date cycle time data, scrap lots are neglected. Use of the out-date time basis under-estimates the true process cycle time mean.

Process Yield Data.

Figures 3.9 and 3.10 show the process yield data for the overall process. The out-date yield series contains some missing data at t = 57, 58 and 59. A casual examination suggests that both series are stationary. The observations seem to fluctuate randomly around a fixed mean, and the variances seem to be constant over time. This random behavior is confirmed by the estimated ACF and the PACF for both the in-date and the out-date yield data, as shown in Figures 3.11 and 3.12. The EACFs displayed in Tables 3.8 and 3.9 show a triangular region of '0' values where p=0 and q=0.

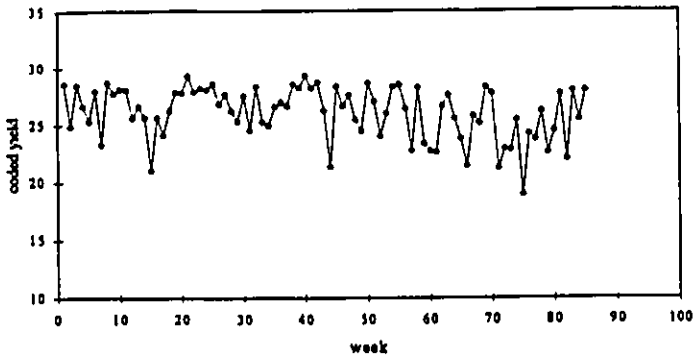

Figure 3.9 **Plot of the Coded In-date Yield for the Overall Process**

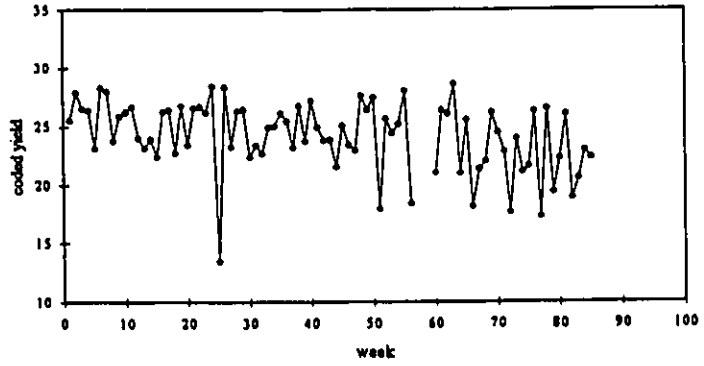

Figure 3.10 **Plot of the Coded Out-date Yield for the Overall Process**

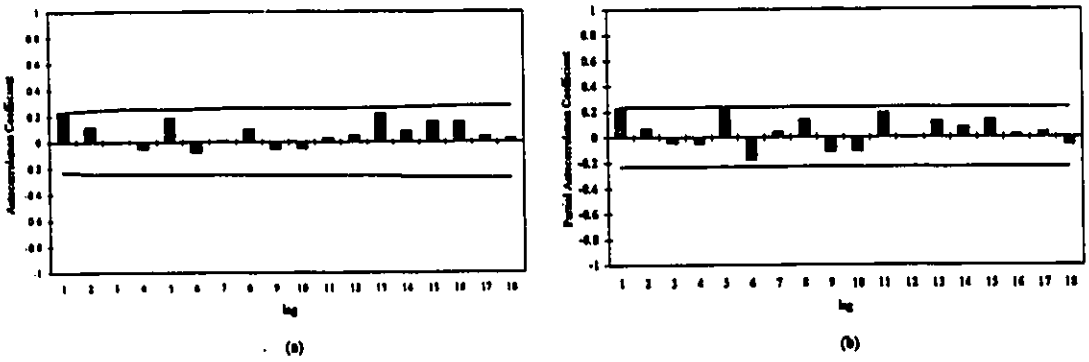

Figure 3.11 **Autocorrelation Function and Partial Autocorrelation Function of the Coded In-date Yield for the Overall Process**

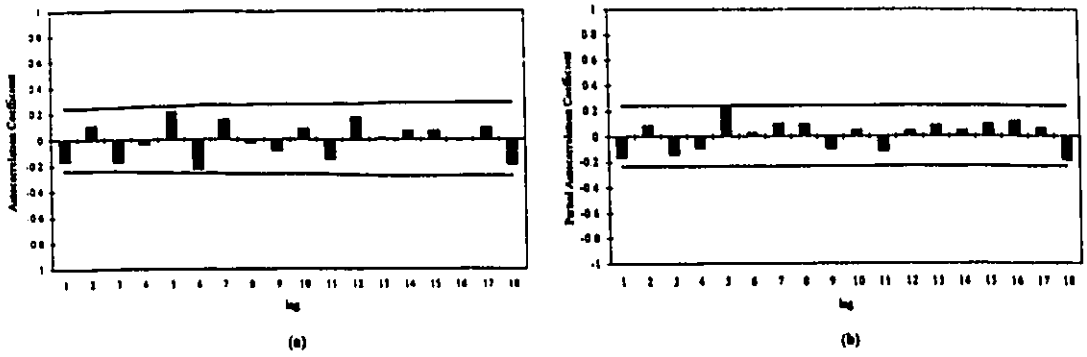

Figure 3.12 **Autocorrelation Function and Partial Autocorrelation Function of the Coded Out-date Yield for the Overall Process**

Based on these observations, a good initial choice is the white noise model,

$$Z_t = \mu + a_t \tag{3.67}$$

Note that in this case the constant C is just the mean of the series μ.

Table 3.8 **Simplified EACF of the Coded In-date Yield for the Overall Process**

(Q-->)	0	1	2	3	4	5	6	7	8	9	10	11	12
(P= 0)	O	O	O	O	O	O	O	O	O	O	O	O	O
(P= 1)	X	O	O	O	O	O	O	O	O	O	O	O	O
(P= 2)	O	O	O	O	O	O	O	O	O	O	O	O	O
(P= 3)	X	O	O	O	O	O	O	O	O	O	O	O	O
(P= 4)	O	O	O	O	O	O	O	O	O	O	O	O	O
(P= 5)	X	O	O	O	O	O	O	O	O	O	O	O	O
(P= 6)	O	O	O	O	O	O	O	O	O	O	O	O	O

Table 3.9 **Simplified EACF of the Coded Out-date Yield for the Overall Process**

(Q-->)	0	1	2	3	4	5	6	7	8	9	10	11	12
(P= 0)	O	O	O	O	O	O	O	O	O	O	O	O	O
(P= 1)	X	O	O	O	O	O	O	O	O	O	O	O	O
(P= 2)	X	O	O	O	O	O	O	O	O	O	O	O	O
(P= 3)	X	X	O	O	O	O	O	O	O	O	O	O	O
(P= 4)	X	X	O	O	O	O	O	O	O	O	O	O	O
(P= 5)	O	O	O	X	O	O	O	O	O	O	O	O	O
(P= 6)	X	O	O	X	O	O	O	O	O	O	O	O	O

Modeling results, using the joint estimation of model parameters and outlier effects for the above model are presented in Table 3.10. The mean of the out-date yield series, μ_O=25.1, is lower than the mean of the in-date yield series, μ_I=26.3. This difference may be explained by the fact that when using the in-date time basis, split lots are joined to their main lot using some weights, as discussed in Section 2.3. Resulting yield data are then pooled values and less weight is given to split lots. On the other hand, using the out-date time basis, split lots are treated as independent entities (i.e. all lots are given the same weight). Since split lots have generally lower yield values than normal lots, the out-date yield data are being under-estimated. The out-date yield data show five outliers that appear in the model as intervention components, i.e. pulse functions $P_t^{(25)}$, $P_t^{(51)}$, $P_t^{(56)}$, $P_t^{(66)}$ and $P_t^{(72)}$. No outliers were detected in the in-date yield data. The ACF of the residual series, see Figure 3.13, do not reveal anomalies in the fitted models, i.e. all autocorrelation coefficients are randomly distributed within the limits.

Table 3.10 ARIMA Joint Detection-Estimation of the Coded Yield for the Overall Process Using (a) In-date Time Basis (b) Out-date time basis

(a)

PARAMETER LABEL	VARIABLE NAME	NUM./ DENOM.	FACTOR	ORDER	CONS-TRAINT	VALUE	STD ERROR	T VALUE
1 CNST		CNST	1	0	NONE	26.3	.2522	104.27
TOTAL NUMBER OF OBSERVATIONS.							72	
EFFECTIVE NUMBER OF OBSERVATIONS.							72	
RESIDUAL STANDARD ERROR						.232646E+01		

(b)

PARAMETER LABEL	VARIABLE NAME	NUM./ DENOM.	FACTOR	ORDER	CONS-TRAINT	VALUE	STD ERROR	T VALUE
1 CNST		CNST	1	0	NONE	25.15	.2332	107.87
2	B25SER	NUM.	1	0	NONE	-11.4359	1.8871	-6.06
3	B51SER	NUM.	1	0	NONE	-6.9604	1.8661	-3.73
4	B56SER	NUM.	1	0	NONE	-6.4953	1.8865	-3.48
5	B66SER	NUM.	1	0	NONE	-6.7530	1.8855	-3.62
6	B72SER	NUM.	1	0	NONE	-7.2968	1.8567	-3.93
TOTAL NUMBER OF OBSERVATIONS.							72	
EFFECTIVE NUMBER OF OBSERVATIONS.							72	
RESIDUAL STANDARD ERROR						.210679E+01		

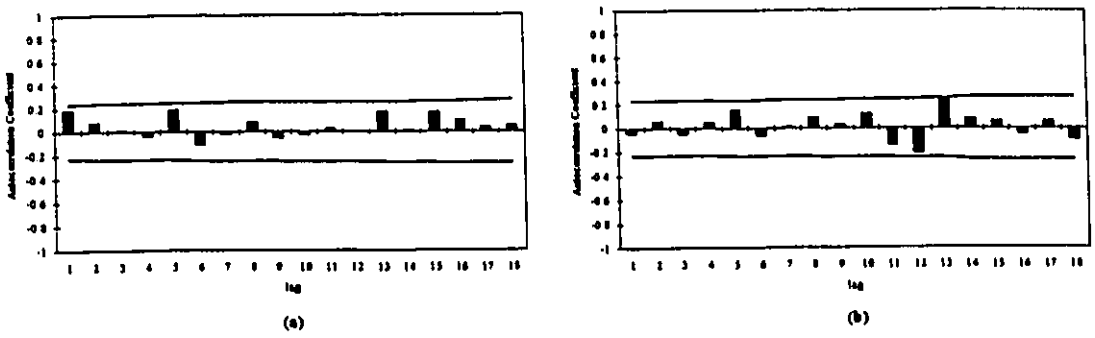

Figure 3.13 **Autocorrelation Function of the Yield Residual Series from the Fitted White Noise Model for the Overall Process Using the (a) In-date Time Basis (b) Out-date Time Basis**

The yield data for the overall process may then be represented by equation 3.68 for the in-date time basis and (3.69) for the out-date time basis,

$$Z_t = 26.3 + a_t \tag{3.68}$$

$$Z_t = 25.2 + a_t \tag{3.69}$$

No correlation was then found within the yield series. However, these results could also indicate the presence of some large noise masking the inherent dynamics of the series. In order to model the inherent dynamics of the yield series, the variability within the process should be diminished. Also, as showed by Harris and Ross (1991), a stationary series approaches a white noise sequence when sampled slowly. Thus, one could catch the dynamics of the yield series if one would sample more frequently.

3.3.2 Cycle Times and Yields for Individual Technologies

Process Cycle Time Data

As discussed previously, the overall process may be broken down, depending on the type of transistor produced, into four process-technologies: CMOS (1.5μm dlm), CMOS (1.2μm dlm), CMOS (1.08μm dlm) and CMOS (1.2μm tlm). The same three

stage procedure was used to build adequate models to fit the cycle time and the yield data for each of the four process-technologies. However, only the CMOS (1.08μm dlm) will be discussed as an example. Results for the other three technologies are given in Appendix C. Plots of the in-date and out-date cycle time for the CMOS (1.08μm dlm) are shown in Figures 3.14 and 3.15, respectively.

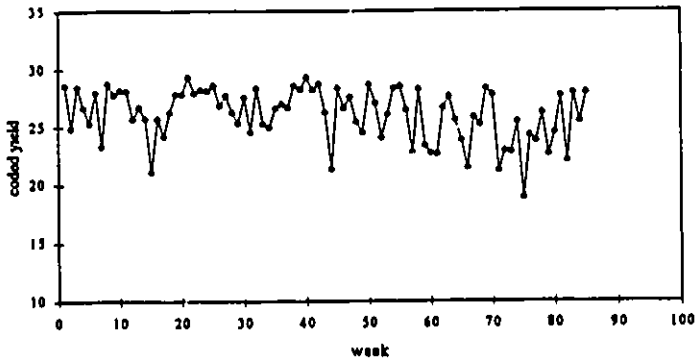

Figure 3.14 **Plot of the Coded In-date Cycle Time for the CMOS (1.08μm dlm) Technology**

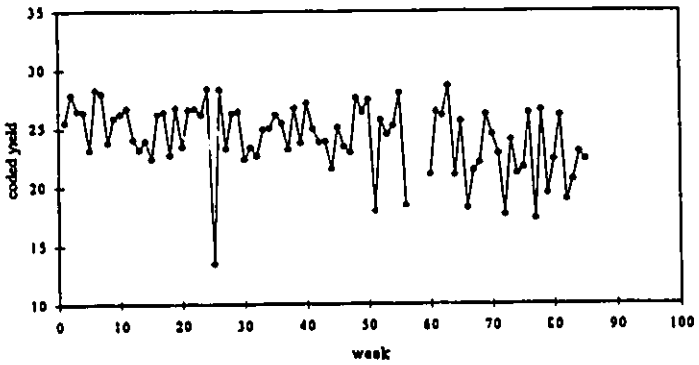

Figure 3.15 **Plot of the Coded Out-date Cycle Time for the CMOS (1.08μm dlm) Technology**

Figures 3.16 and 3.17 suggest fitting an AR(1) model,

$$Z_t = C + \phi Z_{t-1} + a_t = \mu + \frac{1}{(1-\phi)} a_t \tag{3.70}$$

since the ACF decays rapidly to zero while the PACF cuts off to zero after lag 1. Estimation results, using the joint detection-estimation procedure, are presented in Table 3.11.

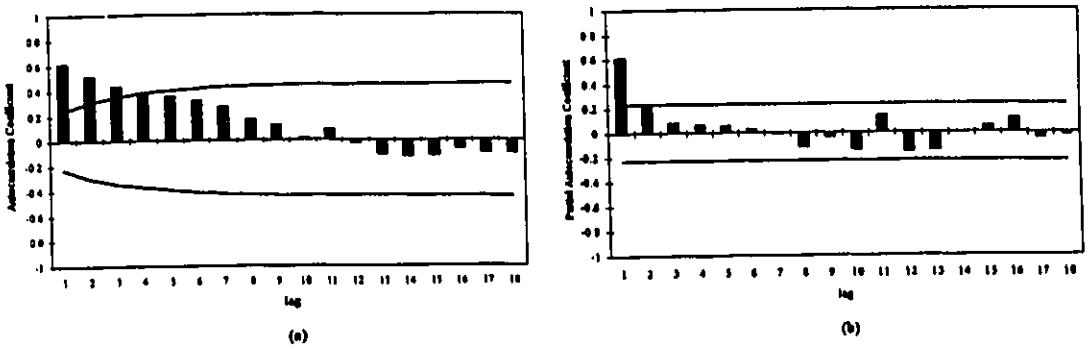

Figure 3.16 **Autocorrelation Function and Partial Autocorrelation Function of the Coded In-date Cycle Time for the CMOS (1.08μm dlm) Technology**

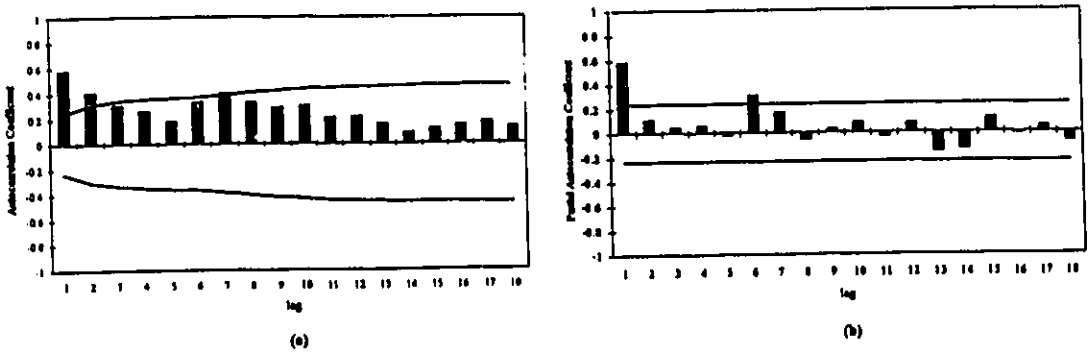

Figure 3.17 **Autocorrelation Function and Partial Autocorrelation Function of the Coded Out-date Cycle Time for the CMOS (1.08μm dlm) Technology**

Table 3.11 **ARIMA Joint Detection-Estimation Results for the Coded Cycle Time for the CMOS (1.08μm dlm) Technology Using (a) In-date time basis (b) Out-date Time Basis**

(a)

PARAMETER LABEL		VARIABLE NAME	NUM./ DENOM.	FACTOR	ORDER	CONS-TRAINT	VALUE	STD ERROR	T VALUE
1	CNST1		CNST	1	0	NONE	13.4011	0.9868	13.58
2		B14SER	NUM.	1	0	NONE	3.5501	0.8920	3.98
3		B30SER	NUM.	1	0	NONE	3.9726	0.8848	4.49
4		B51SER	NUM.	1	0	NONE	4.1118	0.9814	4.19
5		B51SER	DENM	1	1	NONE	.8552	.0705	12.13
6		B57SER	NUM.	1	0	NONE	3.8651	3.0433	3.73
7		B57SER	DENM	1	1	NONE	.7537	.8996	.84
8		B58SER	NUM.	1	0	NONE	3.4147	10.1718	.93
9		B58SER	DENM	1	1	NONE	.7206	1.0131	.71
5		B61SER	NUM.	1	0	NONE	-4.8208	0.8075	-5.97
6	PH1	CXOVDSSI	D-AR	1	1	NONE	.5990	.0555	10.78

TOTAL NUMBER OF OBSERVATIONS. 72
EFFECTIVE NUMBER OF OBSERVATIONS. 71
RESIDUAL STANDARD ERROR . . . . . .12837E+01

(b)

PARAMETER LABEL		VARIABLE NAME	NUM./ DENOM.	FACTOR	ORDER	CONS-TRAINT	VALUE	STD ERROR	T VALUE
1	CNST1		CNST	1	0	NONE	13.3987	0.3458	38.74
2		B34SER	NUM.	1	0	NONE	-1.2193	0.3859	-3.16
3	PHO	CTOVDSSO	D-AR	1	1	NONE	.7773	.0726	10.71

TOTAL NUMBER OF OBSERVATIONS. 72
EFFECTIVE NUMBER OF OBSERVATIONS. 71
RESIDUAL STANDARD ERROR . . . . . .131013E+01

The in-date and the out-date cycle time series are then given by equations 3.71 and 3.72, respectively,

$$Z_t = 13.4 + \frac{1}{(1-0.60B)}a_t \tag{3.71}$$

$$Z_t = 13.4 + \frac{1}{(1-0.78B)}a_t \tag{3.72}$$

As for the overall process, the model for the out-date cycle time was a quite correlated AR(1) process, ϕ_O=0.78. The in-date cycle time series did not contain as much correlation, ϕ_I=0.60. Also, both series had approximately the same estimated mean, $\mu_O=\mu_I$=13.4. Of note is the larger number of outliers detected when using the in-date time basis. This result seems to indicate that there are some significant masking effects in outlier detection when using the out-date time basis. The estimated ACF of the residuals, shown in Figure 3.18, confirm the adequacy of the above models, AR(1), to represent the cycle time data for the CMOS (1.08μm dlm).

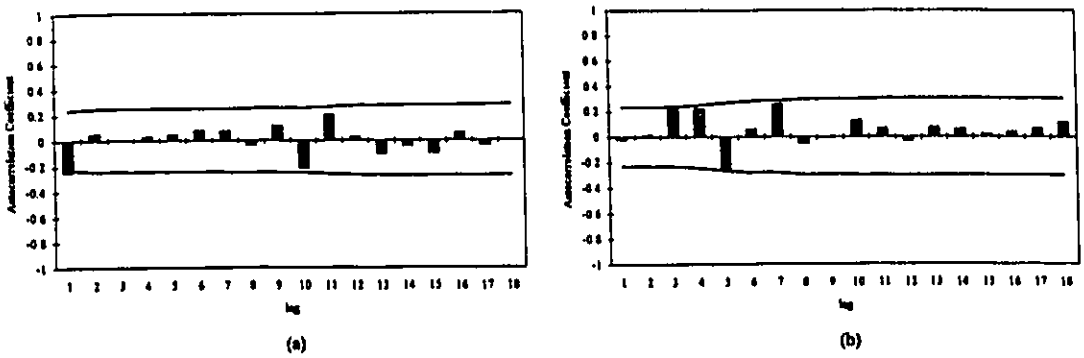

Figure 3.18 **Autocorrelation Function of the Cycle Time Residual Series from the Fitted AR(1) Model for the Overall Process Using the (a) In-date Time Basis (b) Out-date Time Basis**

The same three stage procedure was used to derive ARIMA models fitting the cycle time data for the three other technologies, which are shown in Appendix B. A summary of the resulting intervention models for each technology is displayed in Tables 3.12 and 3.13. The complete results for the identification, the joint detection-estimation and the diagnostic checking steps may be found in Appendix C. No significant difference was noticed between cycle time models using the in-date and the out-date time basis.

However, models for the individual process technologies were not as reliable as those derived for the overall process. The first reason is that the ARIMA models were constructed based on only 72 data points. Also, each data point which represents a weekly averaged, was not calculated using enough information. Moreover, there are many missing data which can significantly alter the estimates of the model parameters, especially when they occur in a sequence. Given that only 72 data points were available for modeling, missing observations can strongly bias model parameters and eventually give a non-adequate model form.

Table 3.12 **Summary of Cycle Time Models for the Four Technologies Using (a) In-date Time Basis (b) Out-date Time Basis**

a)

Process Technology CMOS	Fitted ARIMA Model	Residuals Standard Error
(1.5μm dlm)	$Z_t = 12.1 + \frac{(7.7)}{(1-0.81B)} P_t^{(38)} + \frac{1}{(1-0.54B)} a_t$	1.26
(1.2μm dlm)	$Z_t = 12.5 + (4.4) P_t^{(61)} + (-5.0) P_t^{(37)} + (-5.5) P_t^{(28)} + (6.5) P_t^{(39)} + \frac{1}{(1-0.48B)} a_t$	1.28
(1.08μm dlm)	$Z_t = 13.4 + (3.6) P_t^{(14)} + (4.0) P_t^{(38)} + \frac{(4.1)}{(1-B)} P_t^{(37)} + (-4.4) P_t^{(38)} + \frac{1}{(1-0.60B)} a_t$	1.28
(1.2μm tlm)	$Z_t = 15.0 + \frac{(-7.2)}{(1-0.81B)} P_t^{(25)} + (-5.1) P_t^{(30)} + (13.5) P_t^{(38)} + (4.4) P_t^{(66)} + \frac{1}{(1-0.64B)} a_t$	1.57

b)

Process Technology CMOS	Fitted ARIMA Model	Residuals Standard Error
(1.5μm dlm)	$Z_t = 11.9 + (-4.5) P_t^{(13)} + (-5.4) P_t^{(46)} + \frac{1}{(1-0.75B)} a_t$	1.19
(1.2μm dlm)	$Z_t = 11.9 + (-6.6) P_t^{(27)} + \frac{(4.0)}{(1-0.9B)} P_t^{(37)} + \frac{1}{(1-0.48B)} a_t$	1.29
(1.08μm dlm)	$Z_t = 13.4 + (-9.4) P_t^{(34)} + \frac{1}{(1-0.78B)} a_t$	1.31
(1.2μm tlm)	$Z_t = 14.6 + (-3.9) P_t^{(19)} + (-5.8) P_t^{(27)} + \frac{1}{(1-0.82B)} a_t$	1.59

Process Yield Data

Yields for the CMOS(1.08μm dlm) technology using the in-date and the out-date time basis are displayed in Figures 3.19 and 3.20, respectively. Plots of the yields for the other three technologies are given in Appendix B. The yield series shown below seem to contain a lot of noise. The ACFs and the PACFs, presented in Figures 3.21 and 3.22,

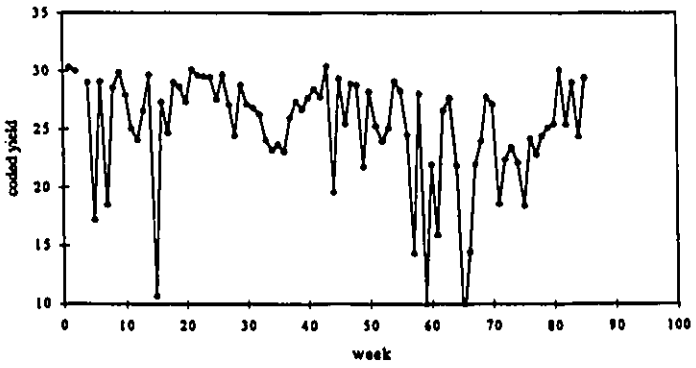

Figure 3.19 **Plot of the Coded In-date Yield for the CMOS (1.08μm dlm) Technology**

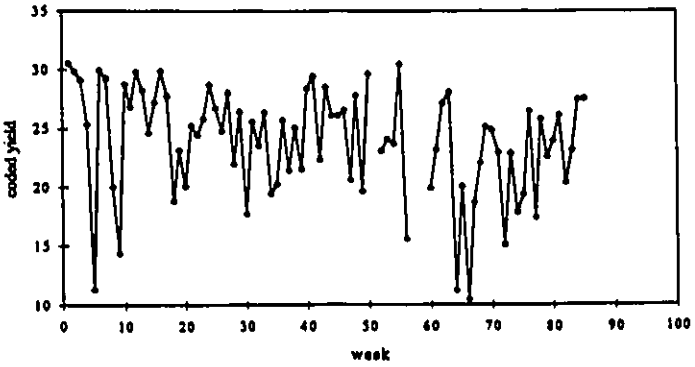

Figure 3.20 **Plot of the Coded Out-date Yield for the CMOS (1.08μm dlm) Technology**

show that autocorrelation and partial autocorrelation coefficients are generally not significant suggesting a white noise model to fit the yield data for the CMOS(1.08μm dlm)technology

$$Z_t = \mu + a_t \tag{3.73}$$

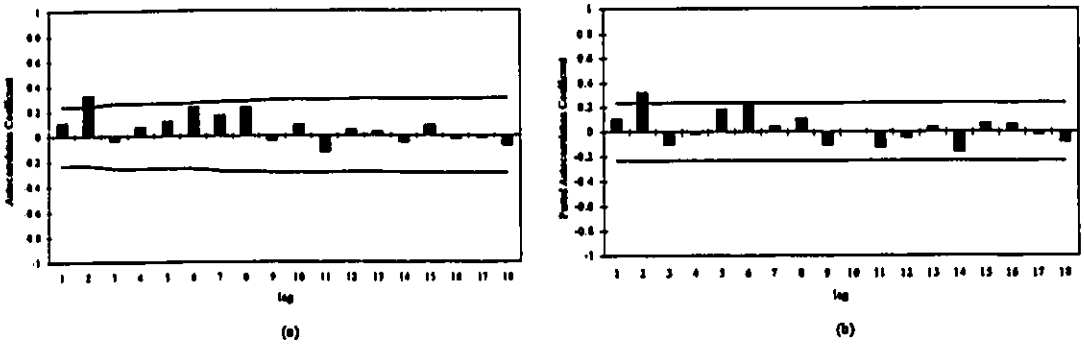

Figure 3.21 **Autocorrelation Function and Partial Autocorrelation Function of the In-date Yield for the CMOS (1.08μm dlm) Technology**

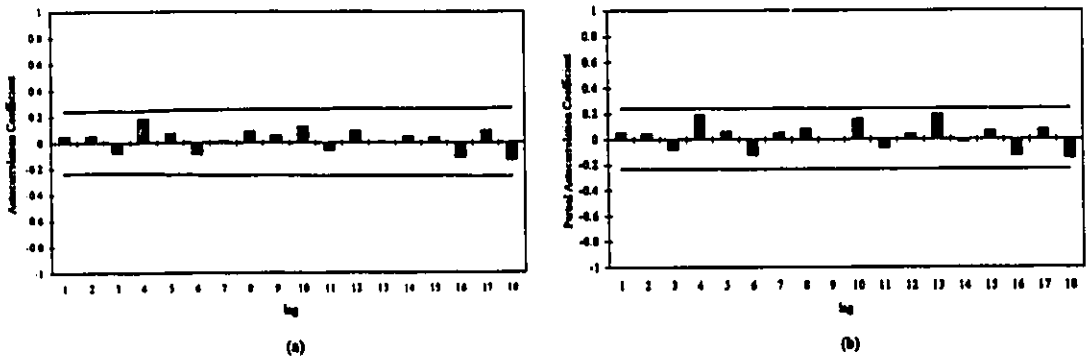

Figure 3.22 **Autocorrelation Function and Partial Autocorrelation Function of the Out-date Yield for the CMOS (1.08μm dlm) Technology**

Estimation results for this model are shown in Table 3.13. The ACF of the residuals, given in Figure 3.23, indicate that the fitted models accounted for all the inherent correlation that exist within the series, i.e. the autocorrelations are randomly distributed and not significant at about the 5% level.

Table 3.13 **ARIMA Joint Detection-Estimation Results for the Coded Yield for the CMOS (1.08μm dlm) Technology Using (a) In-date time basis (b) Out-date Time Basis**

(a)

PARAMETER LABEL	VARIABLE NAME	NUM./ DENOM.	FACTOR	ORDER	CONS-TRAINT	VALUE	STD ERROR	T VALUE
1		CNST	1	0	NONE	28.14	0.2918	96.47
2	B5SER	NUM.	1	0	NONE	-10.7250	1.6261	-6.60
3	B7SER	NUM.	1	0	NONE	-9.4220	1.6217	-5.81
4	B15SER	NUM.	1	0	NONE	-17.2760	1.6360	-10.56
5	B57SER	NUM.	1	0	NONE	-12.9460	1.7050	-7.59
6	B59SER	NUM.	1	0	NONE	-27.3348	1.6894	-16.18
7	B59SER	DENM	1	1	NONE	.9818	.1238	7.93
8	B60SER	NUM.	1	0	NONE	22.6197	4.9496	4.57
9	B60SER	DENM	1	1	NONE	1.0047	.1169	8.59
10	B65SER	NUM.	1	0	NONE	-18.4144	2.9245	-9.41
11	B65SER	DENM	1	1	NONE	.5858	.0854	6.86
12	B33SER	NUM.	1	0	NONE	-5.3976	1.2760	-4.23
13	B33SER	DENM	1	1	NONE	.7764	.0803	9.66
14	B44SER	NUM.	1	0	NONE	-7.9980	1.6256	-4.92
15	B49SER	NUM.	1	0	NONE	-4.1718	1.2758	-3.27
16	B49SER	DENM	1	1	NONE	.7889	.1038	7.60
17	B61SER	NUM.	1	0	NONE	-7.7615	1.8747	-4.14
18	B71SER	NUM.	1	0	NONE	-10.0615	2.5602	-3.93
19	B71SER	DENM	1	1	NONE	.7074	.2398	2.95

TOTAL NUMBER OF OBSERVATIONS. 72
EFFECTIVE NUMBER OF OBSERVATIONS. 72
RESIDUAL STANDARD ERROR . . . . . .18294E+01

(b)

PARAMETER LABEL	VARIABLE NAME	NUM./ DENOM.	FACTOR	ORDER	CONS-TRAINT	VALUE	STD ERROR	T VALUE
1		CNST	1	0	NONE	25.01	0.547	51.44
2	B5SER	NUM.	1	0	NONE	-13.8974	3.7811	-3.57
3	B64SER	NUM.	1	0	NONE	-12.2966	3.0590	-4.02
4	B64SER	DENM	1	1	NONE	.7934	.0823	9.64

TOTAL NUMBER OF OBSERVATIONS. 72
EFFECTIVE NUMBER OF OBSERVATIONS. 72
RESIDUAL STANDARD ERROR . . . . . .400475E+01

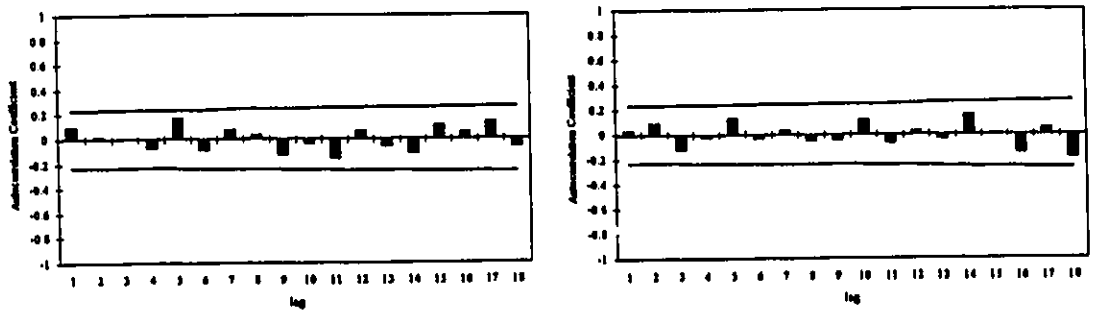

Figure 3.23 **Autocorrelation Function of the Yield Residuals from the Fitted White Noise Model for the CMOS(1.08μm dlm) Technology Using (a) In-date Time Basis (b) Out-date Time Basis**

A summary of the estimation results for all four process-technologies is presented in Table 3.14. As for the overall process, no correlation was found within the yield series. These results could indicate the presence of some large noise masking the inherent dynamics of the series. Also, infrequent sampling could cause the resulting process to approach a sequence of identically and independently distributed random variables, i.e. a white noise sequence.

Moreover, the in-date yield series always have a greater mean value than the out-date yield series. This is in accordance with the results found for the overall process. As discussed previously, the difference may be due to the fact that split lots are treated as independent entities in the out-date series. Those split lots are given the same weight as the normal lots. As a result, the mean of the out-date yield series are deflated.

The out-date yield models do not fit the data as well as the in-date yield models since the standard error of the residuals are larger for the out-date time basis case. As a matter of fact, out-date yield series seem to contain a lot more noise than in-date yield series. The large noise within those out-date series is masking the inherent dynamics of the process. Moreover, as shown in Table 3.14, many more outliers are detected when using the in-date time basis. There are some significant masking effects in outlier detection when using the out-date time basis.

One can also notice that most of the estimated outliers have a negative impact on the estimated means; usually an outlier results in a decrease of the observed yield values. As a result of the inadequacy of out-date yield models to detect outliers, the estimated mean is always smaller in the out-date yield series than in the in-date yield series. So, the presence of some very large noise within the out-date yield series is not only producing poorer ARIMA models but it is also underestimating the yield of the process.

Table 3.14 **Summary of Yield Models for the Four Technologies Using (a) In-date Time Basis (b) Out-date Time Basis**

a)

Process Technology CMOS	Fitted ARIMA Model	Residuals Standard Error
(1.5μm dlm)	$Z_t = 28.9 + \frac{(-9.7)}{(1-0.58B)} P_t^{(16)} + (9.1) P_t^{(30)} + a_t$	2.98
(1.2μm dlm)	$Z_t = 27.9 + \frac{(-6.1)}{(1-0.77B)} P_t^{(12)} + (-10.6) P_t^{(26)} + (-8.8) P_t^{(29)} + + \frac{(-13.0)}{(1-0.63B)} P_t^{(60)} + (8.5) P_t^{(62)} + a_t$	2.58
(1.08μm dlm)	$Z_t = 28.2 + (-10.7) P_t^{(3)} + (-9.4) P_t^{(7)} + (-17.3) P_t^{(13)} + (-12.9) P_t^{(37)} + + \frac{(-27.3)}{(1-B)} P_t^{(39)} + \frac{(22.6)}{(1-B)} P_t^{(39)} + \frac{(18.4)}{(1-0.59B)} P_t^{(42)} + + \frac{(-5.4)}{(1-0.78B)} P_t^{(33)} + (-8.0) P_t^{(44)} + \frac{(-4.2)}{(1-0.79B)} P_t^{(49)} + + (-7.8) P_t^{(61)} + \frac{(-10.6)}{(1-0.71B)} P_t^{(71)} + a_t$	1.83
(1.2μm tlm)	$Z_t = 27.0 + (-10.6) P_t^{(7)} + (-1.4) P_t^{(34)} + (-9.2) P_t^{(36)} + (-11.4) P_t^{(38)} + + (-8.0) P_t^{(60)} + a_t$	2.33

b)

Process Technology CMOS	ARIMA Model Fitting Available Yield Data	Residuals Standard Error
(1.5μm dlm)	$Z_t = 27.7 + (-17.2) P_t^{(13)} + (-15.7) P_t^{(25)} + (-14.0) P_t^{(46)} + a_t$	3.50
(1.2μm dlm)	$Z_t = 25.8 + (-16.0) P_t^{(23)} + a_t$	4.19
(1.08μm dlm)	$Z_t = 25.0 + (-13.9) P_t^{(5)} + \frac{(-12.3)}{(1-0.79B)} P_t^{(64)} + a_t$	4.00
(1.2μm tlm)	$Z_t = 24.2 + a_t$	4.67

3.3.3 Forecasting

Process Cycle Time Data

In the previous Section, univariate time series models were constructed to represent the cycle time and yield data. Modeling provided a better understanding of the process understudy. But the prime objective of this thesis was to obtain reliable forecasts using these models. The ultimate practical test of a model is its ability to forecast.

Recall that the in-date cycle time series for the overall process was found to inherently follow an AR(1) model

$$Z_t = 12.53 + 0.56 Z_{t-1} + a_t \tag{3.74}$$

From the above equation one can see that the one-step-ahead ARIMA forecast, $Z_t(l)=Z_{t+l}$, is given by,

$$\hat{Z}_{t+l} = 12.53 + 0.56 Z_t \tag{3.75}$$

Notice that since a_{t+l} is unknown when forecasting for time t+1, it is set equal to its expected value of zero. Forecasts for lead times l = 1, 2, 3, 4 and 5 from origin t = 72 appear in Table 3.15. The observed value for Z_{72} = 11.35.

Table 3.15 **Forecasts of the Coded In-date Cycle Time for the Overall Process for Lead Times l = 1, 2, 3, 4 and 5 from Origin t = 72**

TIME	FORECAST	STD. ERROR	ACTUAL IF KNOWN
73	11.89	0.8049	13.11
74	12.17	0.9233	15.52
75	12.39	0.9578	14.70
76	12.49	0.9683	17.90
77	12.53	0.9716	15.30

The forecasts are converging to the estimated mean, μ = 12.53. A model with AR terms tends to converge less rapidly to the estimated mean than a pure MA model (Pankratz, 1983). As discussed in Section 3.2.1, this is a characteristic particularity of stationary ARIMA models. How rapidly this convergence occurs depends on the form of the model. Also, the further into the future one forecasts, the more uncertain the forecasts become. This is indicated by the increasing standard error of the residuals at longer lead

times. Since the first forecast, $l = 1$, is the only forecast based solely on observed values, it is more accurate than the later forecasts. The forecast with lead time l=1 from origin t = 72, based on equation 3.74 is calculated from,

$$\hat{Z}_{73} = \hat{Z}_{72}(1) = (12.53)(1-0.56)+(0.56)(11.35) = 11.89 \qquad (3.76)$$

Substituting observed values for Z_{72} and Z_{73}, we get the forecast at lead time $l = 2$,

$$\hat{Z}_{74} = \hat{Z}_{73}(1) = (12.53)(1.056)+(0.56)(11.89) = 12.17 \qquad (3.77)$$

All other forecasts are entirely based on previous forecasts which increases the uncertainty associated with the predicted values. This illustrates why it is desirable to reestimate ARIMA models as new data become available. Figure 3.24 shows the forecasts along with 95% confidence intervals. The model gave very poor forecasts since the 95% confidence limits established around the forecast values do not contain any of the five observed values. However, the data seem to be drifting upward at approximately t = 74; a new outlier may have entered into the series.

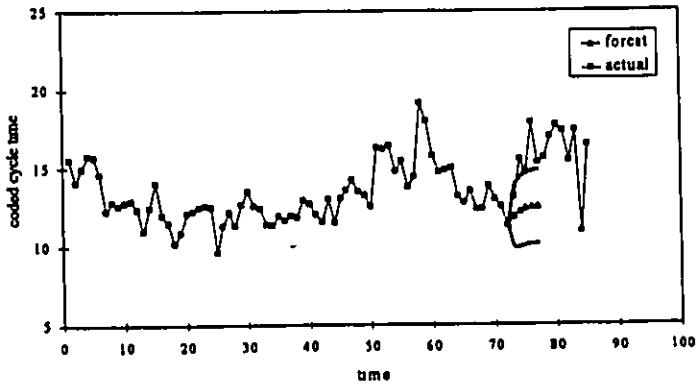

Figure 3.24 **Forecast Plot of the Coded In-date Cycle Time for the Overall Process for Lead Times l = 1, 2, 3, 4 and 5 from the Origin t = 72**

One can see the improvements in the forecasts by updating the series by a few observations and re-estimating the current model. Estimation results are tabulated below. Table 3.16 indicates the presence of two IO outliers at t = 74 and 76.

Table 3.16 ARIMA Joint Detection-Estimation Results for the Coded In-dateCycle Time for the Overall Process

	PARAMETER LABEL	VARIABLE NAME	NUM./ DENOM.	FACTOR	ORDER	CONS-TRAINT	VALUE	STD ERROR	T VALUE
1	CNST2		CNST	1	0	NONE	12.5800	.2477	50.77
2		B25SER	NUM.	1	0	NONE	-2.6950	0.7245	-3.62
3	PH2	B25SER	DENM	1	1	EQ 01	.5443	.0707	7.70
4		B51SER	NUM.	1	0	NONE	4.1309	0.8001	5.16
5		B51SER	DENM	1	1	NONE	.8664	.0648	13.36
6		B58SER	NUM.	1	0	NONE	5.2060	0.8779	5.93
7		B58SER	DENM	1	1	NONE	.6964	.1213	5.74
8		B74SER	NUM.	1	0	NONE	2.7899	0.8637	3.23
***	PH2	B74SER	DENM	1	1	EQ 01	.5443	.0707	7.70
9		B76SER	NUM.	1	0	NONE	4.3301	0.8490	5.10
***	PH2	B76SER	DENM	1	1	EQ 01	.5443	.0707	7.70
***	PH2	CXOVALI	D-AR	1	1	EQ 01	.5443	.0707	7.70

TOTAL NUMBER OF OBSERVATIONS. 77
EFFECTIVE NUMBER OF OBSERVATIONS. 76
RESIDUAL STANDARD ERROR . . . . . .991711E+00

Since outliers are by definition unexpected, the presence of two outliers very soon after the forecast origin, t = 72, could not be taken into account when forecasting. This explains the very poor forecasting performance of the model. Based on the above model, forecasts at lead time l = 1, 2, 3, 4 and 5 are calculated and plotted along with 95% confidence intervals, as shown in Figure 3.25. The same performance is obtained when starting to forecast from origin t = 77. The forecasts converge very rapidly towards the estimated mean, giving very poor predictions.

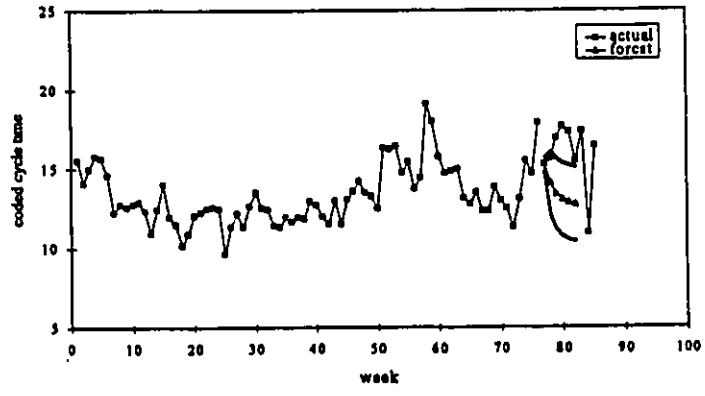

Figure 3.25 Forecast Plot of the Coded In-date Cycle Time for the Overall Process for Lead Times l = 1, 2, 3, 4 from the Origin t = 77

However, as discussed by Pankratz (1991), ARIMA models are especially suited for short term forecasting. They are the optimal univariate models, i.e. models that generate the minimum mean squared error forecasts. So the very poor forecasting performance of the model is due to two factors: the presence of unexpected events (outliers) and the "natural" inadequacy of ARIMA models for long-term forecasts.

Table 3.17 and Figure 3.26 show one-step-ahead forecasts of the in-date cycle time data for the overall process. In this case, the ARIMA model is updated as new data becomes available. This means repeating the three stage modeling procedure each time. The one-step-ahead forecasts seem quite satisfactory. The above results confirm the adequacy of the constructed ARIMA models for short term forecasting.

Table 3.17 One-step-ahead Forecasts of the Coded In-date Cycle Time for the Overall Process Starting from Origin $t = 72$

TIME	FORECAST	STD. ERROR	ACTUAL IF KNOWN
73	11.89	1.0043	13.11
74	12.91	1.0043	15.52
75	14.25	1.0043	14.70
76	13.77	1.0056	17.90
77	15.50	1.0056	15.30
78	14.09	0.9917	15.61
79	15.66	0.9891	16.96
80	16.66	1.0198	17.69
81	17.04	1.0198	17.32
82	16.98	1.0170	15.45
83	15.98	1.0170	17.37
84	17.00	1.0170	10.93
85	13.56	1.0170	16.43

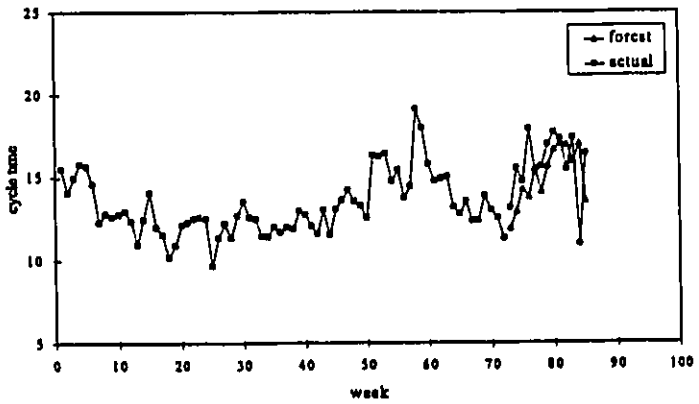

Figure 3.26 One-step-ahead Forecasts of the Coded In-date Cycle Time Series for the Overall Process Starting from Origin $t = 72$.

Considering the out-date cycle time data, forecasts for lead times l = 1, 2, 3, 4 and 5 from origin t = 72 are displayed in Table 3.18 and in Figure 3.27. The 95% confidence limits seem to contain all five forecasts. From Figure 3.27, one may think that the out-date cycle time model was accurate in calculating forecasts.

Table 3.18 Forecasts of the Coded Out-date Cycle Time at Lead Times l = 1, 2, 3, 4 and 5 from Origin t = 72 for the Overall Process

TIME	FORECAST	STD. ERROR	ACTUAL IF KNOWN
73	13.78	0.9920	14.29
74	13.67	1.2430	15.08
75	13.57	1.3950	15.87
76	13.49	1.4950	16.28
77	13.42	1.5640	13.80

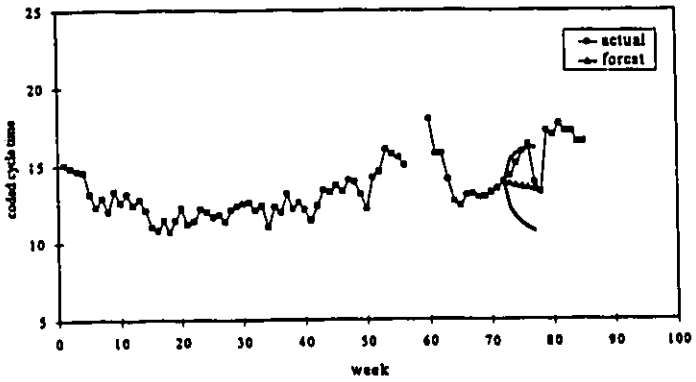

Figure 3.27 Forecast Plot of the Coded Out-date Cycle Time for the Overall Process for Lead Times l = 1, 2, 3, 4 and 5 from Origin t = 72

However, comparing Table 3.18 to Table 3.15, one can see that the out-date cycle time forecasts have a larger standard error than the in-date cycle time forecasts. The only conclusion that can be drawn from those results, is that the in-date cycle time model produces more precise forecasts than the out-date cycle time model. The one-step ahead out-date cycle time forecasts were quite satisfactory, as shown in Figure 3.28. This confirms the adequacy of the ARIMA models for short-term forecasting.

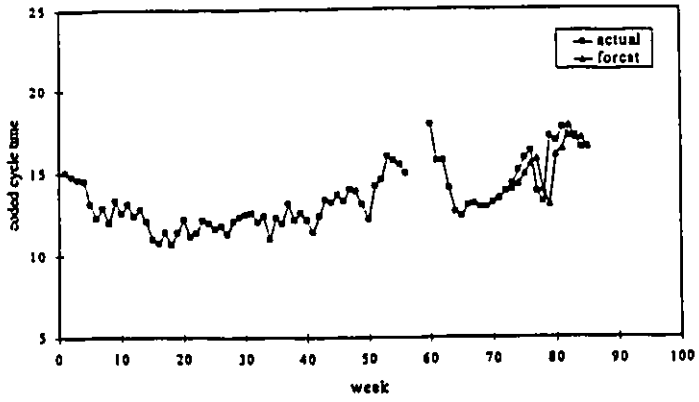

Figure 3.28 **One-step-ahead Forecasts of the Coded Out-date Cycle Time for the Overall Process Starting from Origin $t = 72$**

The same procedure was used to calculate in-date and out-date cycle time forecasts for each of the four technologies. The same trend as for the overall process was found, i.e. long-term forecasts were poor whereas short-term forecasts were quite satisfactory. Figures 3.29 to 3.32 illustrate the case of the CMOS (1.08μm dlm) technology. However, complete results for the three other technologies are presented in Appendix C.

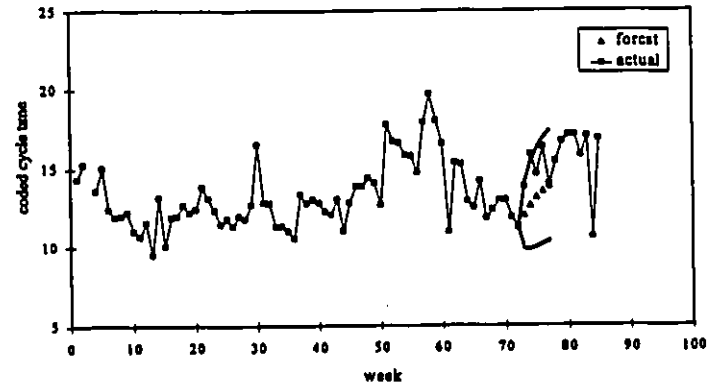

Figure 3.29 **Forecast Plot of the Coded In-date Cycle Time for the CMOS(1.08μm dlm) Technology for Lead Times $l = 1, 2, 3, 4$ and 5 from Origin $t = 72$**

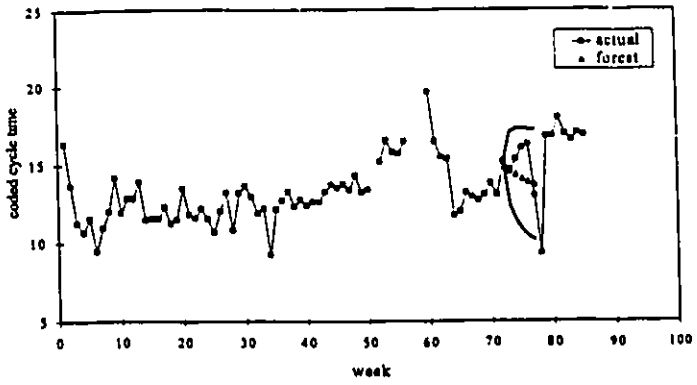

Figure 3.30 Forecast Plot of the Coded Out-date Cycle Time for the CMOS(1.08μm dlm) Technology for Lead Times $l = 1, 2, 3, 4$ and 5 from Origin $t = 72$

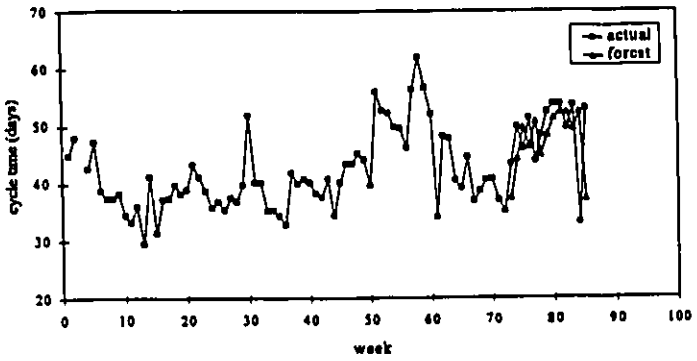

Figure 3.31 One-step-ahead Forecasts of the Coded In-date Cycle Time for the CMOS (1.08μm dlm) Technology from Origin $t = 72$

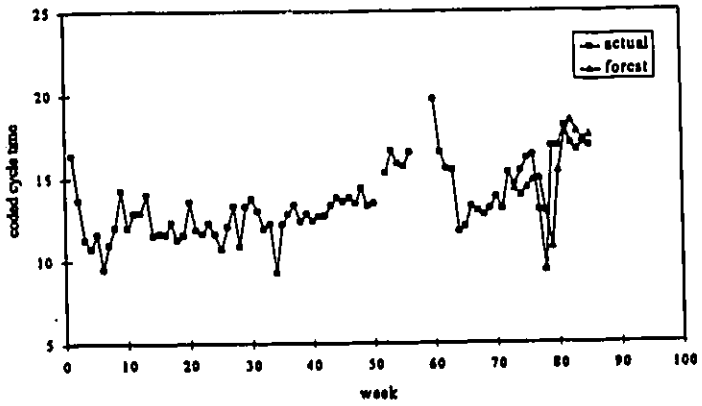

Figure 3.32 One-step-ahead Forecasts of the Coded Out-date Cycle Time for the CMOS (1.08μm dlm) Technology from Origin $t = 72$

In summary, while the fitted ARIMA models produced quite satisfactory one-step-ahead forecasts, the long-term forecasts were very poor. Two factors may explain this result. First, ARIMA models are not recommended for long-term forecasts because the forecasts converge very rapidly to the estimated mean of the series. Second, the process under study was frequently subjected to significant outliers. This is not surprising since, as discussed in Chapter 2, the process is continuously evolving and is also often affected by external events, such as, shift changes, pieces of equipment going down, power failures, etc.

Process Yield Data

Recall from Section 3.3, that the process yields follow a white noise process, i.e. the in-date and out-date yield data are randomly distributed around a constant mean,

$$Z_t = \mu + a_t \tag{3.78}$$

From the above equation, one can see that the forecasts at any lead time, l, from any origin, t, is equal to the estimated mean of the series,

$$\hat{Z}_t(l) = \hat{\mu} \tag{3.79}$$

Forecast results for the overall yield series are presented in Figures 3.33 and 3.34. As expected, the forecasts for lead times l = 1, 2, 3, 4 and 5 from origin t = 72 are constant.

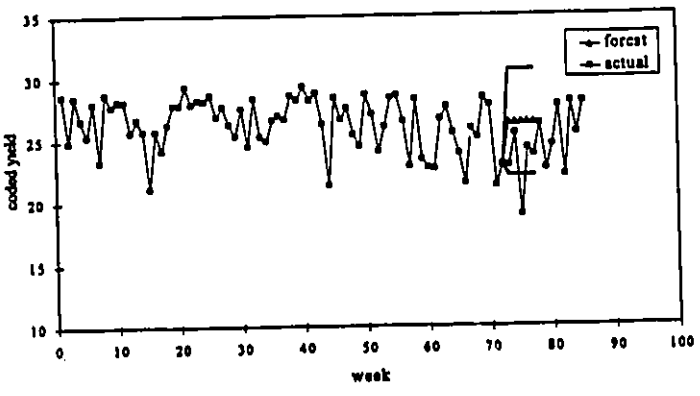

Figure 3.33 **Forecast Plot of the Coded In-date Yield for the CMOS(1.08μm dlm) Technology for Lead Times l = 1, 2, 3, 4 and 5 from Origin t = 72**

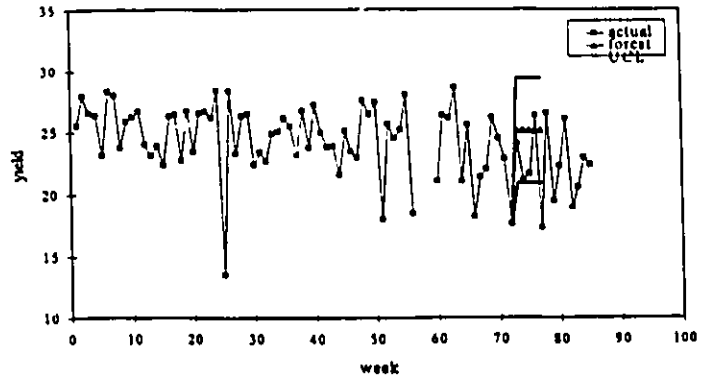

Figure 3.34 **Forecast Plot of the Coded Out-date Yield for the CMOS(1.08μm dlm) Technology for Lead Times l = 1, 2, 3, 4 and 5 from Origin t = 72**

Apparently the use of ARIMA models did not improve the current non formal forecasting method used by the engineers at Northern Telecom. The method consists of taking previous month yield average as next week forecast. Since this technique is based on only five observations, as opposed to the whole series when ARIMA forecasts are used, the precision of the estimate should be better now.

Furthermore, some benefits are gained from the above ARIMA forecasts when an outlier enters into the series. If the outlier is identified soon enough, the forecasts could be highly improved by adjusting the forecasting model. Given that the process under study is frequently subjected to significant outliers, ARIMA models should be used in the forecasting procedure. This case is illustrated in Table 3.19 and Figure 3.34, where the one-step-ahead forecast for the in-date yield has actually changed from time t = 73 to t = 75. Since the change was caused by an TC outlier, the one-step-ahead forecasts converged quite rapidly to the estimated mean of the series, as shown in Table 3.19. Figure 3.34 does not show very well the change on the value of the forecasts, because the outlier did not have a large effect on the mean of the series.

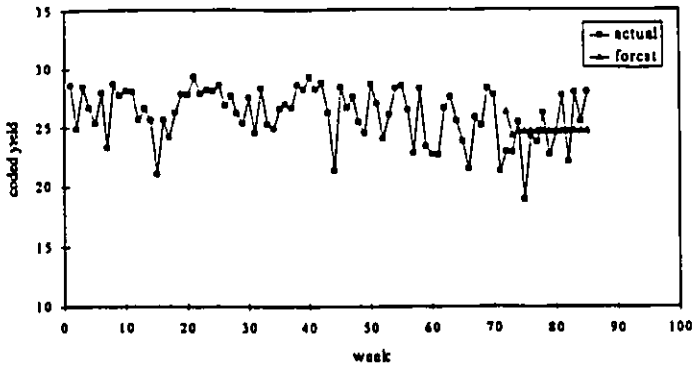

Figure 3.35 **One-step-ahead Forecasts of the Coded Out-date Cycle Time for the CMOS (1.08μm dlm) Technology from Origin $t = 72$**

Table 3.19 **One-step-ahead Forecasts of the Coed In-date Yield for the CMOS(1.08μm dlm) Technology from Origin $t = 72$**

TIME	FORECAST	STD. ERROR	ACTUAL IF KNOWN
73	23.96	2.1331	22.87
74	22.14	2.0048	25.43
75	22.47	1.7484	18.92
76	22.47	1.7380	24.27
77	22.47	1.7380	23.77
78	22.47	1.7380	26.21
79	22.47	1.7380	22.65
80	22.47	1.7380	24.51
81	22.47	1.7380	27.70
82	22.47	1.7380	22.06
83	22.47	1.7380	27.97
84	22.47	1.7380	25.50
85	22.47	1.7380	27.99

3.4 Conclusions and Recommendations

3.4.1 Conclusions

1. Cycle times were found to follow an AR(1) model for the overall process as well as for the different technologies. This result suggests that an observation at time $t = T$ is directly dependent on the previous observation at time $t = T-1$.

2. Yields were found to follow a white noise process. However, this does not ensure that the inherent yield process does not have any dynamics. Two reasons could explain this estimated white noise behavior:
    - large noise within the process could be masking the dynamics of the series;
    - infrequent sampling could make the observed yield approach a white noise process.
3. In general, the in-date time basis gave better results than the out-date time basis. Out-date cycle times and yields were underestimated. ARIMA models fitted the in-date data much better than the out-date data. Out-date cycle times were more highly correlated. Many more outliers were detected using the in-date time basis. This suggests the presence of some masking effects in outlier detection when the out-date time basis is used.
4. Joint estimation of outliers and model parameters was essential in this work since outliers were found to significantly alter model parameters. For cycle time data, outliers inflated the ϕ term in the AR(1) model suggesting a more highly correlated process. Intervention models that corrected for the outlier effects fitted the data much better than the traditional ARIMA models.

3.4.2 Recommendations

1. More data should be collected to increase the precision in the estimated model parameters and the sensitivity to outlier detection.
2. In order to check if the yields follow a white noise process two things should be done
    - data should be collected more frequently;
    - noise should be minimized.

Chapter Four

FORECASTING CYCLE TIMES AND YIELDS WITH TRANSFER FUNCTION MODELS

4.1 Introduction

Forecasts using ARIMA models are said to be optimal forecasts, that is, no other forecasts produced from a single time series have a smaller mean squared forecast error. The models of cycle times and yields developed in Chapter 3 provided one-step-ahead cycle time and yield forecasts. However, the long-term ARIMA forecasts were not very reliable. This is a characteristic of ARIMA whose forecasts become equal to the mean of the series within a short lead time. Moreover, the process under study was frequently subjected to significant outliers giving very poor long-term terms forecasts.

One approach to improving these forecasts is to use information from other process variables as predictors of the yields and cycle times for different stages in fabrication. The new model involves the sum of a deterministic transfer function model

describing how the predictors affect the cycle times and the yields and a stochastic noise model. The objective of this stage of the work was to develop transfer function models to improve the forecasts of yields and cycle times.

Basic background and a review of literature pertaining to the development of transfer function models is presented in Section 4.2. Results and discussion of this model building exercise and an evaluation of their effectiveness are then given.

4.2 Background and Literature Survey

4.2.1 Introduction

One way of relating a response variable to one or more explanatory variables is through linear regression models,

$$Y_t = \beta_0 + \beta_1 X_{t1} + \beta_2 X_{t2} + \ldots + \beta_m X_{tm} \qquad (4.1)$$

However, these models are very deficient when observations are serially correlated (Pankratz, 1991).

In such cases, it is possible to relate the response of one series to its own past values, and also to the past and present values of other time series. In this way, the basic concepts of regression models are combined with that of ARIMA models to give a family of statistical models called transfer function (TF) models. A transfer function model describes how a response (output) variable, Y_t, is linearly related to current and past values of one or more explanatory (input) variable, $X_{1t}, X_{2t}, \ldots, X_{mt}$. Assuming that the input and output variables are both stationary time series, the general form of the single-input, single-output transfer function can be expressed as

$$Y_t = C + \upsilon_1(B) X_{t1} + N_t \qquad (4.2)$$

where N_t represents the noise in the process and follows an ARIMA model

$$N_t = \frac{\theta(B)}{\phi(B)} a_t \tag{4.3}$$

and the linear operator

$$\upsilon(B) = \upsilon_0 + \upsilon_1 B + \upsilon_2 B^2 + \ldots \tag{4.4}$$

is the transfer function or impulse response function relating X_t to Y. The individual weights $\upsilon_0, \upsilon_1, \upsilon_2 \ldots$ are either called the impulse response weights or the transfer function weights. The linear operator $\upsilon(B)$ shows how Y_t responds through time to a given change in X_t; υ_1 states how Y_t reacts to a change in X_{t-1}; and more generally, υ_m states how Y_t reacts to a change in X_{t-m} (Hudak and Liu, 1992). The linear operator $\upsilon(B)$ can also be represented in terms of the operator polynomials $\omega(B)$ and $\delta(B)$,

$$\begin{aligned} \omega(B) &= \omega_0 + \omega_1 B + \ldots + \omega_s B^s \\ \delta(B) &= 1 - \delta_1 B - \ldots - \delta_r B^r \end{aligned} \tag{4.5}$$

The parameters of the numerator polynomial, $\omega(B)$, describe the initial effects of the input whereas the denominator polynomial, $\delta(B)$, characterizes the decay pattern of initial effects in the response. These operators are related to the linear operator, $\upsilon(B)$, according to

$$\upsilon(B) = \frac{\omega(B) B^b}{\delta(B)} \tag{4.6}$$

where b denotes the number of sampling periods of delay or dead time. Usually, the number of terms in $\omega(B)$ and $\delta(B)$ is small. If $\delta(B) = 1$, then $\upsilon(B) = \omega(B)$ and $\upsilon(B)$ has a finite number of terms. If $\delta(B) \neq 1$, then $\upsilon(B)$ has an infinite number of terms. Since the transfer function is assumed to be stable, the coefficients $\upsilon_0, \upsilon_1, \upsilon_2 \ldots$ diminish to zero regardless of the order of the $\delta(B)$ polynomial. The transfer function model may then be expressed in its rational form as

$$Y_t = C + \frac{\omega(B)B^b}{\delta(B)} X_t + N_t \tag{4.7}$$

Such a model assumes that the input series X_t does not respond in any way to changes in the output series Y_t. That is the relationship between the input series and the output series is unidirectional.

Pankratz (1991) defines the steady-state gain of the transfer function, g, as the *full (equilibrium) change over time* in Y_t in response to a unit change in X_t. It is represented by the sum of all impulse response weights,

$$g = \upsilon_0 + \upsilon_1 + \upsilon_2 + \ldots \tag{4.8}$$

or equivalently,

$$g = \frac{\omega_0 + \omega_1 + \ldots + \omega_s}{1 - \delta_1 - \delta_2 - \ldots - \delta_r} \tag{4.9}$$

We see that g is finite, and the transfer function is stable, only if the series $\upsilon_0 + \upsilon_1 + \upsilon_2 + \ldots$ converges.

The single-input transfer function model given by equation 4.7 can be easily extended to its multiple-input form,

$$Y_t = C + \frac{\omega_1(B)B^b}{\delta_1(B)} X_{1t} + \frac{\omega_2(B)B^b}{\delta_2(B)} X_{2t} + \ldots + \frac{\omega_m(B)B^b}{\delta_m(B)} X_{mt} + N_t \tag{4.10}$$

However, for purposes of simplicity, only the single-input modeling is presented in what follows.

A transfer function model consists of two main parts: a deterministic and a stochastic part. The deterministic part is a set of transfer functions with their associated input series whereas the disturbance series represents the stochastic part. The objective is then to find parsimonious models for these two parts based on the available data. As in the case of ARIMA modeling, there are three stages for transfer function modeling: identification, estimation and diagnostic checking.

As a preliminary analysis in transfer function modeling, it is good practice to build ARIMA models for both the output and the input series (Pankratz, 1991). ARIMA forecasts of the inputs may be necessary to generate transfer function forecasts of the output, while ARIMA forecasts of the output series may provide a basis for assessing output forecasts from transfer function models. In general, such separate ARIMA models may provide useful modeling information.

4.2.2 Identification

The identification stage of transfer function modeling involves three main parts (Hudak and Liu, 1988):

- the estimation of a set of transfer function weights;
- the determination of the form of the ARIMA model for the disturbance, N_t;
- the determination of the form of a rational polynomial to represent the estimated transfer function weights if these weights display a 'die-out pattern' (i.e., they diminish to zero)..

Traditionally, the cross correlation function (CCF) method, introduced by Box and Jenkins (1976), has been used for such a purpose. In this method, tentative orders for $v(B)$ and $\delta(B)$ are obtained by analyzing the sample cross correlation function between residuals of an ARMA model of the input series, and a series obtained by filtering (prewhitening) the output series by the same ARMA model. The model given by equation 4.10 is estimated with $N_t = a_t$ and residuals from this fit are used to model N_t. However, the CCF method does not easily handle multiple inputs. Moreover, Box and Jenkins give a detailed discussion of the CCF only for single-input transfer function modeling.

Another identification method is the linear transfer function approach (LTF), first introduced by Liu and Hanssens (1982). This method is detailed in Liu et. al. (1986), Liu and Hudak (1985), Liu (1986, 1987), and Pankratz (1991). The LTF method is a

practical and simple model identification procedure and it can handle multiple inputs with relative ease.

The first step of the LTF identification method consists of an initial estimation of a preliminary linear transfer function model of the form

$$Y_t = C + (v_0 + v_1 B + v_2 B^2 + \ldots + v_k B^k) X_t + N_t \tag{4.11}$$

by judiciously specifying the maximum number of lags, k, and a proxy for the disturbance, N_t. The number of lags, k, should be sufficiently large to take into account the longest lagged-time response. The choice of the initial number of significant transfer function weights is a potential weakness of the LTF method, since these weights are often chosen arbitrarily. Ideally, its choice is based on some physical understanding of the process under study.

Another key element in the LTF approach is the choice of the proxy used for the disturbance term. Contrary to the CCF method, the disturbance N_t is not approximated by the white noise series, a_t, which should provide more efficient estimates of the transfer function (TF) weights. For non-seasonal time series, the disturbance is best approximated by an AR(1) process:

$$N_t = \frac{1}{1 - \phi B} a_t \tag{4.12}$$

This approximation procedure suggested by Liu (1986) is related to the common filter approach of Liu and Hanssens (1982). The approximation is useful since

- it is correct if the disturbance is really AR(1);
- it is a good approximation if the disturbance is pure MA;
- it provides an indication of differencing if $\phi \approx 1$ or if the ACF of N_t decays slowly to zero;
- it validates a white noise representation for N_t if $\phi \approx 0$.

In the second step, the TF weights given by equation 4.11 are evaluated and the estimated disturbance series is checked to discover any gross errors in the model, such as

nonstationarity. In such a case, both the output and the input series are differenced to induce stationarity. Then steps 1 and 2 are repeated until a stationary disturbance is obtained, by successive differencing.

Once a stationary disturbance is achieved, the most recent set of estimated TF weights are examined to tentatively identify a rational form for the transfer function model, $\omega(B)B^b/\delta(B)$ to represent $\upsilon(B)$. Often, a visual comparison of the estimated TF weights with some theoretical impulse response weight functions is sufficient to determine some reasonable values for the orders r, s and b of the rational transfer function form. Usually, the polynomial numerator $\omega(B)$ only involves a few number of terms and the order of the denominator polynomial $\delta(B)$ is either $r = 0$ or $r = 1$. Such patterns are relatively easy to identify visually by inspecting the TF weights. However, it is sometimes difficult to distinguish a pattern in these impulse response weights. In such cases, the Corner method proposed by Liu and Hanssens (1982) can be used to determine the orders in a corresponding rational transfer function, $\omega(B)B^b/\delta(B)$. The method employs a Corner table which consists of determinants of matrices, $C(f,g)$, composed of the TF weights υ,

$$C(f,g) = \begin{vmatrix} \upsilon_f & \upsilon_{f-1} & \cdots\cdots & \upsilon_{f-g+1} \\ \upsilon_{f+g-1} & \upsilon_f & \cdots\cdots & \upsilon_{f-g+2} \\ \upsilon_{f+g-1} & \upsilon_{f+g-2} & \cdots\cdots & \upsilon_f \end{vmatrix} \qquad (4.13)$$

where f refers to rows ($f = 0, 1, 2,...$) and g refers to columns ($g = 1, 2, 3,...$). If the orders associated with $\omega(B)$ and $\delta(B)$ are b, s and r, then the corner table has the pattern shown in Table 4.1. The symbol 'o' indicates a value not significantly different from 0, while the symbol 'x' indicates a value that is significantly different from 0. Note that in the table shown below, the elements in the first b rows and in the lower right-hand corner beginning at the row labeled $s+b$ and column $r+1$ are all zeros. Although, a clear cut pattern may be difficult to distinguish from the corner table, it still provides some good

estimates for b, s and r. In such cases, the principal of parsimony should always be favored.

Table 4.1. Corner Table

4.2.3 Estimation

Once a transfer function model is identified, the next stage of the modeling strategy is to estimate the parameters of the identified TF model using the available data. There are a variety of estimation methods that give approximate maximum likelihood (ML) estimates. Approximate ML estimates are based on the conditional likelihood function (Box and Jenkins, 1976). This involves choosing coefficients that minimize the sum of squared residuals (Σa_t^2). Hillmer and Tiao (1979) suggested a more exact approximation to ML estimates. This method generates better estimates of MA coefficients (only) but is more computing intensive.

In the first step, using the initial coefficient values estimated in the LTF identification method, the following series is computed,

$$\hat{Y}_t = C + (v_0 + v_1 B + v_2 B^2 + \ldots + v_k B^k) X_t \qquad (4.14)$$

In step 2, estimates of the stationary disturbance series are computed using

$$\hat{N}_t = Y_t - \hat{Y}_t \tag{4.15}$$

Then the residual series are recursively computed by

$$\hat{a}_t = \theta_1 a_{t-1} + \cdots + \theta_q a_{t-q} + N_t - \phi_1 N_{t-1} - \cdots - \phi_p N_{t-p} \tag{4.16}$$

As discussed in Section 3.2.2, for stochastic model estimation, the effects of transients can be minimized if the difference equations are started off from a value of t for which all previous X's (X^*), Y's (Y^*), N's (N^*) and a's (a^*) are known. From equation 4.14, $t = k + p$. If starting values of the a's are set equal to their expected values of zero, the conditional sum of squares function is

$$S^*(\nu,\phi,\theta) = \sum_{k+p}^{n} \hat{a}_t^2\left(\nu,\phi,\theta \middle| X^*,Y^*,N^*,a^*\right) \tag{4.17}$$

where n is the last time period for which data are available. Then a nonlinear least-squares routine, such as the Gauss-Marquardt method (1963), is used to obtain coefficients for the TF parameters. Then, using the new transfer function outputs, the above steps are repeated until a set of transfer function parameters minimizes the sum of squared residuals (SSR) value. This minimal value will give the optimal estimates for the linear TF model.

As for ARIMA models, the outlier detection procedure (Chen and Liu, 1993) may be combined with the above estimation procedure to give a joint detection-estimation procedure of outlier effects and model parameters. The transfer function models include then detected outliers as intervention components.

4.2.4 Diagnostic Check.

Once a TF model is identified and its parameters are estimated, the next stage is to perform a check adequacy of the TF model for lack of fit and to reformulate (or re-identify) it if necessary. As for ARIMA models, model inadequacy can usually be detected

by examining the autocorrelation function (ACF) of the residuals. In practice, the residual ACF is the main tool used at the checking stage. The transfer function model is adequate when the residuals are insignificant and randomly distributed (i.e., white noise). If this is not the case, the CCF tool is used to suggest the type of modification needed.

An important assumption in a TF model is that the (stationary) input series X_t is independent of the disturbance series, N_t. The CCF between such a series and a_t should have no significant values. The residual CCF gives the relationship between the residuals from the TF model $\{a_t\}$ and the residuals of the ARIMA model of an input series X_t. If the model is adequate there should be no cross correlations between these two series, especially at low lags.

4.2.5 Forecasting

Frequently, forecasts of a time series Y_t, Y_{t-1},..., may be considerably improved by using information coming from some associated series X_t, X_{t-1},.... A transfer function model relating these two series is then built up, using the procedure just described,

$$Y_t = \frac{\omega(B)B^b}{\delta(B)}X_t + \frac{\phi(B)}{\nabla^d\theta(B)}a_t \tag{4.18}$$

The above equation is multiplied through by $\delta(B)\nabla^d\theta(B)$ to give

$$\delta(B)\nabla^d\phi(B)Y_t = \nabla^d\phi(B)\omega(B)X_{t-b} + \delta(B)\theta(B)a_t \tag{4.19}$$

or equivalently,

$$\delta^*(B)Y_t = \omega^*(B) + \theta^*(B)a_t \tag{4.20}$$

where

$$\begin{aligned}\delta^*(B) &= 1-\delta^*_1B-\ldots-\delta^*_{p+d+r}B^{p+d+r}\\ \omega^*(B) &= \omega^*_0+\omega^*_1B+\ldots+\omega^*_{p+d+s}B^{p+d+s}\\ \theta^*(B) &= 1-\theta^*_1B-\ldots-\theta^*_{q+r}B^{q+r}\end{aligned} \tag{4.21}$$

Optimal forecasts, $\hat{Y}_t(l)$, that minimize the mean square forecast errors, are generated by taking the conditional expectation of Y_{t+l} at time t,

$$\begin{aligned}\hat{Y}_t(l) = E[Y_{t+l}] = \delta^*_1 E[Y_{t+l-1}] + \ldots + \delta^*_{p^*+r} E[Y_{t+l-p^*-r}] \\ + \omega^*_0 E[X_{t+l-b}] - \ldots - \omega^*_{p^*+s} E[X_{t+l-b-p^*-s}] \\ + E[a_{t+l}] - \theta^*_1 E[a_t] - \ldots - \theta^*_{q+r} E[a_{t+l-q-r}]\end{aligned} \tag{4.22}$$

where

$$\begin{aligned}E[Y_{t+l}] &= \begin{cases} Y_{t+l} & l \le 0 \\ \hat{Y}_t(l) & l > 0 \end{cases} \\ E[X_{t+l}] &= \begin{cases} X_{t+l} & l \le 0 \\ \hat{X}_t(l) & l > 0 \end{cases} \\ E[a_{t+l}] &= \begin{cases} a_{t+l} & l \le 0 \\ 0 & l > 0 \end{cases}\end{aligned} \tag{4.23}$$

For dead time, $b<1$, the value of $\hat{a}_t$ is obtained utilizing the usual ARIMA model given by equation 4.3, or if $b \ge 1$, from

$$\hat{a}_t = Y_t - \hat{Y}_{t-1}(1) \tag{4.24}$$

The forecasts $\hat{X}_t(l)$ are also obtained in the usual way, as discussed in Section 3.2.2, by taking the conditional expectations on the ARIMA model represented by equation 3.30.

Equation 4.18 may rewritten in the form

$$Y_t = \nu(B) X_t + \psi(B) a_t \tag{4.25}$$

where

$$\begin{aligned}\nu(B) &= \frac{\omega(B) B^b}{\delta(B)} \\ \psi(B) &= \frac{\phi(B)}{\nabla^d \theta(B)}\end{aligned} \tag{4.26}$$

Assume that an adequate model for the leading series is

$$X_t = \frac{\phi_x(B)}{\nabla^{d_x} \theta_x(B)} \alpha_t \tag{4.27}$$

where α_t is the residual series. Now equation 4.25 may be written

$$Y_t = \vartheta(B)\alpha_t + \psi(B)a_t \tag{4.28}$$

where

$$\vartheta(B) = \frac{\phi_x(B)}{\nabla^{d_x}\theta_x(B)}\nu(B) \tag{4.29}$$

The forecast $\hat{Y}_t(l)$ of Y_{t+l} made at origin t is then of the form

$$\hat{Y}_t(l) = \sum_{j=0}^{l-1} \vartheta_j X_{t+l-j} + \psi_j a_{t+l-j} \tag{4.30}$$

where a_t are the residuals from the noise series, N_t, and α_t are the residuals from the input series, X_t. The variance of the lead-l forecast error is then given by

$$V(l) = E[Y_{t+l} - \hat{Y}_t(l)]^2 = \sigma_a^2 \sum_{j=b}^{l-1} \vartheta_j^2 + \sigma_a^2 \sum_{j=0}^{l-1} \psi_j^2 \tag{4.31}$$

4.3 Results and Discussion

In Chapter 3, univariate models were built to forecast cycle time and yield data. While the one-step-ahead forecasts were satisfactory, the longer term forecasts were quite poor. In this Section the use of transfer function models to improve longer-term forecasts is presented.

4.3.1 Process Cycle Time Models

Modeling

As discussed in Chapter 2, each process technology consists of eight main procedures: Well Formation, Device Isolation, Gate Formation, Capacitor Formation, Source/Drain Formation, First Metallization, Second Metallization and Passivation. Process cycle time data may be collected for each procedure. Figure 4.1 shows plots of in-date cycle times of the eight procedures for the CMOS (1.08μm dlm) technology. The first step was to identify the procedures that are most critical to the technology cycle time data. This was done by examining the cross correlation function between the cycle time of a specific technology and the cycle time of its related procedures. Results of the cross correlation functions for the CMOS (1.08μm dlm) technology with the critical procedures are shown in Tables 4.2 to 4.5. These cross correlation functions suggest that procedures Well Formation, Device Isolation, Source/Drain Formation and Second Metallization are the most critical procedures for the in-date cycle time data of the CMOS (1.08μm dlm) technology.

Cycle times from these procedures were used as leading indicator series, X_t's , to build transfer function models for the technology in-date cycle time. As discussed by Pankratz (1991), some ARIMA modeling should precede the construction of a transfer function model. This involved the development of separate ARIMA models for all series in our proposed model.

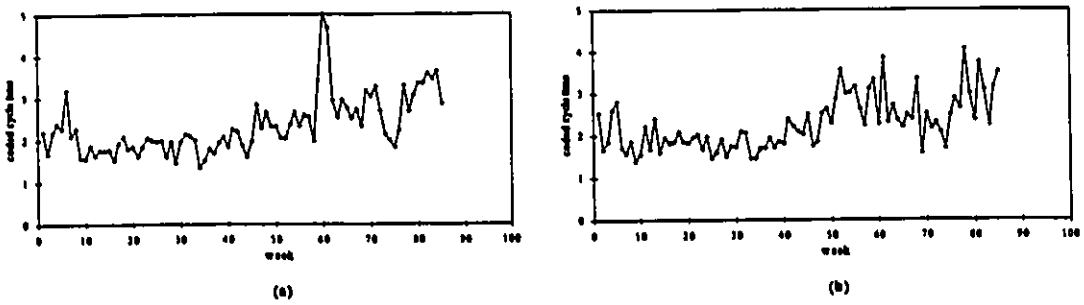

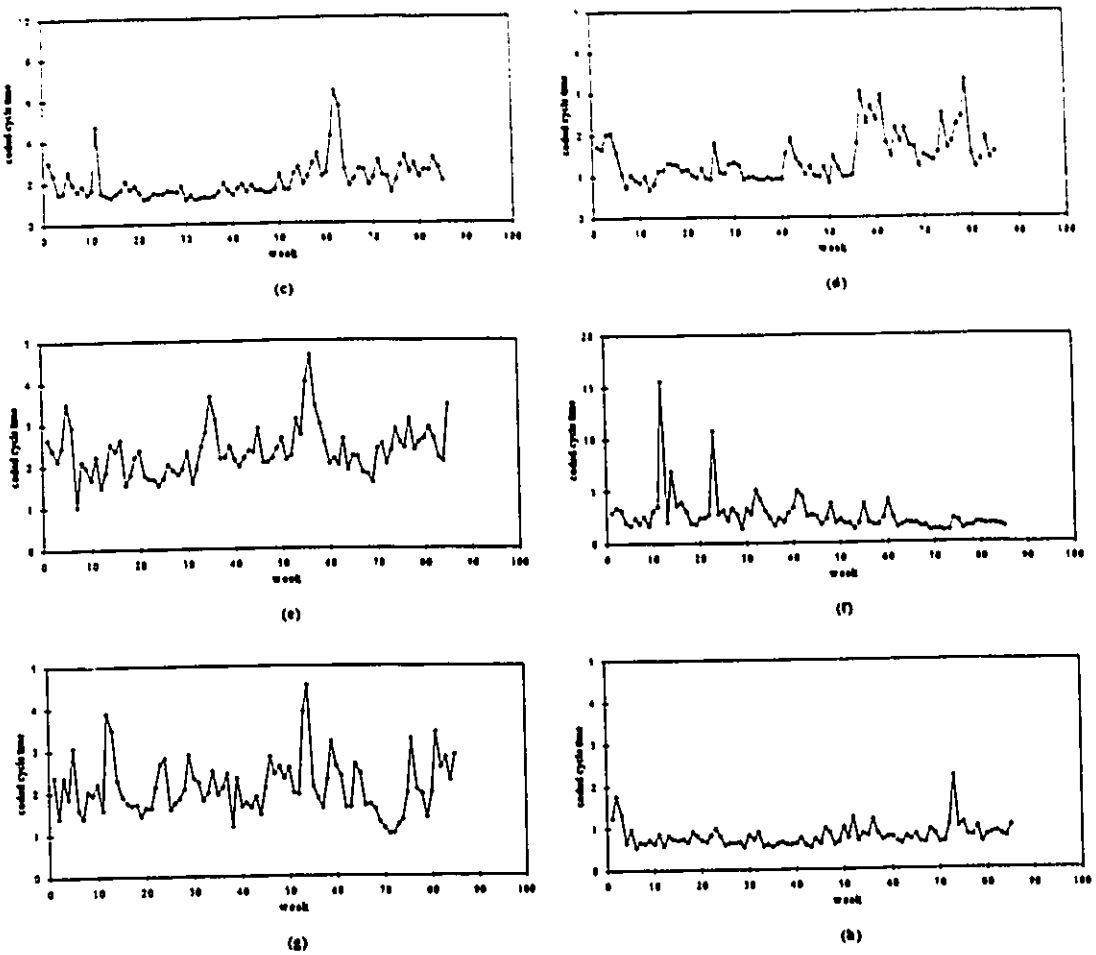

Figure 4.1 **Plots of the In-date Cycle Time Data for the Procedures of the CMOS (1.08μm dlm) Technology (a) Well Formation (b) Device Isolation (c) Gate Formation (d) Capacitor Formation (e) Source/Drain Formation (f) First Metallization (g) Second Metallization (h) Passivation**

Table 4.2 **Cross Correlation Function of the In-date Cycle Time Relating the CMOS(1.08μm dlm) Technology to its Well Formation Procedure**

```
                -1.0  -.8  -.6  -.4  -.2   .0   .2   .4   .6   .8  1.0
                +----+----+----+----+----+----+----+----+----+----+
                                          I
-12     .17                       +      IXXXX +
-11     .20                       +      IXXXXX+
-10     .24                       +      IXXXXXX
 -9     .27                       +      IXXXXX+X
 -8     .29                       +      IXXXXX+X
 -7     .42                       +      IXXXXX+XXXXX
 -6     .47                       +      IXXXXX+XXXXXX
 -5     .46                         +    IXXXX+XXXXXX
 -4     .46                         +    IXXXX+XXXXXXX
```

```
-3    .45                    +    IXXXX+XXXXXX
-2    .53                    +    IXXXX+XXXXXXX
-1    .63                    +    IXXXX+XXXXXXXXXX
 0    .66                    +    IXXXX+XXXXXXXXXX
 1    .61                    +    IXXXX+XXXXXXXXX
 2    .34                    +    IXXXX+XXXX
 3    .29                    +    IXXXX+XX
 4    .29                    +    IXXXX+XX
 5    .30                    +    IXXXX+XX
 6    .21                   +     IXXXXX+
 7    .18                   +     IXXXX +
 8    .17                   +     IXXXX +
 9    .05                   +     IX    +
10    .09                   +     IXX   +
11    .13                   +     IXXX  +
12    .13                   +     IXXX  +
```

Table 4.3 **Cross Correlation Function of the In-date Cycle Time Relating the CMOS(1.08μm dlm) Technology to its Device Isolation Procedure**

```
          -1.0  -.8  -.6  -.4  -.2   .0   .2   .4   .6   .8  1.0
          +----+----+----+----+----+----+----+----+----+----+
                                     I
-12   .00                    +     I     +
-11   .09                    +     IXX   +
-10   .11                    +     IXXX  +
 -9   .10                    +     IXX   +
 -8   .22                    +     IXXXXXX
 -7   .18                    +     IXXXX +
 -6   .27                    +     IXXXXX+X
 -5   .22                     +    IXXXXX
 -4   .32                     +    IXXXX+XXX
 -3   .37                     +    IXXXX+XXXX
 -2   .46                     +    IXXXX+XXXXXX
 -1   .54                     +    IXXXX+XXXXXXXX
  0   .60                     +    IXXXX+XXXXXXXXXX
  1   .58                     +    IXXXX+XXXXXXXXXX
  2   .52                     +    IXXXX+XXXXXXXX
  3   .58                     +    IXXXX+XXXXXXXXXX
  4   .43                     +    IXXXX+XXXXXX
  5   .45                     +    IXXXX+XXXXXX
  6   .45                    +     IXXXXX+XXXXX
  7   .35                    +     IXXXXX+XXX
  8   .28                    +     IXXXXX+X
  9   .29                    +     IXXXXX+X
 10   .22                    +     IXXXXXX
 11   .12                    +     IXXX  +
 12   .16                    +     IXXXX +
```

Table 4.4 **Cross Correlation Function of the In-date Cycle Time Relating the CMOS(1.08μm dlm) Technology to its Source/Drain Procedure**

```
          -1.0  -.8  -.6  -.4  -.2   .0   .2   .4   .6   .8  1.0
          +----+----+----+----+----+----+----+----+----+----+
                                     I
-12   -.04                   +     XI    +
-11   -.05                   +     XI    +
-10   -.01                   +      I    +
 -9   -.03                   +     XI    +
 -8   -.08                   +    XXI    +
 -7   -.06                   +     XI    +
 -6    .05                   +      IX   +
 -5    .10                    +     IXX  +
 -4    .20                    +     IXXXXX
 -3    .30                    +     IXXXX+XXX
```

```
-2    .35                    +     IXXXX+XXXX
-1    .32                    +     IXXXX+XXX
 0    .27                    +     IXXXX+XX
 1    .28                    +     IXXXX+XX
 2    .39                    +     IXXXX+XXXXX
 3    .40                    +     IXXXX+XXXXX
 4    .45                    +     IXXXX+XXXXXX
 5    .47                    +     IXXXX+XXXXXXX
 6    .38                   +      IXXXXX+XXX
 7    .19                   +      IXXXXX+
 8    .16                   +      IXXXX +
 9    .09                   +      IXX   +
10    .08                   +      IXX   +
11    .01                   +      I     +
12    .00                   +      I     +
```

Table 4.5 **Cross Correlation Function of the In-date Cycle Time Relating the CMOS(1.08μm dlm) Technology to its 2nd Metallization Procedure**

```
          -1.0  -.8  -.6  -.4  -.2   .0   .2   .4   .6   .8  1.0
         +----+----+----+----+----+----+----+----+----+----+----+
                                      I
-12   -.29                    X+XXXXXI     +
-11   -.17                     + XXXXI     +
-10   -.15                     + XXXXI     +
 -9   -.11                     +  XXXI     +
 -8   -.06                     +   XXI     +
 -7   -.02                     +     I     +
 -6    .14                     +     IXXX  +
 -5    .28                      +    IXXXX+XX
 -4    .20                      +    IXXXXX
 -3    .14                      +    IXXXX+
 -2    .09                      +    IXX  +
 -1    .17                      +    IXXXX+
  0    .55                      +    IXXXX+XXXXXXXX
  1    .30                      +    IXXXX+XXX
  2    .24                      +    IXXXX+X
  3    .10                      +    IXXX +
  4    .06                      +    IXX  +
  5    .04                      +    IX   +
  6    .21                     +     IXXXXX+
  7    .15                     +     IXXXX +
  8    .08                     +     IXX   +
  9   -.08                     +   XXI     +
 10   -.14                     +  XXXI     +
 11    .02                     +     IX    +
 12   -.12                     +  XXXI     +
```

The LTF method, discussed in Section 4.2, was used to identify a reasonable transfer function model representing the in-date cycle time data for the technology. Estimation results are presented in Table 4.6. Notice that the joint detection-estimation procedure, discussed in Chapter 3, was used in this case. Five outliers were detected and included in the estimated model as intervention components: B11SER, B30SER, B44SER, B61SER and B67SER.

Table 4.6 **Transfer Function Joint Detection-Estimation Results of the Coded In-date**

Cycle Time for the CMOS (1.08μm dlm) Technology

	PARAMETER LABEL	VARIABLE NAME	NUM./ DENOM.	FACTOR	ORDER	CONS-TRAINT	VALUE	STD ERROR	T VALUE
1	CNST		CNST	1	0	NONE	5.3897	0.5662	9.35
2	A0	X1t	NUM.	1	0	NONE	.4850	.0808	6.01
3	B1	X2t	NUM.	1	1	NONE	0.5218	.0966	5.40
4	B3	X2t	NUM.	1	3	NONE	.4642	.0961	4.83
5	C5	X3t	NUM.	1	5	NONE	.4306	.0773	5.57
6	D0	X4t	NUM.	1	0	NONE	.4576	.0693	6.60
7		B11SER	NUM.	1	0	NONE	-2.6927	0.4950	-5.44
8		B11SER	DENM	1	1	NONE	.5731	.1009	5.68
9		B30SER	NUM.	1	0	NONE	5.2337	0.6010	8.71
10		B44SER	NUM.	1	0	NONE	-2.7959	0.5547	-5.04
11		B61SER	NUM.	1	0	NONE	-3.6369	0.5502	-6.61
12		B67SER	NUM.	1	0	NONE	-1.8603	0.4662	-3.99
13		B67SER	DENM	1	1	NONE	.5959	.1437	4.15
14	PHI	CXOVDSSI	D-AR	1	1	NONE	-.4840	.1109	-4.36

TOTAL NUMBER OF OBSERVATIONS. 72
EFFECTIVE NUMBER OF OBSERVATIONS. 66
RESIDUAL STANDARD ERROR (WITHOUT OUTLIER ADJUSTMENT). . .79678E+00

The in-date cycle time data for the overall process could then be represented by the following transfer function model

$$\begin{aligned} Y_t &= C + (A0)X_{1t} + (B1*B + B3*B^3)X_{2t} + (C5*B^5)X_{3t} + (D0)X_{4t} \\ &\quad + N_t \\ &= 5.4 + (0.49)X_{1t} + (0.52B + 0.46B^3)X_{2t} + (0.43B^5)X_{3t} + (0.46)X_{4t} \\ &\quad + \frac{1}{(1+0.48B)}a_t \end{aligned} \tag{4.32}$$

The ACF of the residuals, see Figure 4.2, does not indicate any anomalies. The lack of fit test described in Section 3.2.2, gave a value of $Q_l = 10.5$ which, when referred to a $\chi_{17}^2 = 27.59$, at the 5% level showed not significant lack of model fit.

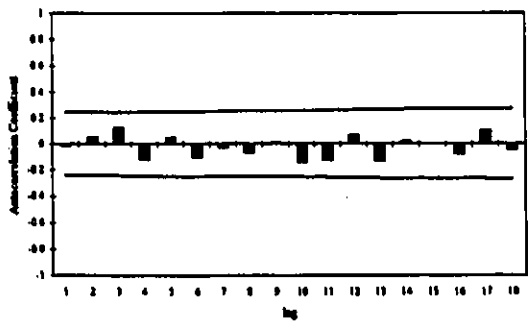

Figure 4.2 **Autocorrelation Function of the Residuals from the Fitted TF Model of the Coded In-date Cycle Time for the CMOS(1.08μm dlm) Technology**

The out-date cycle time for the eight procedures related to the CMOS (1.08μm dlm) technology are presented in Figure 4.3. As for the in-date time basis, the LTF method was used to identify an adequate transfer function model for the out-date cycle time data. Table 4.7 gives the joint detection-estimation results for the CMOS(1.08μm dlm) technology using the out-date data.

Table 4.7 **Transfer Function Joint Detection-Estimation Results of the Out-date Cycle Time Data for the CMOS (1.08μm dlm) Technology**

	PARAMETER LABEL	VARIABLE NAME	NUM./ DENOM.	FACTOR	ORDER	CONS-TRAINT	VALUE	STD ERROR	T VALUE
1	CNST		CNST	1	0	NONE	5.3180	0.5856	9.08
2	A0	X1t	NUM.	1	0	NONE	0.6105	.1051	5.81
3	B0	X2t	NUM.	1	0	NONE	0.5746	0.1147	5.01
4	C0	X3t	NUM.	1	0	NONE	0.5469	0.0987	5.54
5	D0	X4t	NUM.	1	0	NONE	0.4651	0.0914	5.09
6		B58SER	NUM.	1	0	NONE	-5.2290	0.9320	-5.61
7		B60SER	NUM.	1	0	NONE	3.9012	0.8727	4.47
8		B60SER	DENM	1	1	NONE	.5601	.1260	4.45
9		B57SER	NUM.	1	0	NONE	-2.8187	0.8147	-3.46

TOTAL NUMBER OF OBSERVATIONS. 72
EFFECTIVE NUMBER OF OBSERVATIONS. 72
RESIDUAL STANDARD ERROR . . . . . .97810E+00

The out-date cycle time data for the overall process could then be represented by the following transfer function model

$$Y_t = 5.3 + (0.61)X_{1t} + (0.57)X_{2t} + (0.55)X_{3t} + (0.47)X_{4t} + a_t \qquad (4.33)$$

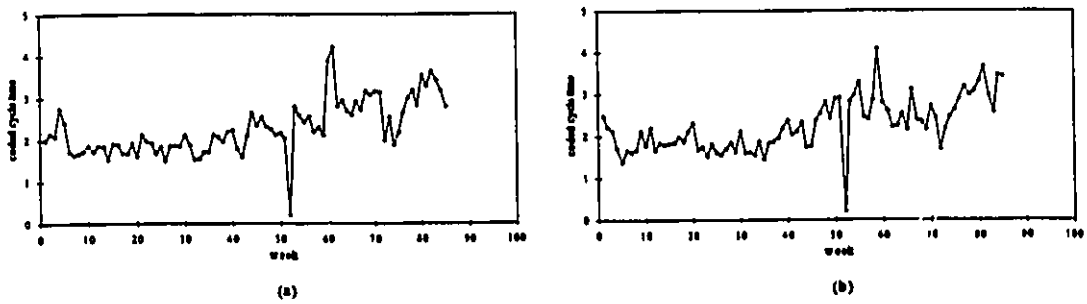

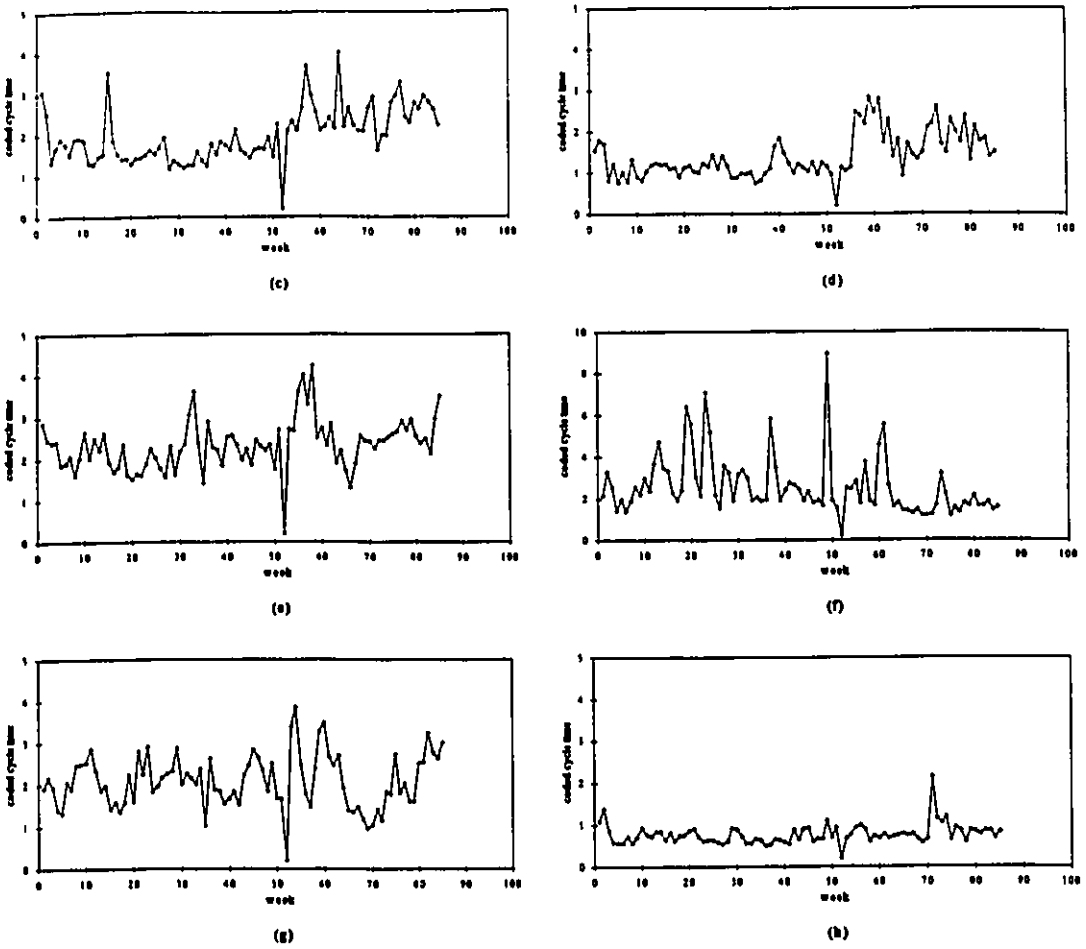

Figure 4.3 **Plots of the Out-date Cycle Time Data for the Procedures of the CMOS(1.08μm dlm) Technology (a) Well Formation (b) Device Isolation (c) Gate Formation (d) Capacitor Formation (e) Source/Drain Formation (f) First Metallization (g) Second Metallization (h) Passivation**

The ACF of the residuals obtained from fitting the above model to the available data appears randomly distributed within the warning limits, as shown in Figure 4.4. This suggests that the model is adequately representing the process. The resulting noise term, N_t, does not contain any dynamics; it is white noise. This means that the input series explained the correlation contained within the output series.

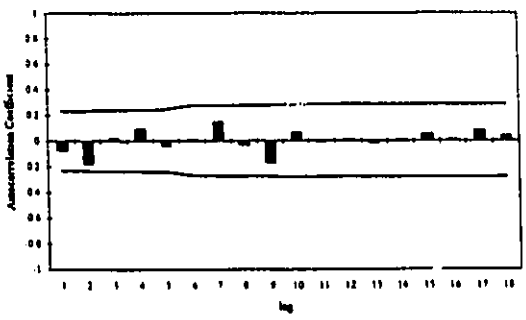

Figure 4.4 **Autocorrelation Function of the Residuals from the Fitted TF Model of the Coded Out-date Cycle Time for the CMOS(1.08μm dlm) Technology**

For this model, $Q_O = 20.5$. Comparison with the $\chi^2_{17,.05}$ indicates the model is adequate. However, since Q_I is significantly smaller than Q_O (10.5 < 20.5) the in-date time basis seems to give a better representation of the cycle time data for the CMOS (1.08μm dlm) technology. This is confirmed by the fact that the residuals from the in-date transfer function model have a smaller standard error value than the ones from the out-date model.

A summary of the modeling results for all the four technologies, using the in-date and the out-date time basis, is given in Tables 4.8 and 4.9 respectively. The shaded areas represent the procedures that were found to be most critical to the technology data. The cycle time data from these critical procedures were used to build transfer function models for the technology cycle time data.

Table 4.8 **Summary of the Modeling Results for the In-date Cycle Time for the CMOS (1.08μm dlm) Process (Shaded Models Represent Most Critical Procedures)**

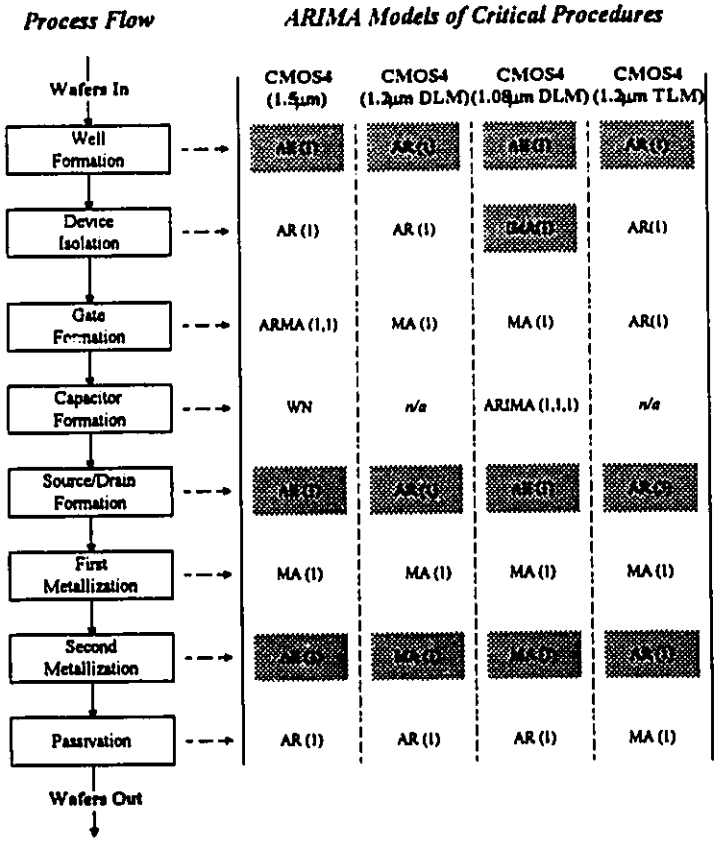

A number of points deserve emphasis from Tables 4.8 and 4.9. First, many of the procedures for the out-date cycle time model follow a white noise process. As discussed in Chapter 3, this indicates the presence of some large noise in the series. This noise is apparently masking the inherent dynamics of the series. These dynamics are identified when the in-date time basis is used instead of the out-date time basis. Table 4.8, suggests that the Well Formation, Device Isolation, Source/Drain Formation and Second Metallization procedures are the most critical procedures for predicting the technology in-date cycle time data. Results from Table 4.9 indicate that procedures Device Isolation,

Table 4.9 **Summary of the Modeling Results for the Out-date Cycle Time for the CMOS (1.08μm dlm) Process (Shaded Models Represent Most Critical Procedures)**

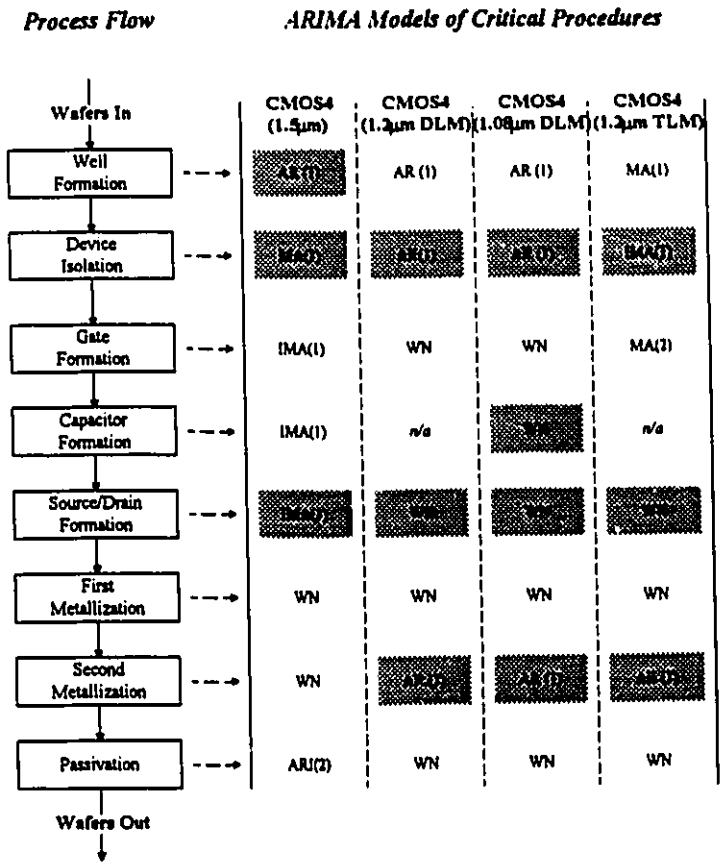

Source/Drain Formation, Capacitor Formation and Second Metallization are the most critical procedures for the out-date time basis cycle time data. Both time bases indicate that Source/Drain Formation and Second Metallization are the most critical procedures in the CMOS manufacturing process. As discussed in Chapter 3, missing data can have a significant effect on the model parameter estimates. Except for the CMOS (1.08μm dlm) technology, the other three process-technologies contain a lot of missing data. Thus, models that were constructed for those series may not be very reliable.

Forecasting

Since our current estimated transfer function models appear to be adequate, we

may use them for forecasting. As mentioned earlier, the transfer function forecasts of the cycle time data for the various technologies are dependent on the forecasts of cycle times of critical procedures. Table 4.10 shows the ARIMA forecasts for lead times $l = 1, 2, 3, 4$ and 5 from origin $t = 72$ for the four inputs series of the transfer function model.

Table 4.10 ARIMA Forecasts of the Coded In-date Cycle Timefor Lead Times $l = 1, 2, 3, 4$ and 5 from Origin $t = 72$ for the CMOS (1.08μm dlm) Technology

(a) Input 1 (Well Formation)

5 FORECASTS, BEGINNING AT 72

TIME	FORECAST	STD. ERROR
73	2.0148	0.5293
74	2.0262	0.5582
75	2.0311	0.5632
76	2.0332	0.5641
77	2.0340	0.5643

(b) Input 2 (Device Isolation)

5 FORECASTS, BEGINNING AT 72

TIME	FORECAST	STD. ERROR
73	2.1493	0.5542
74	2.1493	0.5641
75	2.1493	0.5736
76	2.1493	0.5830
77	2.1493	0.5921

(c) Input 3 (Drain/Source Formation)

5 FORECASTS, BEGINNING AT 72

TIME	FORECAST	STD. ERROR
73	2.4368	0.6559
74	2.2842	0.6853
75	2.2285	0.6891
76	2.2082	0.6896
77	2.2010	0.6896

(d) Input 4 (Second Metallization)

5 FORECASTS, BEGINNING AT 72

TIME	FORECAST	STD. ERROR
73	1.8711	0.6559
74	2.0743	0.6853
75	2.0743	0.6891
76	2.0743	0.6896
77	2.0743	0.6896

Table 4.11 TF Forecasts of the Coded In-date Cycle Time for Lead Times $l = 1, 2, 3, 4$ and 5 from Origin $t = 72$ for the CMOS (1.08μm dlm) Technology

(a) Transfer Function

5 FORECASTS, BEGINNING AT 72

TIME	FORECAST	STD. ERROR
73	13.3736	0.9485
74	16.1262	1.0991
75	13.7730	1.1153
76	13.0882	1.2316
77	13.5181	1.2440

(b) ARIMA

5 FORECASTS, BEGINNING AT 72

TIME	FORECAST	STD. ERROR
73	11.9833	1.2838
74	12.6034	1.5997
75	13.1100	1.7759
76	13.5242	1.8833
77	13.8626	1.9515

(c)

ACTUAL
13.8049
15.8572
14.6221
16.2941
13.9715

Table 4.11 shows five forecasts and standard errors from the transfer function model along with five forecasts and standard errors from the ARIMA model. Also listed are the five future observed values. All forecasts are based on information available at $t = 72$. The forecast standard errors increase at longer forecast lead times. In all cases the standard errors of the TF model forecast are smaller than those for the ARIMA model forecast. This suggests that the TF forecasts are more precise than the ARIMA forecasts.

Comparing the future observed values, one can see that the ARIMA forecasts are more accurate for two of the three forecasts lead times. This emphasizes, as discussed by Pankratz (1991), that the smaller standard error of the forecasts for the transfer function model do not guarantee better forecasts all the time. It only suggests that the transfer function forecasts will be better on average.

The above results are graphically displayed in Figure 4.5.

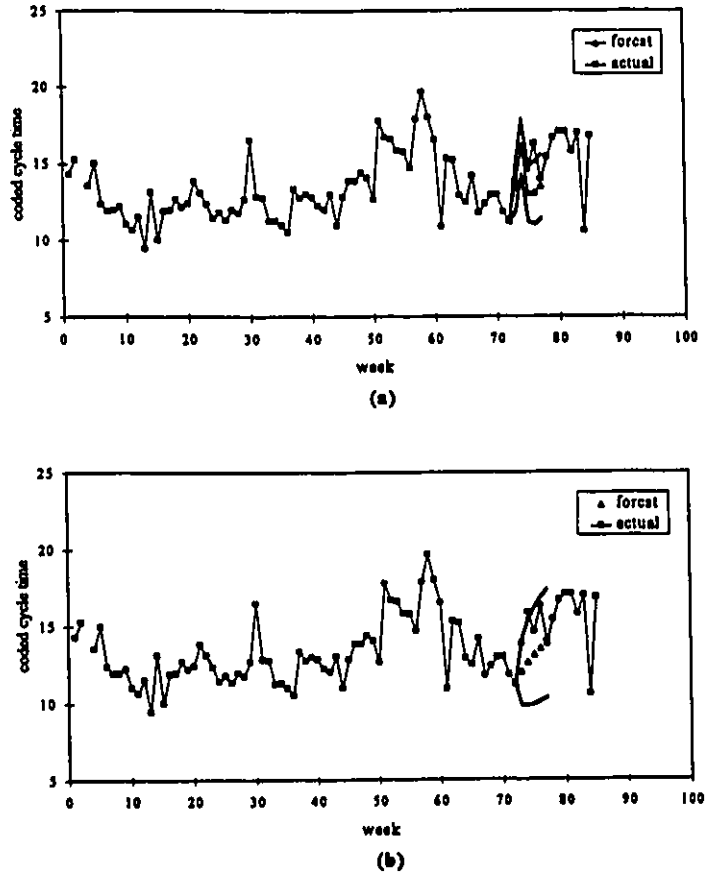

Figure 4.5 **Forecasts of the Coded In-date Cycle Time for Lead Times l = 1, 2, 3, 4 and 5 from Origin t = 72 for the CMOS(1.08μm dlm) Technology Using (a) Transfer Function Model (b) ARIMA Model**

The transfer function forecasts do not converge as rapidly as the ARIMA model forecasts. As discussed in Chapter 3, that is a peculiarity of ARIMA model forecasts. Although, the presence of outliers makes it hard to see, the transfer function forecasts seem to track the

data better than the ARIMA forecasts. The better transfer function forecasts occur because the auxiliary information enables the model to better anticipate the movement of the cycle time data. Since the univariate ARIMA model has no leading indicator, it cannot "anticipate" its own changes. Its forecasts are based uniquely on its prior historical data.

However, due to the presence of significant outliers in the process, no definite conclusions about the level of accuracy of each type of forecasts can be made. By definition, an outlier cannot be anticipated irrelatively to the kind of forecasting model used. In order to adequately compare the accuracy of each type of forecast, the number of outliers should be minimized.

The same procedure may be used for the out-date time basis case. Table 4.12 indicates that the transfer function model should, on average, give more accurate forecasts than the ARIMA model. This is suggested by the smaller standard error forecasts for the transfer function model than the ones for the ARIMA model (i.e. more precise forecasts).

Table 4.12 Forecasts of the Coded Out-date Cycle Time for Lead Times l = 1, 2, 3, 4 and 5 from Origin t = 72 for the CMOS (1.08μm dlm) Technology

(a) Transfer Function			(b) ARIMA			(c) Observed
5 FORECASTS, BEGINNING AT 72			5 FORECASTS, BEGINNING AT 72			ACTUAL
TIME	FORECAST	STD. ERROR	TIME	FORECAST	STD. ERROR	ACTUAL
73	13.2721	1.2814	73	14.7471	1.3736	14.5435
74	12.8469	1.3537	74	14.3814	1.6837	15.3386
75	12.7071	1.3850	75	14.1041	1.8414	16.1181
76	12.6608	1.4002	76	13.8873	1.9288	16.3223
77	12.6654	1.4081	77	13.7196	1.9790	12.9909

However, when compared to the observed values, the ARIMA model forecasts seem, for the five lead times, more accurate than the transfer function model forecasts. Also, the transfer function forecasts seem to rapidly converge to the estimated mean of the series. Thus, contrary to the in-date transfer function model, the out-date transfer function model does not seem to produce better forecasts than the univariate ARIMA model. Transfer function model forecasts for lead times l = 1, 2, 3, 4 and 5 from origin t =77 are given in Table 4.13 and graphically displayed in Figure 4.7. These results seem now to indicate the superiority of the transfer function model forecasts over the ARIMA model forecasts. The

above illustrates the difficulty in assessing the forecasting performance of the TF and the ARIMA models when the series is frequently subjected to significant outliers. Of note is the significant additive outlier (AO) at time $t = 78$.

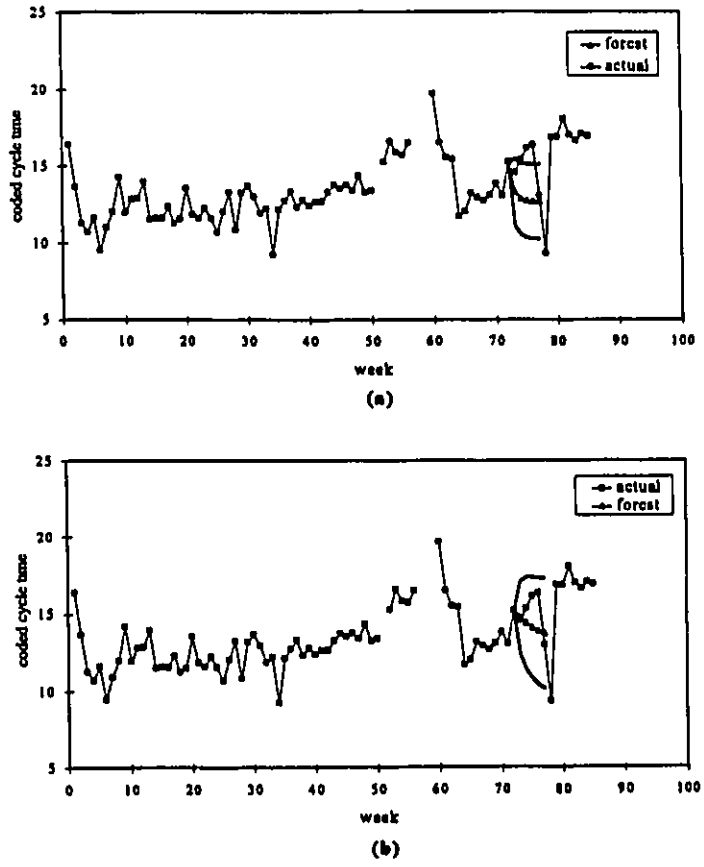

Figure 4.6 **Forecasts of the Coded Out-date Cycle Time for Lead Times $l = 1, 2, 3, 4$ and 5 from Origin $t = 72$ for the CMOS (1.08μm dlm) Technology Using (a) Transfer Function Model (b) ARIMA Model**

Table 4.13 **Forecasts of the Coded Out-date Cycle Time for Lead Times $l = 1, 2, 3, 4$ and 5 from Origin $t = 72$ for the CMOS (1.08μm dlm) Technology**

(a) Transfer Function			(b) ARIMA			(c)
5 FORECASTS, BEGINNING AT 77			5 FORECASTS, BEGINNING AT 77			ACTUAL
TIME	FORECAST	STD. ERROR	TIME	FORECAST	STD. ERROR	ACTUAL

78	13.9397	1.2926	78	13.0419	1.3970	9.3138
79	14.8153	1.3755	79	13.0812	1.7107	16.8410
80	15.3944	1.4116	80	13.1115	1.8690	16.8535
81	15.8709	1.4306	81	13.1347	1.9561	18.0383
82	14.7266	1.4415	82	13.1526	2.0057	16.3981

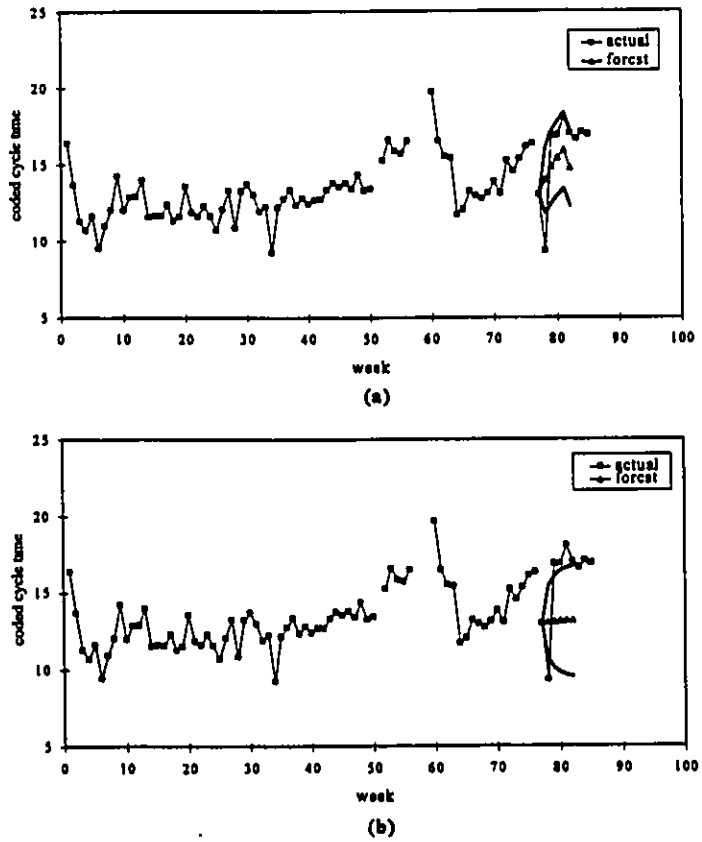

Figure 4.7 **Forecasts of the Coded Out-date Cycle Time for Lead Times $l = 1, 2, 3, 4$ and 5 from Origin $t = 77$ for the CMOS (1.08μm dlm) Technology Using (a) Transfer Function Model (b) ARIMA Model**

In summary, the cycle time transfer function forecasts were, as expected, more precise than the cycle time ARIMA forecasts. This was suggested by the smaller TF forecast standard errors, giving tighter confidence intervals. Although, in general, the TF models seem to qualitatively give better forecasts than the ARIMA models, no thorough comparison could be made due to the significant outliers present in the process.

Overall, better modeling and forecasting results were obtained using the in-date time basis.

4.3.2 Process Yield Data

Modeling

As discussed in Chapter 3, an adequate univariate model for the in-date yield series of the overall process is the white noise process,

$$Z_t = 28.2 + a_t \tag{4.34}$$

whereas, on an out-date time basis, the yield data may be represented by the following white noise process,

$$Z_t = 25.0 + a_t \tag{4.35}$$

Recall from Chapter 3, that forecasts from the above ARIMA models were not very useful since they are equal to the mean of the series. However, it was suggested that the large noise could have some masking effect on the inherent dynamics of the process. If we could relate the process yield data to some other process variables we might then be able to catch these process dynamics. The resulting transfer models should then produce better forecasts than the white noise models given by equations 4.38 and 4.39.

The overall process capacity is believed to affect the yield for the overall process. The process capacity represents either the number of wafers fed to the process, when the in-date time basis is used, or the number of wafers emerging from the process, when out-date time basis is used. The process capacity series for the overall process is shown in Figure 4.8. The cross correlation functions are given in Tables 4.14 and 4.15 for the in-date and out-date time basis, respectively. Table 4.14 shows a one-way positive

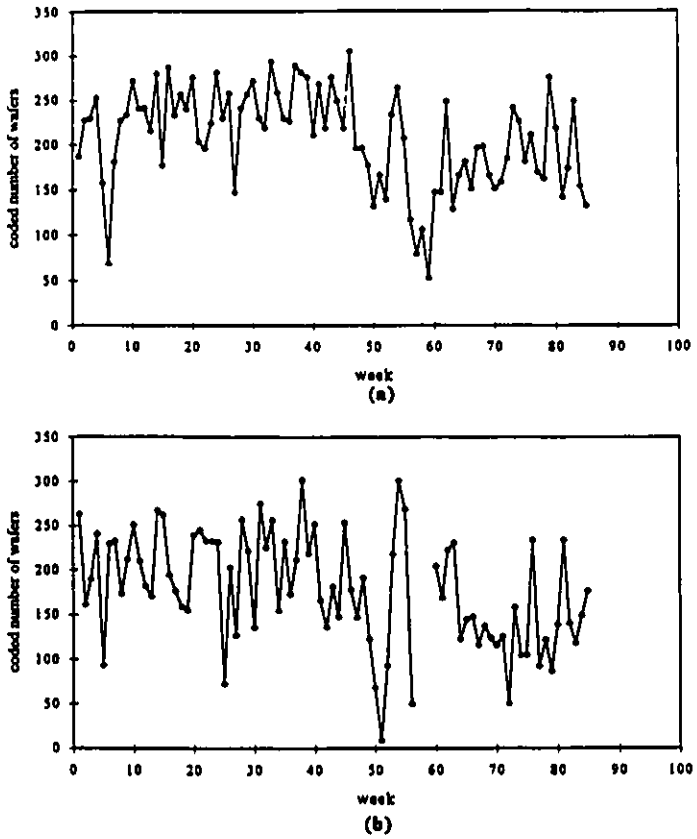

Figure 4.8 **Plots of the Overall Process Capacity Using (a) In-date Time Basis (b) Out-date Time Basis**

correlation between the process yield series and the process capacity series. A one way relationship means that movement in the process capacity series (input) could explain movement in the process yield series (output), but not vice versa. This implies that when a large (low) number of wafers are processed, the yield values increase (decrease). This result may appear surprising at first sight. However, it seems that the number of wafers processed through the fab decreases during sampling periods 55 to 60 corresponding to the Christmas holiday period. The decrease in the yield values may be due to this holiday period. Moreover, for the out-date case, the only instance of significant cross correlation was observed at lag $l = 0$. This suggests that the out-date process capacity series affect the out-date process yield uniquely at lag $l = 0$.

Table 4.14 **Cross Correlation Function Between the Coded In-date Yield and the Coded In-date Process Capacity for the Overall Process**

```
-1.0  -.8  -.6  -.4  -.2   .0   .2   .4   .6   .8  1.0
  +----+----+----+----+----+----+----+----+----+----+
                          I
-12   .08                 +    IXX   +
-11   .04                 +    IX    +
-10   .03                 +    IX    +
 -9   .01                 +    I     +
 -8   .14                 +    IXXXX +
 -7   .13                 +    IXXX  +
 -6   .19                 +    IXXXXX+
 -5   .06                 +    IX    +
 -4   .18                 +    IXXXXX+
 -3   .08                 +    IXX   +
 -2  -.01                 +    I     +
 -1   .14                 +    IXXX  +
  0   .27                 +    IXXXXX+X
  1   .45                 +    IXXXXX+XXXXX
  2   .33                 +    IXXXXX+XX
  3   .11                 +    IXXX  +
  4   .15                 +    IXXXX +
  5   .08                 +    IXX   +
  6   .10                 +    IXXX  +
  7   .26                 +    IXXXXXX
  8   .36                 +    IXXXXX+XXX
  9   .41                 +    IXXXXX+XXXX
 10   .22                 +    IXXXXX+
 11   .09                 +    IXX   +
 12   .21                 +    IXXXXX+
```

Table 4.15 **Cross Correlation Function Between the Coded Out-date Yield and the Coded Out-date Process Capacity for the Overall Process**

```
-1.0  -.8  -.6  -.4  -.2   .0   .2   .4   .6   .8  1.0
  +----+----+----+----+----+----+----+----+----+----+
                          I
-12   .20                 +    IXXXXX+
-11   .03                 +    IX    +
-10   .02                 +    IX    +
 -9   .10                 +    IXX   +
 -8   .01                 +    I     +
 -7   .14                 +    IXXXX +
 -6  -.06                 +   XXI    +
 -5   .20                 +    IXXXXX+
 -4   .05                 +    IX    +
 -3  -.10                 +   XXI    +
 -2   .05                 +    IX    +
 -1  -.12                 +  XXXI    +
  0   .54                 +    IXXXXX+XXXXXXXX
  1   .07                 +    IXX   +
  2   .12                 +    IXXX  +
  3   .01                 +    I     +
  4  -.12                 +  XXXI    +
  5   .03                 +    IX    +
  6   .07                 +    IXX   +
  7   .24                 +    IXXXXXX
  8   .27                 +    IXXXXX+X
  9   .12                 +    IXXX  +
 10   .09                 +    IXX   +
 11  -.21                 +XXXXXI    +
 12   .01                 +    I     +
```

Since there was a one way relationship between the yield data and the process capacity, transfer function models for the overall process were constructed. As discussed earlier, it is necessary to first build ARIMA models for the input series. The modeling strategy discussed in Chapter 3 leads to the following ARIMA models for the overall process capacity (see Appendix D), using the in-date time basis (4.40) and using the out-date time basis (4.41),

$$Z_t = 209.4 + (0.51)Z_{t-1} + a_t \tag{4.36}$$

$$Z_t = 201.5 + a_t \tag{4.37}$$

The mean of the in-date process capacity series is significantly larger than the mean of the out-date process capacity series. As mentioned in Chapter 2, when the out-date time basis is used, split lots and normal lots are given the same weight. Since split lots consist of less number of wafers than the normal lots, the mean of the out-date process capacity is under-estimated. On the other hand, when the in-date time basis is used, split lots are joined to their main lot using some weight factors. Less weight is then given to split lots.

In a transfer function it is very important to decide which inputs to include. Ideally, one should include all relevant and important inputs. If we exclude relevant inputs, and if they are correlated with the included inputs, then the TF model coefficient estimates are biased and inconsistent. As discussed in Section 4.2, the LTF method is used to identify a reasonable transfer function model fitting the available data. Coefficient estimates of the transfer function models, for both the in-date and the out-date time basis, are given in Table 4.16. The above modeling results may be expressed in difference equation form by,

$$Y_t = 21.6 + (0.014B + 0.0089B^9)X_t + a_t \tag{4.38}$$

$$Y_t = 20.8 + (0.0213)X_t + a_t \tag{4.39}$$

As expected, the transfer function model for the out-date time basis (4.43) does not show any dynamics, the out-date process capacity has an immediate and unique impact on the out-date process yield series. The out-date process capacity series cannot be used as a "leading" indicator for the out-date yield series. On the other hand, past observations

in the in-date process capacity series seem to affect future observations, one-step-ahead and eight-step-ahead, in the in-date yield series, as indicated by equation 4.42.

Table 4.16 **Transfer Function Joint Detection-Estimation Results Relating the Coded Yield to the Coded Process Capacity for the Overall Process Using (a) In-date time basis (b) Out-date time basis**

(a)

PARAMETER LABEL	VARIABLE NAME	NUM./ DENOM.	FACTOR	ORDER	CONS-TRAINT	VALUE	STD ERROR	T VALUE
1 CNST		CNST	1	0	NONE	21.5477	0.9522	22.63
2 A1	Xt	NUM.	1	1	NONE	.0141	.0040	3.50
3 A8	Xt	NUM.	1	8	NONE	.0089	.0038	2.93
4	B15SER	NUM.	1	0	NONE	-5.8330	1.6113	-3.62
5	B44SER	NUM.	1	0	NONE	-5.9070	1.5922	-3.71

TOTAL NUMBER OF OBSERVATIONS. 72
EFFECTIVE NUMBER OF OBSERVATIONS. 72
RESIDUAL STANDARD ERROR . . . . . 18157E+01

(b)

PARAMETER LABEL	VARIABLE NAME	NUM./ DENOM.	FACTOR	ORDER	CONS-TRAINT	VALUE	STD ERROR	T VALUE
1 CNST		CNST	1	0	NONE	20.7640	0.8282	25.07
2 A0	Xt	NUM.	1	0	NONE	.0213	.0042	5.10
3	B25SER	NUM.	1	0	NONE	-8.5982	2.1604	-3.98

TOTAL NUMBER OF OBSERVATIONS. 72
EFFECTIVE NUMBER OF OBSERVATIONS. 72
RESIDUAL STANDARD ERROR . . . . . 234072E+01

The ACF of the residuals for the two models, see Figure 4.9, show the adequacy of both models in representing their respective processes. This result is confirmed by the lack of fit test, as discussed by Box and Jenkins (1970). A $Q_I = 16.4$ is associated with the in-date transfer function model while a $Q_O = 18.3$ was found for the out-date transfer function model. Both Q values are smaller than the critical value, $Q_C = 27.59$, found in a χ^2 table with 17 degrees of freedom at the 95% level of confidence. The in-date transfer function model seems to better fit the available data. This is suggested by the difference in the residual standard errors between these two fitted models: the residual standard error is smaller for the in-date transfer function model. The Q-test confirms this result.

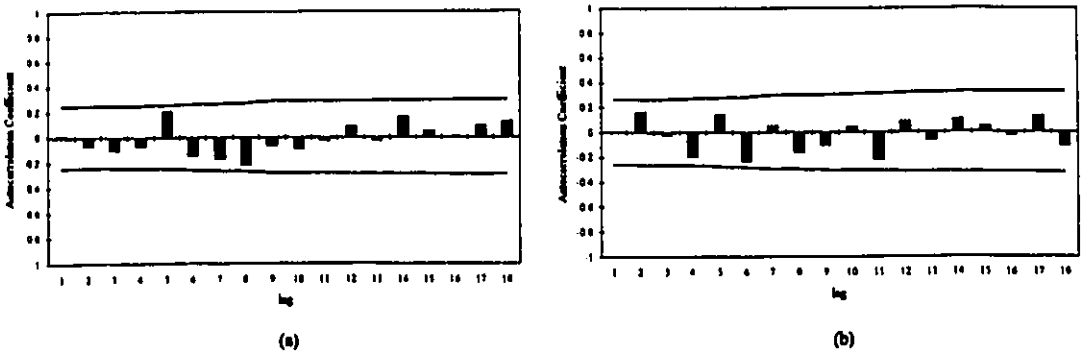

(a) (b)

Figure 4.9 **Autocorrelation Function of the Residuals from the Fitted TF Model of the Coded Yield for the Overall Process Using (a) In-date Time Basis (b) Out-date Time Basis**

Forecasting

Since the above transfer function models seem adequate, they can be used for forecasting. Since the forecasts of the yield data (output series) are dependent on the forecasts of the process capacity data (input series), one must first calculate forecasts for the process capacity series using equations 4.40 and 4.41. These forecasts are displayed in Table 4.17. TF yield forecasts using equation 4.42 for lead times $l = 1, 2, 3, 4$ and 5 from origin $t = 72$ for the overall process, when the in-date time basis is used, appear in Table 4.18 and in Figure 4.10.

Table 4.17 **ARIMA Forecasts of the Coded Process Capacity for Lead Times $l = 1, 2, 3, 4$ and 5 from Origin $t = 72$ for the Overall Process**

(a) In-date

5 FORECASTS, BEGINNING AT 72

TIME	FORECAST	STD. ERROR
73	197.4848	48.6634
74	203.8904	54.6695
75	207.1767	56.1433
76	208.8627	56.5248
77	209.7278	56.6248

(b) Out-date

5 FORECASTS, BEGINNING AT 72

TIME	FORECAST	STD. ERROR
73	201.5239	58.0501
74	201.5239	58.0501
75	201.5239	58.0501
76	201.5239	58.0501
77	201.5239	58.0501

Table 4.18 **TF Forecasts of the Coded In-date Yield for Lead Times $l = 1, 2, 3, 4$ and 5 from Origin $t = 72$ for the Overall Process**

(a) Transfer Function			(b) ARIMA			(c)
5 FORECASTS, BEGINNING AT 72			5 FORECASTS, BEGINNING AT 72			ACTUAL
TIME	FORECAST	STD. ERROR	TIME	FORECAST	STD. ERROR	ACTUAL
73	24.3354	1.6776	73	26.3361	2.3265	22.8683
74	25.1863	1.8401	74	26.3361	2.3265	25.4304
75	25.7188	1.8803	75	26.3361	2.3265	18.9152
76	26.0549	1.8907	76	26.3361	2.3265	24.2676
77	26.2687	1.8934	77	26.3361	2.3265	23.7696

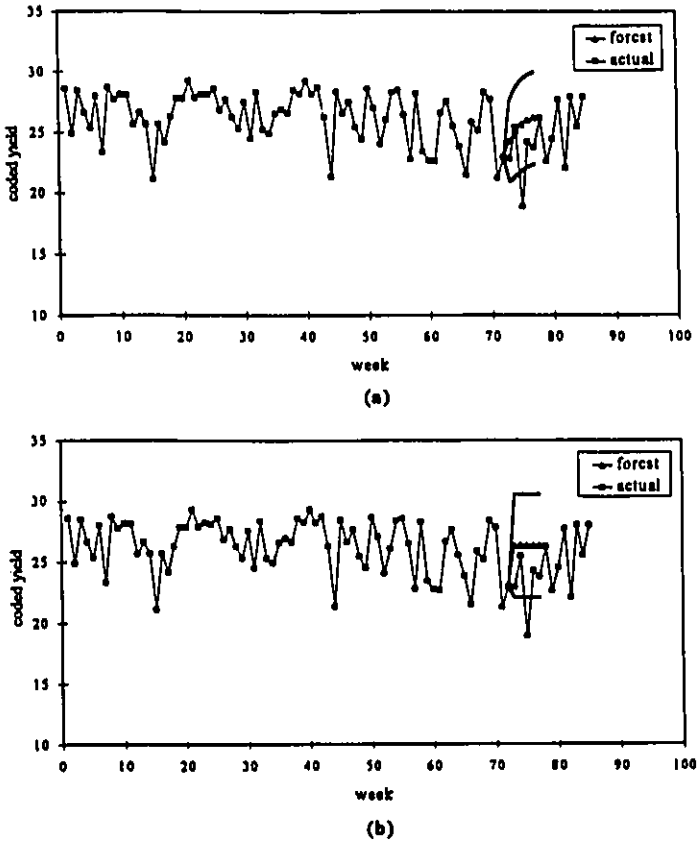

Figure 4.10 **Forecasts of the Coded In-date Yield for Lead Times $l = 1, 2, 3, 4$ and 5 from Origin $t = 72$ for the Overall Process Using (a) Transfer Function Model (b) ARIMA Model**

The standard error forecasts obtained from the in-date transfer function model are significantly smaller than the ones obtained from the ARIMA model, leading to tighter confidence intervals. This suggests that, when the in-date time basis is used, the transfer function model produces more precise forecasts than the ARIMA model. Moreover, the

in-date transfer function forecasts seem to track quite effectively future observations, except for the 75th observation which is an additive outlier (see Figure 4.10). The observed value of the in-date yield can be related to its own past observations, as well as to the past observations of the in-date process capacity. As shown from equation 4.42, future observations of the in-date yield can be anticipated up to eight time intervals before their occurrence. On the other hand the information used to predict future observations is limited, using ARIMA models, to its series own past values. Contrary to the TF yield forecasts, the ARIMA yield forecasts do not have any dynamics. Figure 4.11 shows forecasts for lead times $l = 1, 2, 3, 4$ and 5 starting now from origin $t = 77$.

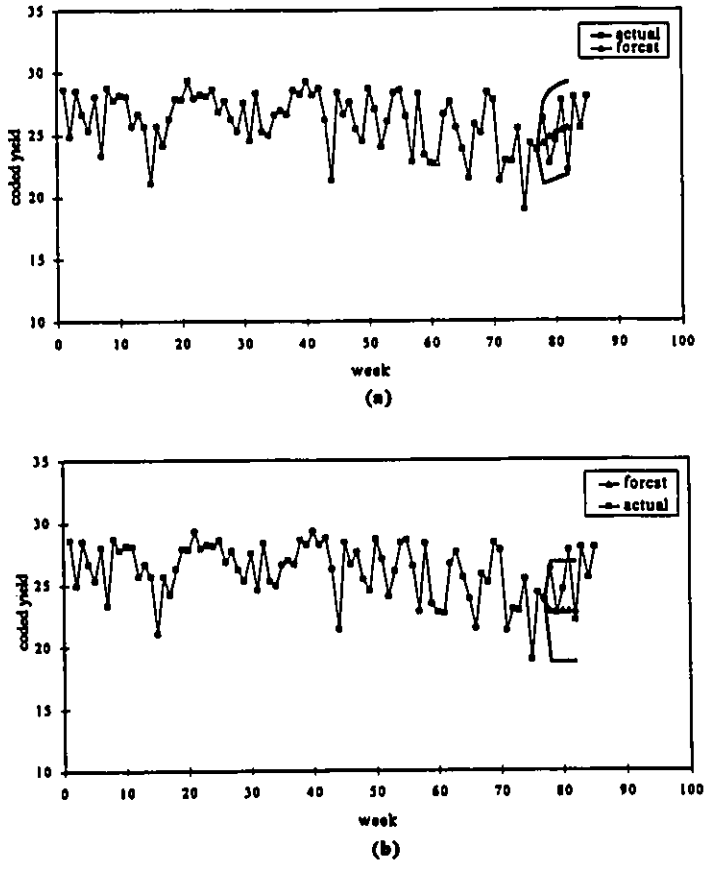

Figure 4.11 **Forecasts of the Coded In-date for Lead Times $l = 1, 2, 3, 4$ and 5 from Origin $t = 72$ for the Overall Process Using (a) Transfer Function Model (b) ARIMA Model**

The transfer function model forecasts appear to be quite robust to the forecasting time origin. Although, the transfer function models seem, in general, to produce better forecasts than the ARIMA models, their effectiveness is diminished by the presence of outliers. Thus, better forecasting could be achieved by minimizing the occurrence and the size of the outliers affecting the process.

Forecasts for the out-date yield data are presented in Table 4.19 and in Figure 4.12. Those results show that the out-date transfer function model gives very similar forecasting performance to the ARIMA model derived in Chapter 3. This result was expected from equation model 4.43. Contrary to the in-date transfer function model where observations are related to past observations of the process capacity series, the out-date yield series is related to present observations of the process capacity series. In other words, the out-date yield series cannot use the out-date process capacity series as a leading indicator for forecasting purposes. Since the out-date transfer function model does not seem to give better forecasts than the out-date ARIMA model, it may not be worth the effort to work with a transfer function model. This is also suggested by the concept of parsimonious parametrization.

Table 4.19 TF Forecasts of the Coded Out-date Yield for Lead Times $l = 1, 2, 3, 4$ and 5 from Origin $t = 72$ for the Overall Process

(a) Transfer Function			(b) ARIMA			(c)
5 FORECASTS, BEGINNING AT 72			5 FORECASTS, BEGINNING AT 72			ACTUAL
TIME	FORECAST	STD. ERROR	TIME	FORECAST	STD. ERROR	ACTUAL
73	23.3221	2.3007	73	25.1475	2.3236	23.9941
74	23.3221	2.3007	74	25.1475	2.3236	21.1529
75	23.3221	2.3007	75	25.1475	2.3236	21.6526
76	23.3221	2.3007	76	25.1475	2.3236	26.3229
77	23.3221	2.3007	77	25.1475	2.3236	17.3186

In summary, the TF models produce more precise forecasts than the ARIMA models, as expected. Due to the presence of significant outliers, no definitive conclusion regarding the accuracy of the different forecasts could be drawn. Since by definition an outlier cannot be anticipated, both types of model could not produce very effective

forecasts. However, except for the out-date yield data, transfer function models seem to produce better forecasts than the ARIMA models. Overall, better modeling and forecasting results were obtained using the in-date time basis.

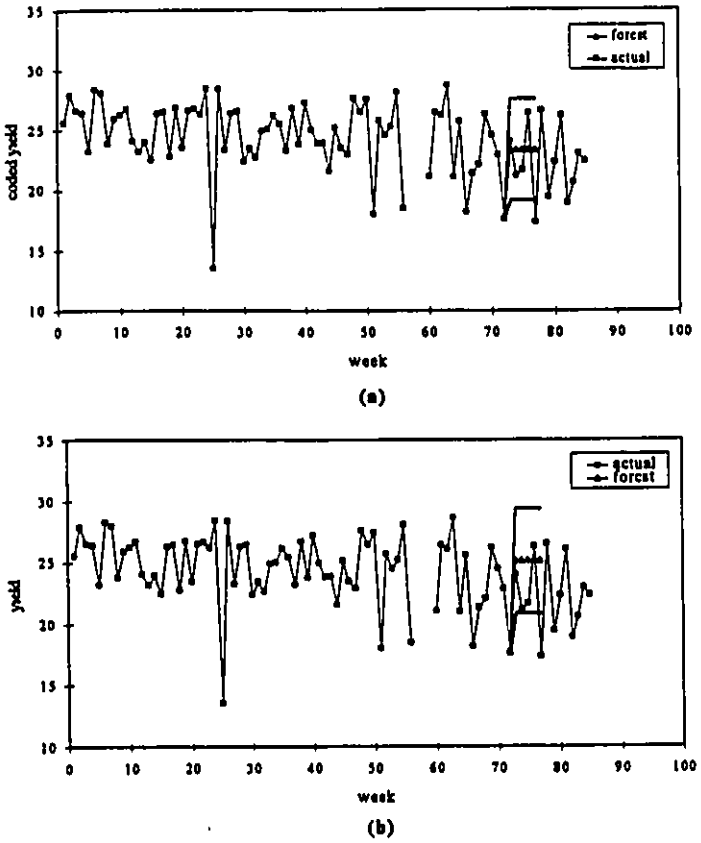

Figure 4.12 **Forecasts of the Coded Out-date Yield for Lead Times l = 1, 2, 3, 4 and 5 from Origin t = 72 for the Overall Process Using (a) Transfer Function Model (b) ARIMA Model**

4.4 Conclusions and Recommendations

4.4.1 Conclusions

1. In general, standard errors of TF forecasts were smaller than those for ARIMA forecasts.
2. Due to the presence of many significant outliers, no obvious improvement was observed when comparing TF forecasts to ARIMA forecasts.
3. Overall, the in-date time basis gave better modeling and forecasting results.

4.4.2 Recommendations

In order to obtain adequate long-term forecasts using the TF models, outliers should be minimized in the process. No matter how good the forecasting models are, they can never anticipate the occurrence of an outlier. Consequently, some process monitoring and control techniques should then be applied to minimize outliers as well as the magnitude of the noise term.

Chapter Five

PROCESS MONITORING, CONTROL AND CONTINUOUS IMPROVEMENT

5.1 Introduction

Statistical Quality Control (SQC) is used in the manufacturing industries where raw materials have to be converted in the most economical way into desired product. SQC seeks better product quality which is the key for profitability. Due to increasing competition, quality control has become one of the major concerns of management. Thus, more efforts have been put towards the improvement of quality control methods. The prime objective of quality control methods is to minimize deviations of critical process output variables from their target levels. This is typically achieved through the use of traditional control charts (e.g., Shewhart, CUSUM, EWMA). These charts monitor variation in process outputs (usually those directly related to product quality) and thereby enable the identification and the removal of special causes (i.e., outliers). Special causes are defined as those that produce a significant shift in the

mean or variability of the controlled output variable. The process is said to be in a state of statistical control if it is only subjected to 'common-cause' disturbances, that is random disturbances that occur under normal operation and that do not require any special control action.

For reliable forecasting, the process should be in a state of statistical control, that is, free of outliers. For example in Section 3.2, very poor forecasts were obtained due to frequent significant outliers. Moreover, minimizing the noise term in the process should allow better modelling and increase the sensitivity of outlier detection methods. Recall from chapter 3, that the extensive noise was suspected of masking the inherent dynamics of the yield process. The objective of this chapter is to present and discuss some methods for improving the forecasting process through the minimization of the noise term and the frequency of outliers. Better forecasting and control should be achieved by combining the joint detection-estimation scheme, discussed in chapter 3, with some traditional control charts. In the first section of this chapter, the use of some control charts for correlated data are examined. In order to account for the effect of outliers, these control charts are combined with the joint detection-estimation. procedure. An alternative charting technique, especially suited for processes frequently subjected to special events, is then proposed. Finally, a strategy for simultaneous outlier treatment and forecasting is suggested. This strategy focuses on the treatment of end-of-series events.

5.2 Background and Literature Survey.

5.2.1 Traditional Shewhart Chart

A widely used charting technique for detecting the occurrence of a significant shift in the mean value of a process variable is the Shewhart chart (Shewhart, 1931). Initially, this technique was based on the assumption that the observations are identically, independently normally distributed with constant variance, that is

$$Y_t = \mu + a_t \tag{5.1}$$

where μ is the mean and a_t is an independent random error with constant variance, σ^2_a, usually arising from measurement and sampling error. This control chart involves plotting the product quality data in time on a chart containing the target value and upper and lower control (action) limits. These limits are placed at the target value plus and minus three standard deviations of the charted quantity such that there is a probability of 0.003 that they are exceeded on chance alone. The Shewhart chart is often combined with run tests (Champ and Woodall, 1978) to improve the power of the chart (i.e., the ability to detect small shifts without generating excessive numbers of false alarms).

5.2.2 Modified Shewhart Chart

The assumption that a measured variable has a constant mean and independent errors, is frequently violated in many manufacturing industries. In such cases, a more realistic approach is to assume a model of the form

$$Y_t = \mu_t + \varepsilon_t \tag{5.2}$$

where the true process mean μ_t varies with time. In this case, equation 5.2 allows the process mean to wander or drift away from the target value in the presence of common cause disturbances only. This autocorrelation in the data is usually caused by the presence of inertial elements such as tanks, reactors and other vessels.

If the observations are autocorrelated, the traditional Shewhart chart must be modified substantially if the average in-control run length, ARL(0), is to be maintained in an acceptable range (Harris and Ross, 1991). The average in-control run length is the frequency of false alarms. A simple way of achieving this is by modifying the contol limits to account for the process dynamics. One approach is to characterize the disturbances by a suitable times series model and the inertial characteristics of the system by a suitable transfer function (Box and Kramer, 1991). As discussed in Section 3.1.1, this approach provides an effective tool for the

modelling process dynamics and stochastic disturbances. This method uses linear difference equations since it supposes that observations are available at discrete, equispaced intervals of time.

For an effective control scheme, it is very important to have some knowledge about the nature of the process and of the nature of the disturbances. Process knowledge is necessary to efficiently detect special cause disturbances and to efficiently estimate the true level of the output deviation from target. A stochastic stationary model assumes that the process fluctuates about a constant mean level. The simplest stochastic model is the stationary white noise model which assumes that the disturbances can be represented by a series of independently, identically distributed random "shocks", a_t , having mean zero and constant variance, σ_a^2. This assumption is, however, not realistic in the process industries since disturbances entering a process are often persistent in nature and dependent on past values.

These kind of disturbances can be represented by an *autoregressive* model of order p (AR(p)) such that

$$\tilde{Z}_t = \phi_1 \tilde{Z}_{t-1} + \phi_2 \tilde{Z}_{t-2} + \ldots + \phi_p \tilde{Z}_{t-p} + a_t \tag{5.3}$$

where $\tilde{Z}_t$ is the deviation of the observed value from the mean of the series,

$$\tilde{Z}_t = Z_t - \mu \tag{5.4}$$

and ϕ_i (i =1,2,...,p) are weighting constants (model parameters). If we define an autoregressive operator of order p by

$$\phi(B) = 1 - \phi_1 B - \phi_2 B^2 - \ldots - \phi_p B^p \tag{5.5}$$

where B is the backward shift operator ($B^n Z_t = Z_{t-n}$). The autoregressive model AR(p) may be written also as

$$\phi(B) \tilde{Z}_t = a_t \tag{5.6}$$

or

$$\tilde{Z}_t = \frac{1}{\phi(B)} a_t = \phi^{-1}(B)\, a_t \tag{5.7}$$

Such a model results from passing white noise through a digital filter $\phi^{-1}(B)$.

Assuming a first order autoregressive process,

$$\tilde{Z}_t = \frac{1}{(1-\phi B)} a_t \tag{5.8}$$

the upper and lower control limits (UCL and LCL) are given by,

$$\begin{aligned} UCL &= \mu_Z + 3\sigma_Z \\ &= \mu_Z + \frac{3}{(1-\phi)}\sigma_a \end{aligned} \tag{5.9}$$

$$\begin{aligned} LCL &= \mu_Z - 3\sigma_Z \\ &= \mu_Z - \frac{3}{(1-\phi)}\sigma_a \end{aligned} \tag{5.10}$$

However, when the data is highly autocorrelated, it becomes difficult to distinguish common causes from special causes (Alwan and Roberts, 1983). Moreover, a special cause may be masked by the large correlation existing in the series. Consequently, the traditional control charts, even with substantially modified control limits, are not appropriate when there is significant correlation in the process.

Montgomery (1985) suggested using the residuals from time series modeling for monitoring purposes. Alwan and Roberts (1987) took a closer look at this monitoring technique in the presence of sequential correlation. They referred to this chart as the *special-cause* chart. Assuming a simple AR(1) process, the residuals are given by

$$\hat{a}_t = (1-\phi B)\tilde{Z}_t \tag{5.11}$$

Since the residuals are independent, this chart can be used in traditional ways to detect any special causes, without the danger of confounding special causes with common-causes. This chart consists of a center-line equal to zero and control limits that correspond to $\pm 3\sigma_a$, where σ_a is the standard deviation of the residual series. However, Harris and Ross (1992) showed

that this chart was very insensitive for detecting outliers when the observations are highly correlated.

5.3 Discussion and Results

5.3.1 Special-cause Chart

As mentioned in the previous chapters, all of the cycle time data followed an AR(1) model. For example, the inherent dynamics of the in-date cycle time data for the overall process can be represented by the following difference equation,

$$(1-0.56B)Z_t = 12.53 + a_t \tag{5.12}$$

or equivalently, in terms of deviation variables,

$$\tilde{Z}_t = \frac{1}{(1-0.56B)} a_t \tag{5.13}$$

The residuals from the above fitted AR(1) model are then given by,

$$\hat{a}_t = (1-0.56B)\tilde{Z}_t \tag{5.14}$$

and are randomly distributed with mean zero and standard deviation σ_a. The special-cause chart, discussed by Alwan and Roberts (1988), for this process is shown in Figure 5.1.

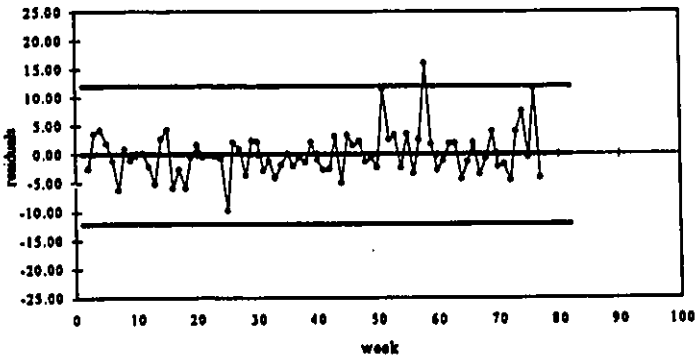

Figure 5.1 **Shewhart Control Chart of the Residuals (Special-cause Chart) of the Coded In-date Cycle Time for the Overall Process**

Compared to the joint outlier detection scheme shown in Table 3.16 (see Section 3.2) one can see that the above special-cause chart is quite insensitive. Only one outlier at $t = 58$ was detected whereas data points at $t = 25$ and 51 were previously identified as outliers by the ARIMA joint detection-estimation procedure. However, the visual representation of the overall process performance including out-of-control situations is seen as a significant advantage by operators . The display of the outlier dynamics may also help diagnose its cause. Furthermore, from Table 3.16, two more outliers were detected at $t = 74$ and 76. Using the above special-cause chart, neither of these out-of-control points were detected.

In theory, the special-cause chart should be updated after the detection and removal of a special cause such as the one found at $t = 58$. This would involve stopping the process monitoring, and collecting enough data to reset the control limits of the residual control chart. That is not always feasible in practice where continuous process monitoring is needed for optimal quality improvement. The use of intervention models to account for these outliers, as done in the joint detection-estimation scheme, could be used to overcome this limitation. This would allow the past data to be kept and thereby maintain the sensitivity of the scheme for detection of outliers. As stated earlier, in the industry there is always a need to continuously monitor the process under study. So usually, when a special cause is detected, charting continues while a search for the origin of the outlier is done. However, the identification and removal of the cause may take a significant period of time. This illustrates another example where the joint detection-estimation procedure is essential to keep, correctly, monitoring while searching for the cause of the detected outlier.

As discussed in Section 3.2, the use of the joint estimation procedure produces residuals with significantly smaller standard error. This should yield tighter control limits on the residual control charts, i.e. an increase in the sensitivity. Such a residual chart will be referred to as an *outlier-adjusted chart*. Figure 5.2 shows an outlier-adjusted chart of the in-date cycle time for the overall process. As expected, the outliers at $t = 25$, 51 and 58 no longer show on the chart since they have been taken into account by the fitted intervention model. However, an observation at time $t = 76$ is beyond the three-sigma limits. On the other hand,

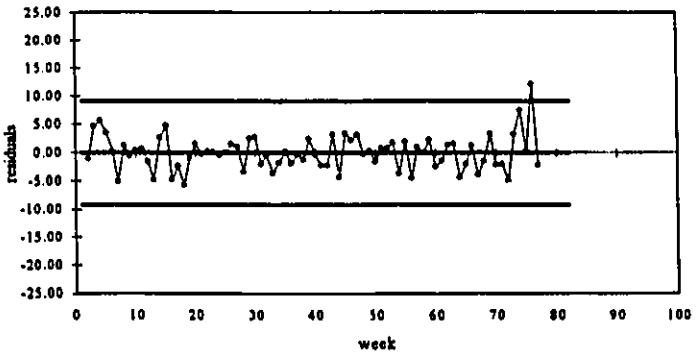

Figure 5.2 **Shewhart Control Chart of the Residuals Combined with the Joint Detection-Estimation Scheme (Outlier-adjusted Chart) of the Coded In-date Cycle Time for the Overall Process**

the outlier detection scheme, shown in Table 3.16 (Section 3.2), indicated two IO outliers at t = 74 and 76. This example seems to suggest that the joint outlier detection scheme developped by Chen and Liu (1993) is still more sensitive than the outlier-adjusted chart.

However, as discussed in Section 3.3.3, outliers occuring near the end of a series are not always reliable. Since 77 data points were used, the two outliers (IOs at t = 74 and 76) occured within the last five data points of the series and may not be correctly identified. Table 5.1 shows the joint estimation results of the intervention model with 77 and 82 data points. Those results show that the IO outlier detected at t = 74, using 77 data points, was actually a spurious outlier, i.e. it was not really an outlier. This result is then in accordance with the improved residual control chart, Figure 5.2. The joint outlier detection scheme initially identified an outlier at t =76 as an IO (see Table 5.1a), whereas that outlier was actually an AO (see Table 5.1b).

Another important result is that the process seems to have changed. The autoregressive parameter, ϕ_1 , has increased from 0.54 to 0.71 which indicates that more correlation has entered into the process. This seems to suggest either that something else has happened to the process other than the outlier at t = 76 or that the outlier has not been

correctly accounted for by the joint scheme. An internal search showed however that some significant management changes took place during that time period which seem to indicate that the process has actually changed. This highligts the importance of regularly refitting the model to check if the process has changed. Consequently, for effective treatment of end-of-series events, the joint detection-estimation scheme (Chen and Liu, 1993) should be combined with the outlier-adjusted chart. A combination of these two techniques should yield optimal both better forecasting and monitoring.

Table 5.1 **ARIMA Joint Detection-Estimation Results of the Coded In-date Cycle Time for the Overall Process Using (a) 77 Data Points (b) 82 Data Points**

(a)

	PARAMETER LABEL	VARIABLE NAME	NUM./ DENOM.	FACTOR	ORDER	CONS-TRAINT	VALUE	STD ERROR	T VALUE
1	CNST2		CNST	1	0	NONE	12.5800	.2477	50.77
2		B25SER	NUM.	1	0	NONE	-2.6950	0.7245	-3.62
3	PH2	B25SER	DENM	1	1	EQ 01	.5443	.0707	7.70
4		B51SER	NUM.	1	0	NONE	4.1309	0.8001	5.16
5		B51SER	DENM	1	1	NONE	.8664	.0648	13.36
6		B58SER	NUM.	1	0	NONE	5.2060	0.8779	5.93
7		B58SER	DENM	1	1	NONE	.6964	.1213	5.74
8		B74SER	NUM.	1	0	NONE	2.7899	0.8637	3.23
***	PH2	B74SER	DENM	1	1	EQ 01	.5443	.0707	7.70
9		B76SER	NUM.	1	0	NONE	4.3301	0.8490	5.10
***	PH2	B76SER	DENM	1	1	EQ 01	.5443	.0707	7.70
***	PH2	CXOVALI	D-AR	1	1	EQ 01	.5443	.0707	7.70

TOTAL NUMBER OF OBSERVATIONS. 77
EFFECTIVE NUMBER OF OBSERVATIONS. 76
RESIDUAL STANDARD ERROR . . . . . .991711E+00

(b)

	PARAMETER LABEL	VARIABLE NAME	NUM./ DENOM.	FACTOR	ORDER	CONS-TRAINT	VALUE	STD ERROR	T VALUE
1	CNST		CNST	1	0	NONE	12.53	0.4451	27.86
2		B25SER	NUM.	1	0	NONE	-2.6308	0.8542	-3.08
3	PHI	B25SER	DENM	1	1	EQ 01	.7066	.0713	9.91
4		B51SER	NUM.	1	0	NONE	3.0630	0.8653	3.54
5		B51SER	DENM	1	1	NONE	.9891	.0160	61.78
6		B58SER	NUM.	1	0	NONE	4.7394	0.9613	4.93
7		B58SER	DENM	1	1	NONE	.5850	.1806	3.24
8		B76SER	NUM.	1	0	NONE	1.1083	0.7942	3.94
***	PHI	CXOVALI	D-AR	1	1	EQ 01	.7066	.0713	9.91

TOTAL NUMBER OF OBSERVATIONS. 82
EFFECTIVE NUMBER OF OBSERVATIONS. 81
RESIDUAL STANDARD ERROR . . . . . .110831E+01

5.3.2 Alternative Chart

Although the combined monitoring techniques give a visual representation of the outliers, they still do not allow a direct visual display of the process variable understudy. Also, throughout this thesis, we observed the tight link that exists between "forecasting" and "monitoring". The forecasting performance of a process is very dependent on the effectiveness on the monitoring technique. It would then be very useful to have a chart that includes all the information needed to assess the performance of a process. Figure 5.3 gives an alternative chart for simultaneous forecasting and monitoring.

This alternative chart consists of a traditional one-step-ahead forecast chart along with control limits. These limits are set equal to ±3 standard error of the one-step-ahead forecasts. The benefit of using such a chart is that all the information is now summarized into one chart. The above chart shows, as expected, an out-of-control point at $t = 76$. On the other hand, data point $t = 74$ seems to be just under the upper control limit.

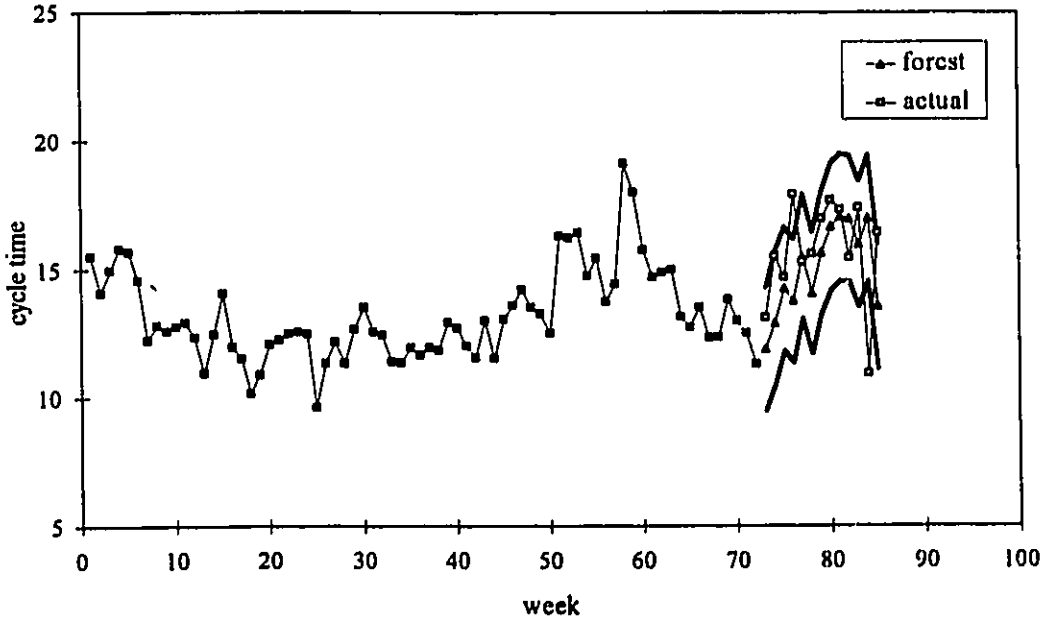

Figure 5.3 Alternative Chart on the In-date Cycle Time for the Overall Process.

5.3.3 Dealing with End-of-Series Events

As illustrated throughout this work, an outlier that occurs at the end of a series can substantially affect the forecasts of a model. Moreover, the effectiveness of outlier detection is decreased if outliers occur near the end of a time series. Forecasts are computed using the parameter estimates of the current model and the observations near the forecast origin. Due to the nature of outliers, a few observations are required, typically four (Liu and Hudak, 1992), after the time of the occurrence of an outlier to correctly identify its type. So at least five observations are needed to accurately identify the type (AO, IO, TC or LS) and the impact of an outlier. As a result, outliers that most impact forecasts are those at the end, or near the end, of a series. The choice of how to treat outliers occurring at the end of a series is therefore very important for the forecasting.

When an outlier is detected at the forecast origin of a series, it will always be *initially* identified as an AO. However, since our process is quite highly correlated, most of the outliers possess dynamics and behave as IOs, TCs and LSs. In forecasting, treating an outlier at the end of a series as an ordinary observation is the same as assuming that it is an IO (Ledolter 1989, Hillmer 1984, or Chen and Liu 1991). Consequently, it is recommended that any AO detected at the end of a series be neglected for forecasting purposes. On the other hand, any other type of outlier detected within the five last observations should be treated as a TC ($\delta = 0.7$) innovation when forecasting. The reason for this is that it is the only type of innovational model that is capable of representing all the others, (i.e. the δ can vary from 0.0 to 1.0). If $\delta = 0.0$ then the outlier is an AO, if $\delta =$ 1.0 then the outlier is an LS and finally if $\delta = \phi$ then the outlier is an IO.

The study of outliers is important in the study of time series analysis. As mentioned by Pankratz (1991), outliers are clues that can lead us to uncover the causes of changes in the behavior of the data. It is highly recommended, in any case, to use *personal judgment* on the nature of an outlier in the forecasting process. One should

always seek information about the potential causes of detected outliers. This may lead to improving the process under study.

The SCA software suggests that the critical value of the control limits be reduced from 3σ to 2.5σ at the end of the series when forecasting. However, the process under study, like many others applications in the manufacturing industry, is highly correlated and frequently subjected to significant outliers. This could lead to a high number of false alarms (type II errors), to spurious outliers and to biased forecasts. So, it is recommended that the 3σ limits be retained for monitoring purposes.

A strategy for simultaneous outlier treatment and forecasting is proposed from the above analysis (see Figure 5.4). This procedure has been used throughout this work for monitoring and forecasting purposes. It focuses on the treatment of end-of-series events in the forecasting process. In this procedure, the series is updated as more data become available. New estimates of the model parameters are then calculated using both the traditional estimation procedure and the joint detection-estimation procedure. If the series is affected by some outliers, they should show in the residuals from the traditional estimation procedures. As discussed in Section 5.2.2, these "infected" residuals are monitored in the special cause chart. Using the joint detection-estimation procedure, a model that indicates an outlier within the last five observations of the fitted data series may not be reliable and consequently is treated as a temporary model. By contrast, a permanent model is one that does not include an outlier within the last five observations of the fitted series. When a permanent model changes, the control limits of the special cause chart are reset. The temporary model is used for forecasting purposes, since it represents the most current available information. Results from the forecasting process, are then used to update the alternative chart. As discussed earlier, AO outliers are neglected whereas all other type of outliers that contain dynamics (IO, LS and TC) are always treated as TC. This is due to the fact that TC models can represent all other innovations during the joint estimation stage.

An interesting point here, is that recent papers and articles (e.g. Chen and Liu, 1993) have been discussing how critical the treatment of outliers occurring near the end of a series can be. However, no specific quantification of the notion "near the end of a series" has been made. In other words, no specific work has been done to determine the number of points needed to detect and correctly identify the type of outlier. Simulations need to be carried out for different forms of ARIMA models and different types of outliers (i.e., AO, IO, TC and LS) with different magnitudes to answer this question. Average Run Lengths could then be determined for each case.

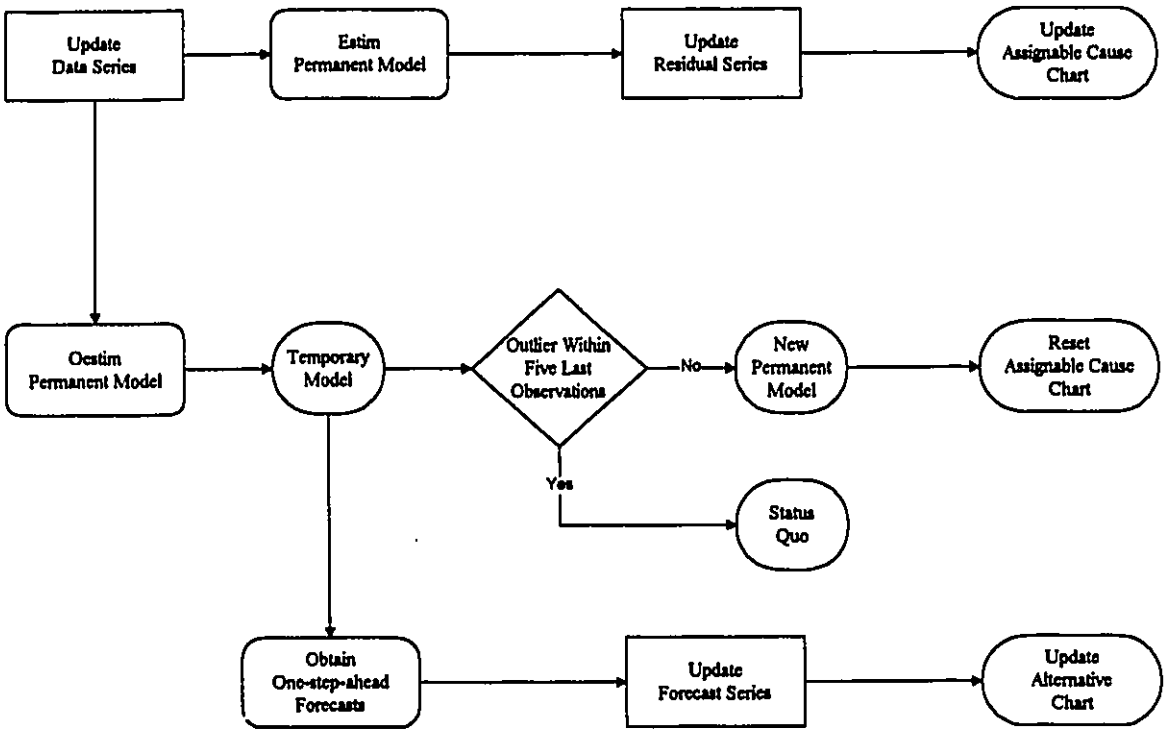

Figure 5.4 Suggested Strategy for Simultaneous Outlier Treatment and Forecasting.

5.4 Conclusions and Recommendations

5.4.1 Conclusions

1. An outlier-adjusted chart has been suggested for processes that are frequently subjected to significant outliers. This chart combines the traditional special-cause chart with the outlier detection scheme. The improved special-cause chart is now more sensitive. Also, when an outlier is detected, this chart can be updated without stopping the monitoring process. This should allow continuous process monitoring which is needed for optimal quality improvement.
2. An alternative chart for simultaneous forecasting and monitoring was also suggested. This chart has the benefit of including all the needed information in one chart.
3. A strategy for simultaneous outlier treatment and forecasting was proposed. This method more fully adresses the treatment of end-of-series events in the forecasting process.

5.4.2 Recommendations

Some simulations should be carried out for different time series models and different forms of outliers to quantify the notion " end-of-series" and to more fully evaluate the proposed detection-forecasting procedure.

Chapter Six

SUMMARY OF CONCLUSIONS, RECOMMENDATIONS AND CONTRIBUTIONS TO KNOWLEDGE

6.1 Conclusions

6.1.1 Forecasting Cycle Times and Yields with ARIMA Models

1. Cycle times were found to follow an AR(1) model for the overall process as well as for the different technologies. This result suggests that an observation at time $t = T$ is directly dependent on the previous observation at time $t = T-1$.
2. Yields were found to follow a white noise process. However, this does not ensure that the inherent yield process does not have any dynamics. Two reasons could explain the observed white noise behaviour:

- infrequent sampling could make the observed yield approach a white noise process.

3. In general, the in-date time basis gave better results than the out-date time basis. Out-date cycle times and yields were underestimated. ARIMA models fitted the in-date data much better than the out-date data. Out-date cycle times were more highly correlated. Many more outliers were detected using the in-date time basis. This suggests the presence of some masking effects in outlier detection when the out-date time basis is used.
4. Joint estimation of outliers and model parameters was essential in this work since outliers were found to significantly alter model parameters. For cycle time data, outliers inflated the ϕ term in the AR(1) model suggesting a more highly correlated process. Intervention models that corrected for the outlier effects fitted the data much better than the traditional ARIMA models.

6.1.2 Forecasting Cycle Times and Yields with TF Models

1. In general, standard errors of TF forecasts were smaller than those for ARIMA forecasts.
2. Due to the presence of many significant outliers, no obvious improvement was observed when comparing TF forecasts to ARIMA forecasts.
3. Overall, the in-date time basis gave better modeling and forecasting results.

6.1.3 Process Monitoring, Control and Continuous Improvement

1. An outlier-adjusted chart has been suggested for processes that are frequently subjected to significant outliers. This chart combines the traditional special-cause chart with the outlier detection scheme. The improved special-cause chart is now more sensitive. Also, when an outlier is detected, this chart can be updated without

stopping the monitoring process. This should allow continuous process monitoring which is needed for optimal quality improvement.

2. An alternative chart for simultaneous forecasting and monitoring was also suggested. This chart has the benefit of including all the needed information in one chart.
3. A strategy for simultaneous outlier treatment and forecasting was proposed. This method more fully adresses the treatment of end-of-series events in the forecasting process.

6.2 Recommendations

6.2.1 Forecasting Cycle Times and Yields with ARIMA Models

1. More data should be collected to increase the precision in the estimated model parameters and the sensitivity to outlier detection.
2. In order to check if the yields follow a white noise process two things should be done
    - data should be collected more frequently;
    - noise should be minimized.

6.2.2 Forecasting Cycle Times and Yields with TF Models

In order to obtain adequate long-term forecasts using the TF models, outliers should be minimized in the process. No matter how good the forecasting models are, they can never anticipate the occurrence of an outlier. Consequently, some process monitoring and control techniques should be applied to minimize outliers as well as the magnitude of the noise term.

6.2.3 Process Monitoring, Control and Continuous Improvement

Some simulations should be carried out for different time series models and different forms of outliers to quantify the notion " end-of-series" and to more fully evaluate the proposed detection-forecasting procedure.

6.3 Contributions to Knowledge

The outlier detection scheme and the intervention analysis were combined to develop "improved" ARIMA and TF models. This allowed better representation of the cycle times and yields.

The alternative time basis (in-date) overcame the difficulties of the current time basis (out-date).

Development of a strategy incorporating two new control charts to continuously monitor and control the process. These charts utilize intervention analysis allowing us to keep using available data while investigating the cause of special events.

Better forecasting should result from using the suggested strategy for simultaneous forecasting and control.

Chapter Seven

REFERENCES

Abraham, B., and Ledolter, "Statistical Methods for Forecasting", Wiley, New York (1983).

Alwan, L.C. and Roberts, H.V., "Time Series Modeling for Statistical Process Control", Journal of Business & Economic Statistics, 6, 87-95, (1985).

Anderson, T.W., "The Statistical Analysis of Time Series", Wiley, New York (1971).

Barlett, M.S., "An Introduction to Stochastic Processes with Special Reference to Methods and Applications", 2nd.ed., Cambridge (1966).

Box, G.E.P and G.M. Jenkins, "Time Series Analysis: Forecasting and Control", Holden Day, San Francisco (1976).

Chang, I., "Effect of Exogeneous Interventions on the Estimation of Time Series Parameters", American Statistical Association, Proceedings of the Business and Economic Statistics Section, Washington (1983).

Chang, I., Tiao, G.C. and Chen, C., "Estimation of Time Series Parameters in the Presence of Outliers", Technometrics, 30, 193-204, (1988).

Chen, C. and Liu, L.M., "Joint Estimation of Model Parameters and Outlier Effects in Time Series", Working Paper Series, Scientific Computing Associates, Illinois, (1993).

Chen, C. and Liu, L.-M., "Forecasting Time Series with Outliers", Working Paper Series, Scientific Computing Associates, Illinois, (1991).

Chen, C and Liu, L.-M, "Joint Estimation of Model Parameters and Outlier Effects in Time Series", SCA Working Paper, 126, Scientific Computing Associates (1992).

Cryer, J.D., "Time Series Analysis", Duxbury Press, Boston (1986).

Guttman, I. and Tiao, G.C., "Effect of Correlation on the Estimation of a Mean in the Presence of Spurious Observations", The Canadian Journal of Statistics, 6, 229-247 (1978).

Harris, T.J. and W.H. Ross, "Statistical Process Control Procedures for Correlated Observations", Can. J. Chem. Eng., 69, 48-57 (1991).

Hillmer, S.C., "Monitoring and Adjusting Forecasts in the Presence of Additive Outliers", Journal of Forecasting, 3, 205-215 (1984).

Hudak, G.B. and Liu, L.-M., "Transfer Function Modeling: Simplification and Applications", SCA Working Papers, 117, Scientific Computing Associates (1988).

Ledolter, J., "The Effect of Outliers on the Estimates and the Forecasts from ARIMA Time Series Models", American Statistical Association 1987 Proceedings of the Business and Economic Statistics Section", 453-458 (1987).

Ledolter, J., "The Effect of Additive Outliers on the Forecasts from ARIMA Models", International Journal of Forecasting, 5, 231-240 (1989).

Liu, L.-M., "Estimation of Rational Transfer Function Models", SCA Workpapers, 107, Scientific Computing Associates (1983).

Liu, L.-M., "Sales Forecasting and Production Planning Using Multi-variable Time Series Methods", SCA Working Papers, 113, Scientific Computing Associates (1985).

Liu, L.-M., "Sales Forecasting Using Multi-Equation Transfer Function Models", Journal of Forecasting, 6, 223-238 (1987).

Liu, L.-M., "Use of Linear Transfer Function Analysis in Econometric Time Series Modeling", SCA Working Papers, 122, Scientific Computing Associates (1991).

Liu, L.-M., Hudak, G.B., Box, G.E.P., Muller, M.E. and Tiao, G.C., "The SCA Statistical System: Reference Manual for Forecasting and Time Series Analysis", DeKalb, IL: Scientific Computing Associates (1993).

Liu, L.-M., and Chen, C., "Recent Developments of Time Series Analysis in Intervention in Environmental Impact Studies", Journal of Environmental Science and Health, A26, 1217-1252 (1991).

Liu, L.-M., "Modeling and Forecasting Time Series Using an Expert System Approach", SCA Working Paper, 127, Scientific Computing Associates (1993).

Ljung, G.M., and Box, G.E.P., "On a measure of Lack of Fit in Time Series Models", Biometrika, 65, 297-304 (1978).

Pankratz, A., "Forecasting with Univariate Box-Jenkin Models: Concepts and Cases", Wiley, New York (1983).

Pankratz, A., "Forecasting with Dynamic Regression Models", Wiley, New York, (1991).

Ryan, T.P., "Statistical Methods for Quality Improvement", Wiley, New York (1989).

Tsay, R.S. and Tiao, G.C. (1984), "Consistent Estimates of Autoregressive Parameters and Extended Sample Autocorrelation Function for Stationary and Non-stationary ARMA Models", J.A.S.A., 79, 84-96, (1984).

Tsay, R.S. and Tiao, G.C., "Use of Canonical Analysis in Time Series Model Identification", Biometrica, 72, 299-315, (1985).

Tsay, R.S., "Outliers, Level Shifts and Variance Changes in Time Series", Journal of Forecasting, 7, 1-20 (1988).

Vandaele, W., "Applied Time Series Analysis and Box-Jenkins Models", Academic Press., New York, (1983).

Wei, W.W.S, "Time Series Analysis: Univariate and Multivariate Methods", CA: Adison-Wesley, Redwood City, (1990).

Wold, H., "A Study in the Analysis of Stationary Time Series", Uppsala: Almquist and Wicksell, (1938).

Appendix A

PROCESS FLOW DIAGRAM FOR CMOS FABRICATION

There are many processing variations for achieving specific MOS transistor structures. However, the processes used by each company usually contain the same fundamental stages. Typically, wafer fabrication involves a series of photolithography (PE) steps, between which are various cycles of oxidation, chemical vapor deposition (CVD), diffusion, ion implantation, etching and stripping. An example of a work flow for wafer fabrication is shown here.

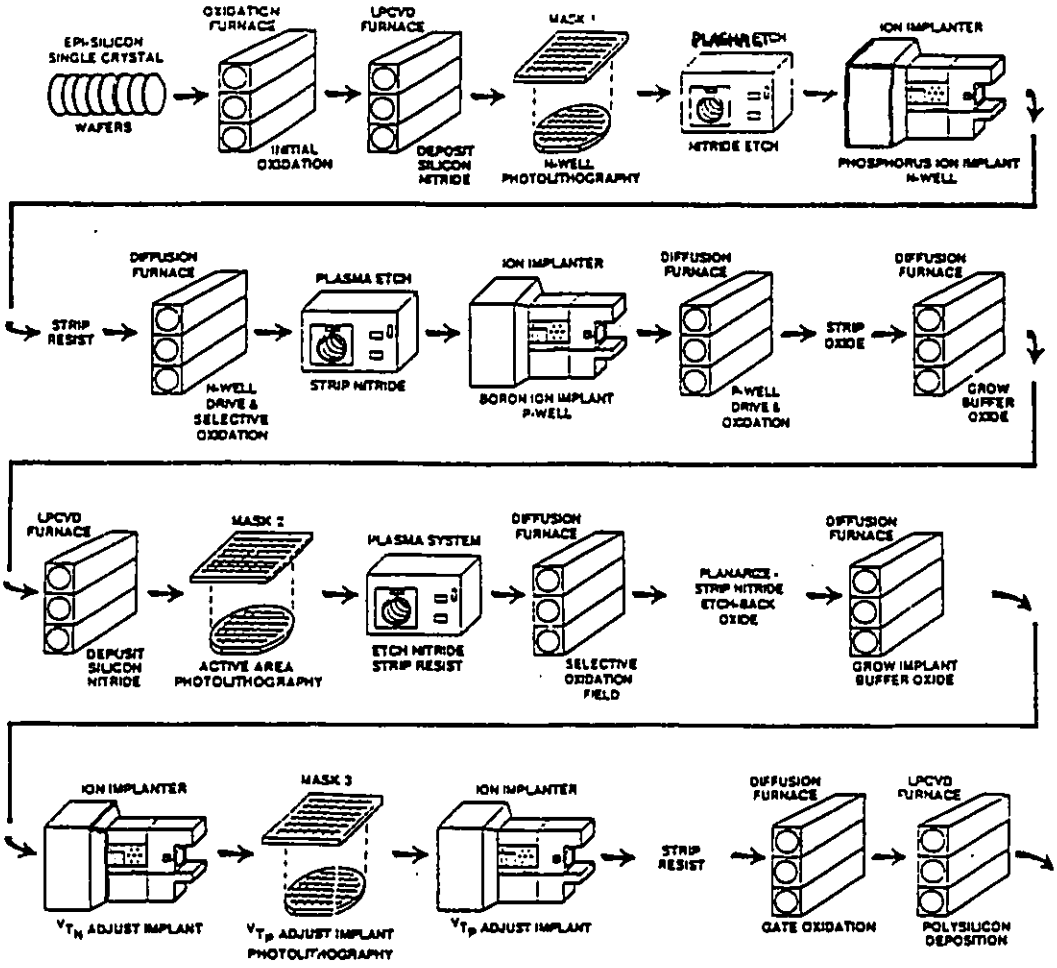

Figure A Process Flow Diagram for CMOS Fabrication

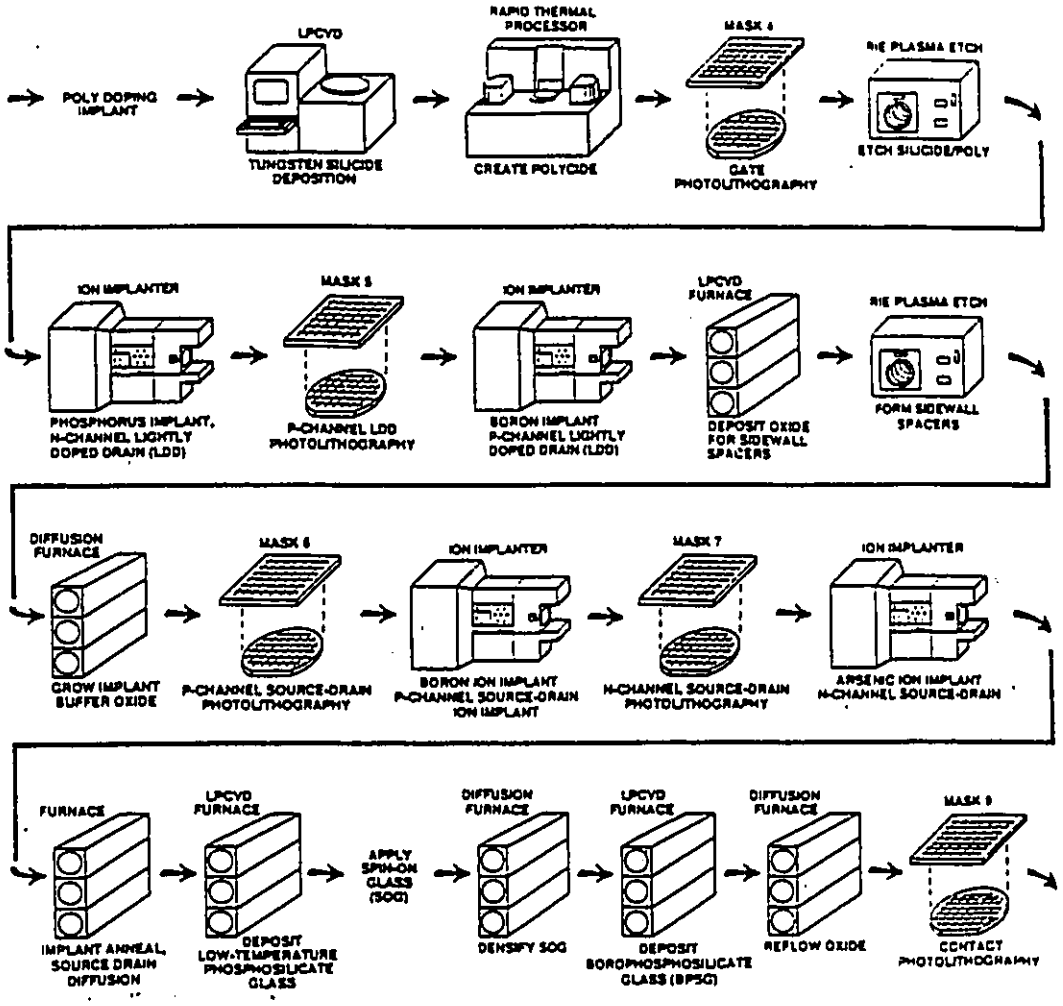

Figure A **Process Flow Diagram for CMOS Fabrication (continued)**

Appendix B

CYCLE TIMES AND YIELDS FOR THREE OTHER TECHNOLOGIES

This appendix contains plots of the cycle time and the yield data for the three technologies: CMOS (1.5μm dlm), CMOS (1.2μm dlm) and CMOS (1.2μm tlm).

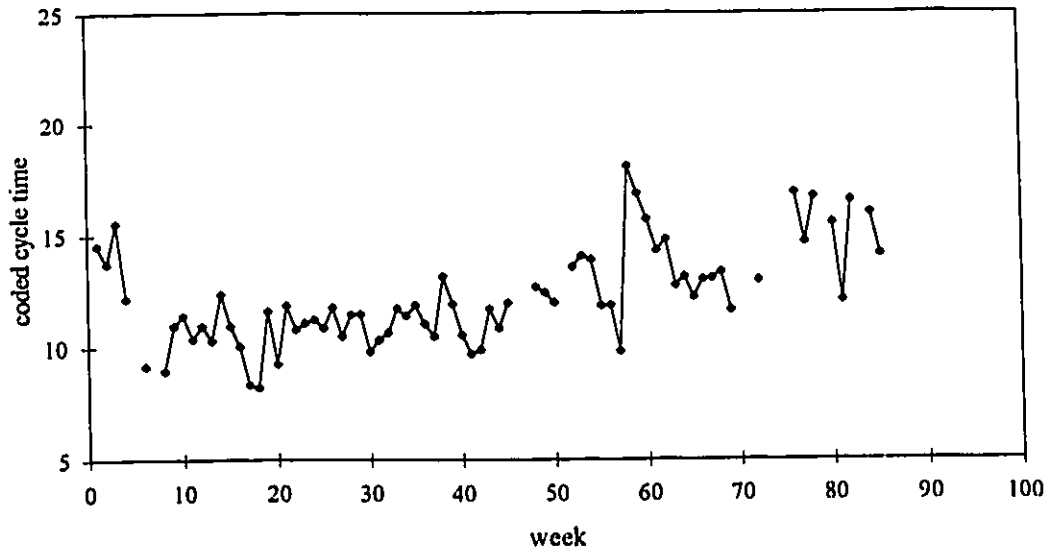

(a)

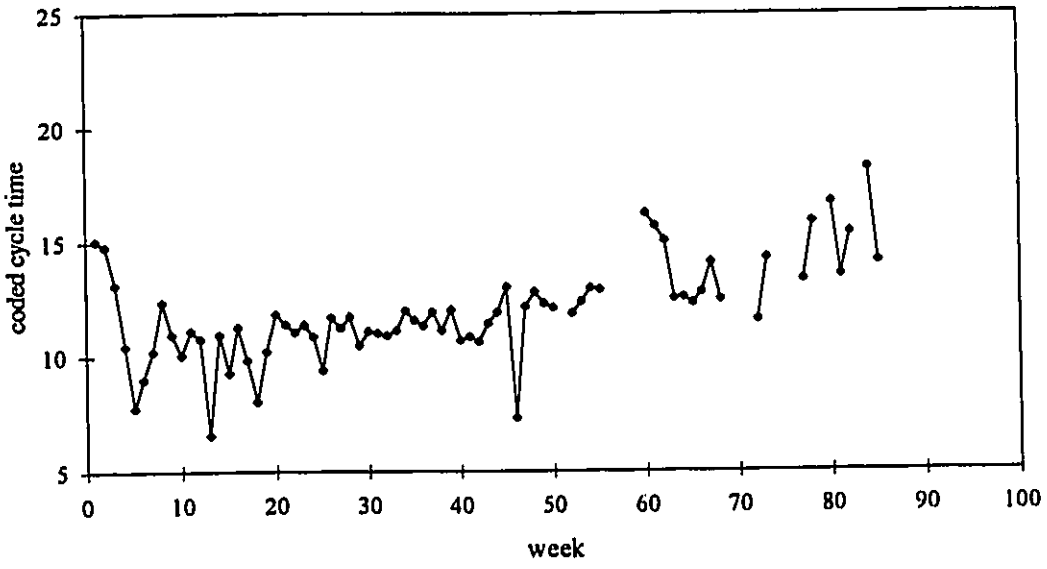

(b)

Figure B.1 Plot of the Coded Cycle Time Data for the CMOS(1.5μm dlm) Technology Using (a) In-date Time Basis (b) Out-date Time Basis

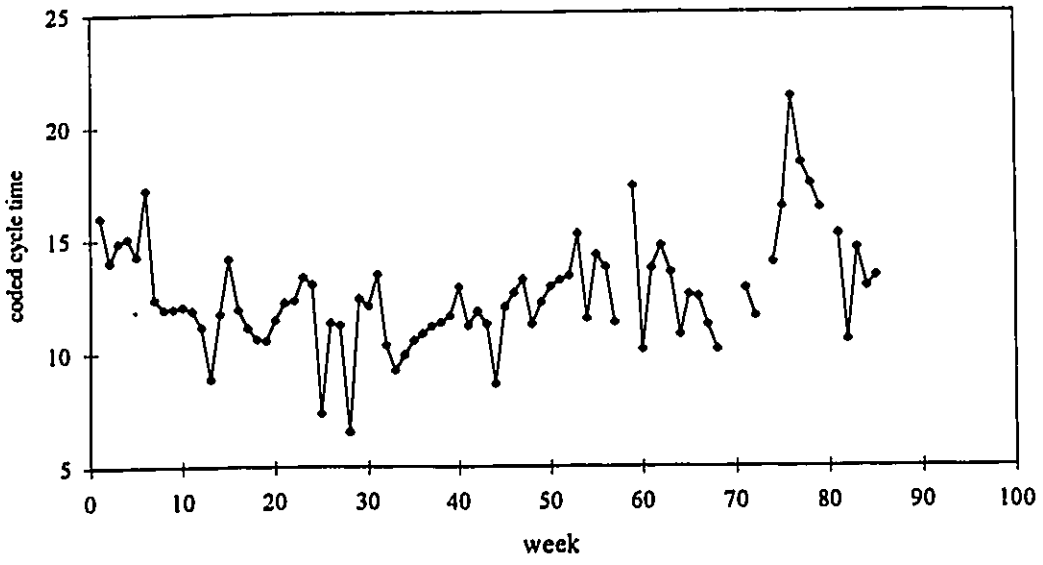

(a)

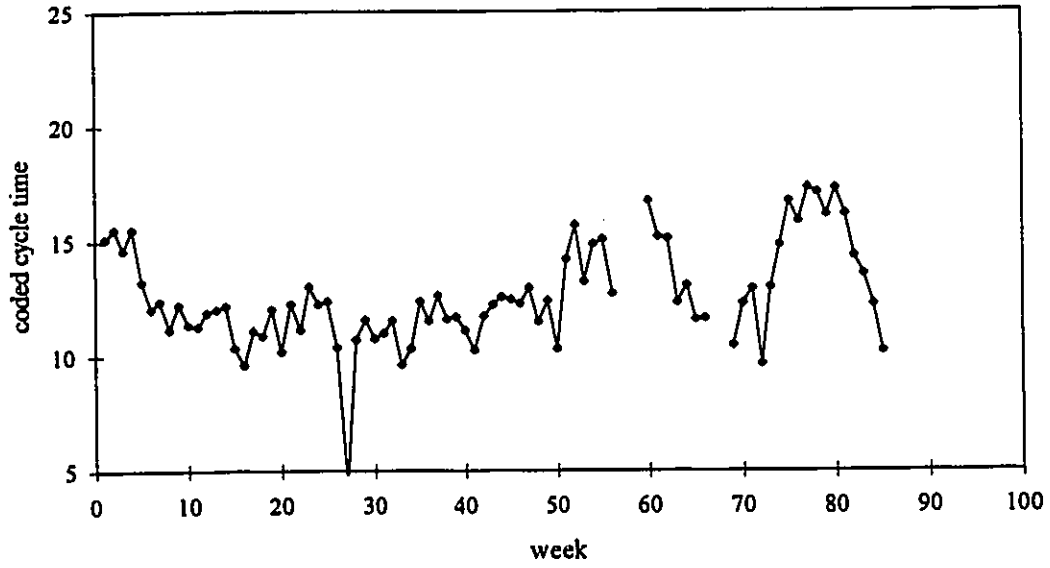

(b)

Figure B.2 Plot of the Coded Cycle Time Data for the CMOS(1.2μm dlm) Technology Using (a) In-date Time Basis (b) Out-date Time Basis

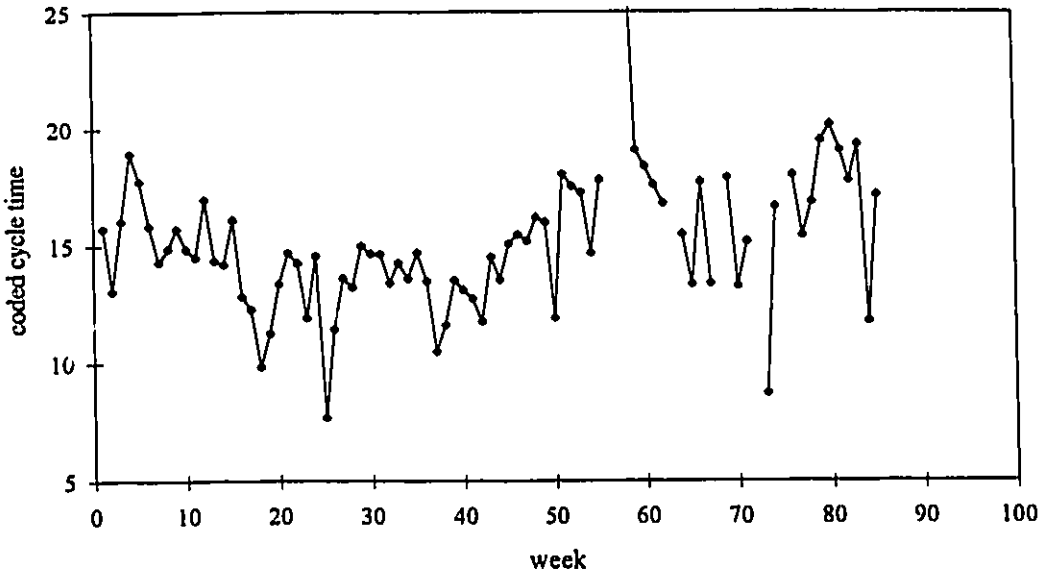

(a)

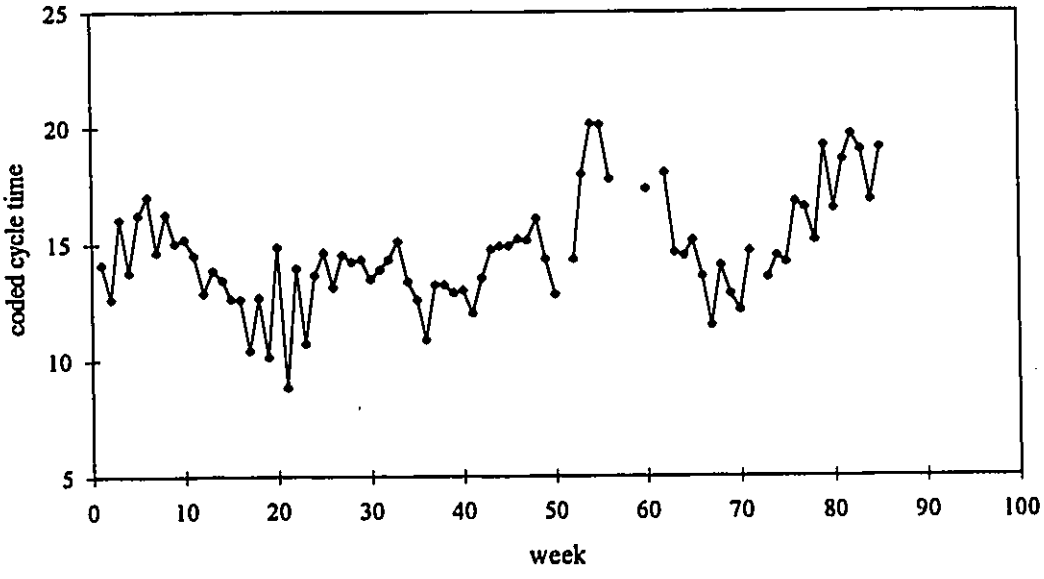

(b)

Figure B.3 Plot of the Coded Cycle Time Data for the CMOS(1.2μm tlm) Technology Using (a) In-date Time Basis (b) Out-date Time Basis

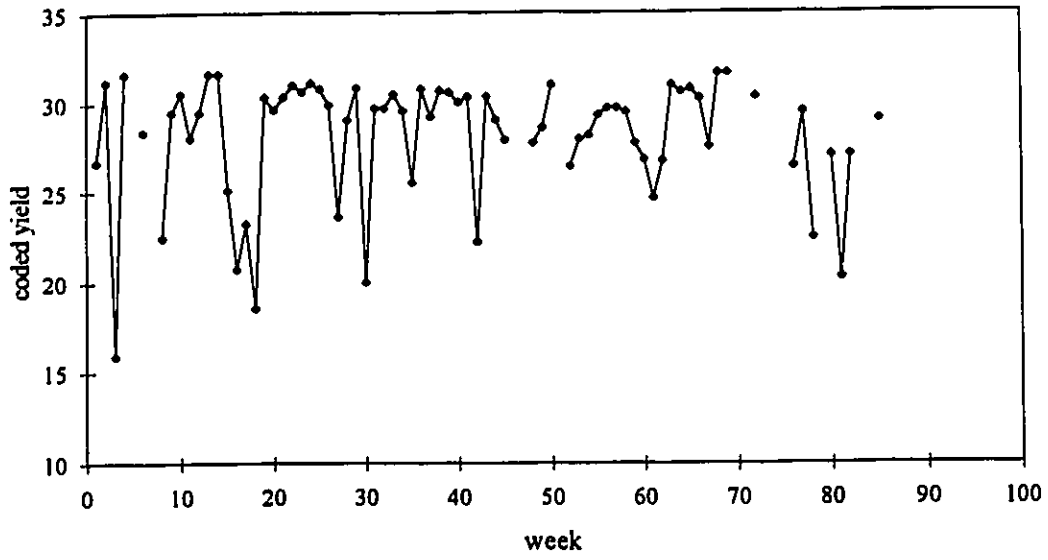

a)

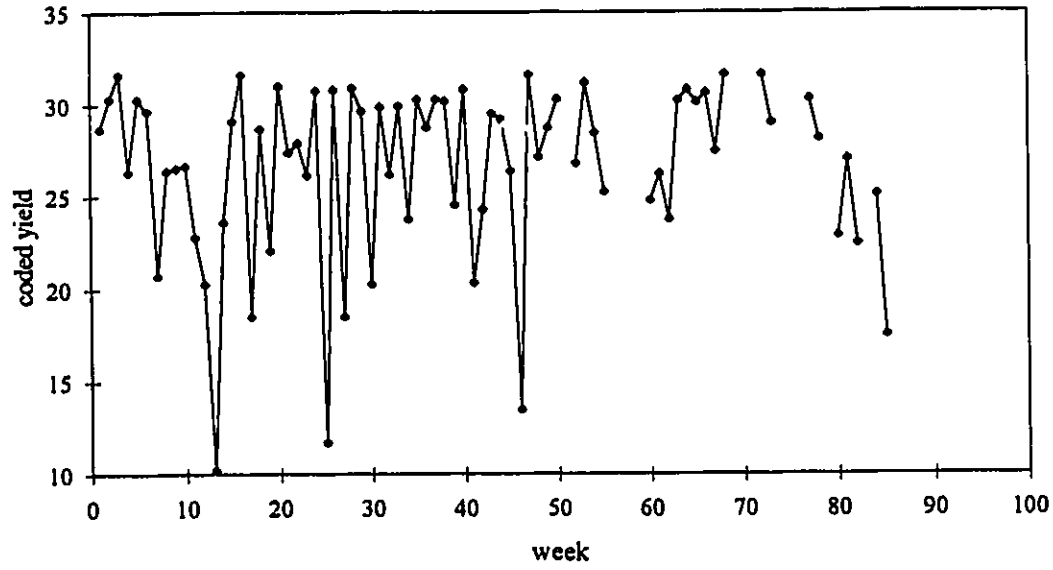

b)

Figure B.4 Plot of the Coded In-date Yield Data for the CMOS(1.5μm dlm) Technology Using (a) In-date Time Basis (b) Out-date Time Basis

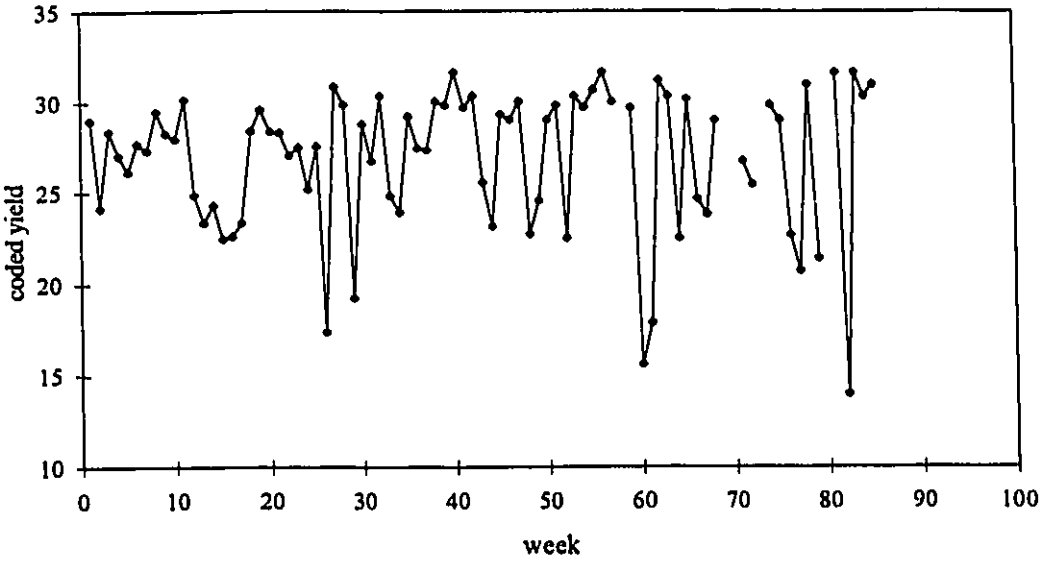

a)

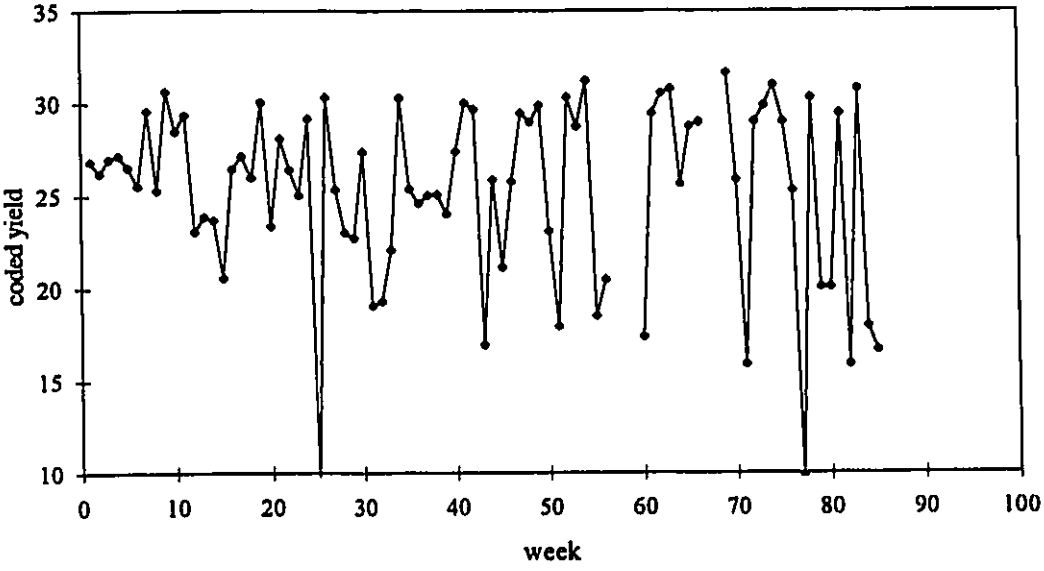

b)

Figure B.5 Plot of the Coded Yield Data for the CMOS(1.2μm dlm) Technology Using (a) In-date Time Basis (b) Out-date Time Basis

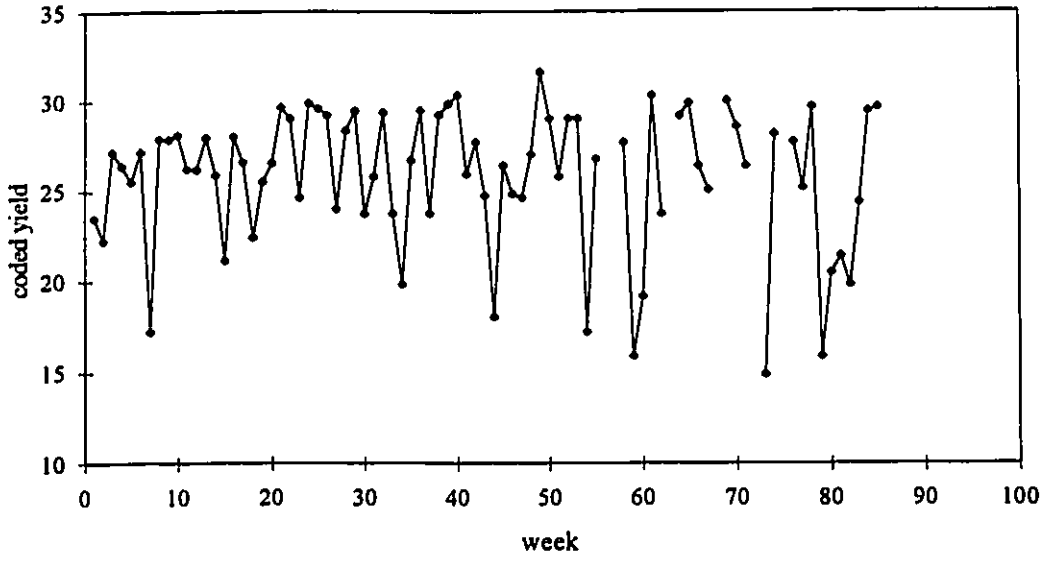

a)

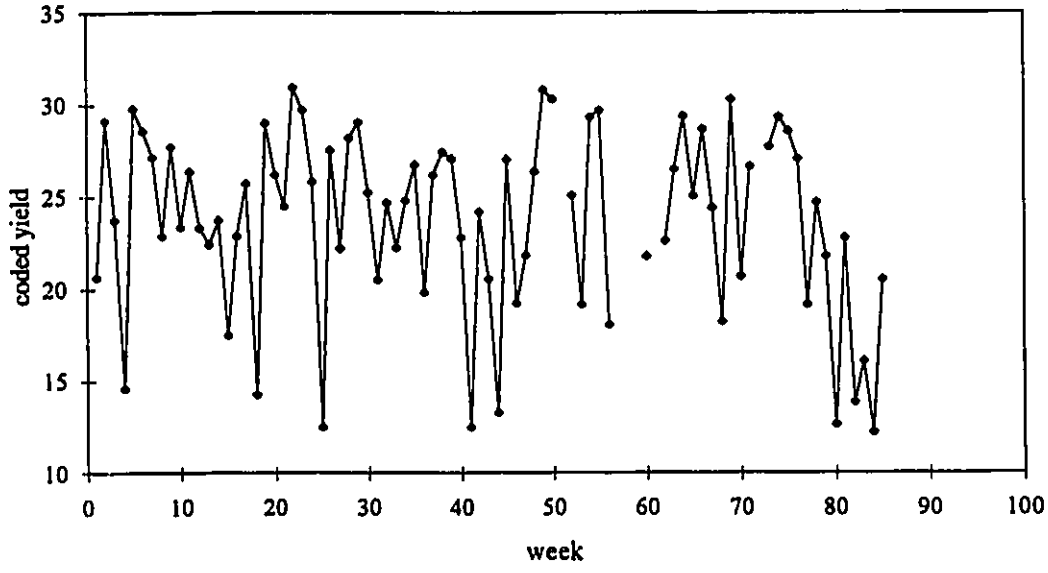

b)

Figure B.6 Plot of the Coded Yield Data for the CMOS(1.2μm tlm) Technology Using (a) In-date Time Basis (b) Out-date Time Basis

Appendix C

JOINT DETECTION-ESTIMATION RESULTS FOR OTHER THREE TECHNOLOGIES

This appendix contains complete joint detection-estimation results (identification, estimation and diagnostic check) of the cycle times and the yields for the three technologies: CMOS (1.5μm dlm), CMOS (1.2μm dlm), CMOS (1.2μm tlm).

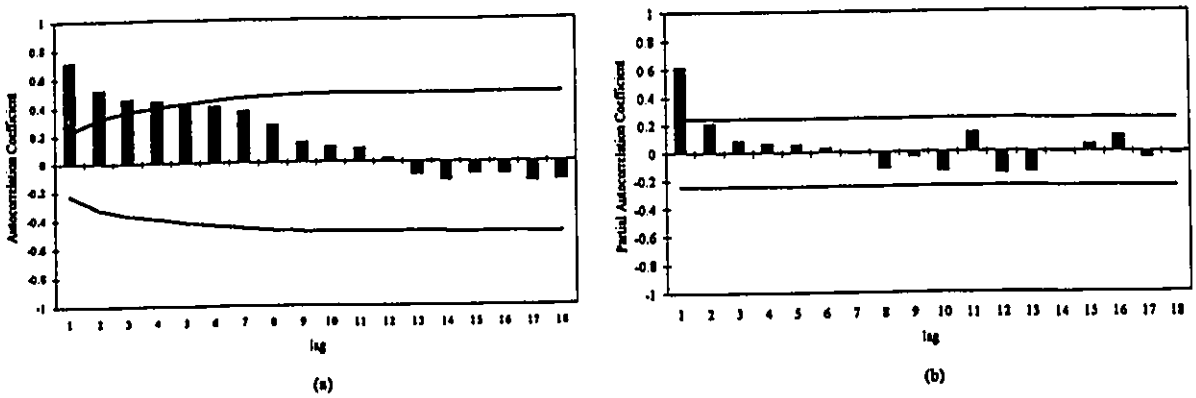

Figure C.1 Coded In-date Cycle Time for the CMOS(1.5μm dim) Process
a) Autocorrelation Function
b) Partial Autocorrelation Function

Table C.1 ARIMA Joint Detection-Estimation Results of the Coded In-date Cycle Time for the CMOS(1.5μm dim) Process

PARAMETER LABEL	VARIABLE NAME	NUM./ DENOM.	FACTOR	ORDER	CONS-TRAINT	VALUE	STD ERROR	T VALUE
1 CNST		CNST	1	0	NONE	12.1000	.3439	35.18
2	B58SER	NUM.	1	0	NONE	7.7000	1.0921	7.05
3	B58SER	DENM	1	1	NONE	.8087	.0554	14.61
4 PHI	Zt	D-AR	1	1	NONE	.5409	.0958	5.71

TOTAL NUMBER OF OBSERVATIONS. 72
EFFECTIVE NUMBER OF OBSERVATIONS. 71
RESIDUAL STANDARD ERROR . . . . . .126332E+01

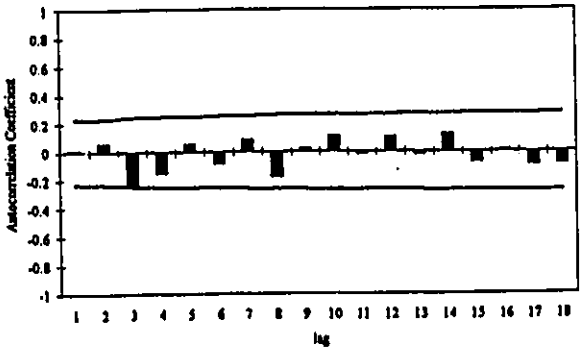

Figure C.2 Autocorrelation Function of the Residuals from the Above Fitted ARIMA Model

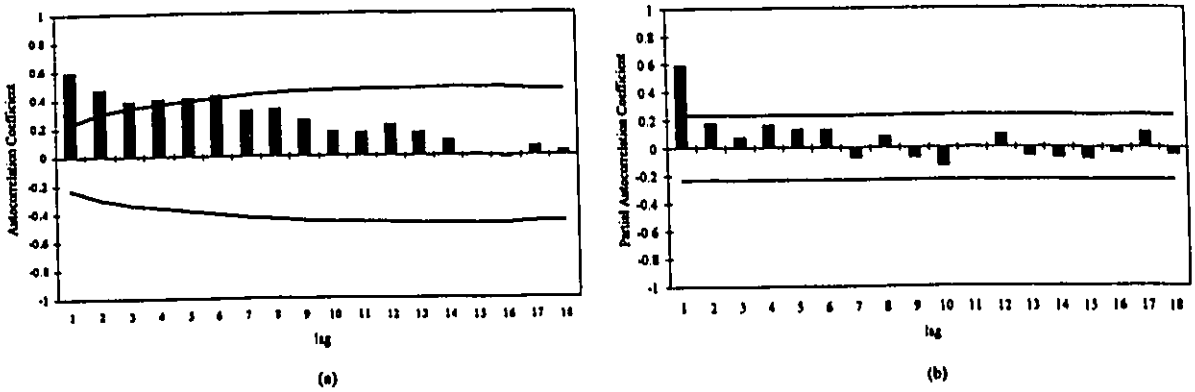

Figure C.3 Coded Out-date Cycle Time Data for the CMOS(1.5μm dlm) Process
a) Autocorrelation Function
b) Partial Autocorrelation Function

Table C.2 ARIMA Joint Detection-Estimation Results of the Coded Out-date Cycle Time for the CMOS(1.5μm dlm) Process

PARAMETER LABEL	VARIABLE NAME	NUM./ DENOM.	FACTOR	ORDER	CONS-TRAINT	VALUE	STD ERROR	T VALUE
1 CNST1		CNST	1	0	NONE	11.8955	0.3624	32.82
2	B13SER	NUM.	1	0	NONE	-4.4764	0.8462	-5.29
3	B46SER	NUM.	1	0	NONE	-5.3875	1.3141	-4.10
4 PHI	Zt	D-AR	1	1	NONE	.7529	.0879	6.52
TOTAL NUMBER OF OBSERVATIONS.							72	
EFFECTIVE NUMBER OF OBSERVATIONS.							71	
RESIDUAL STANDARD ERROR						.119251E+01		

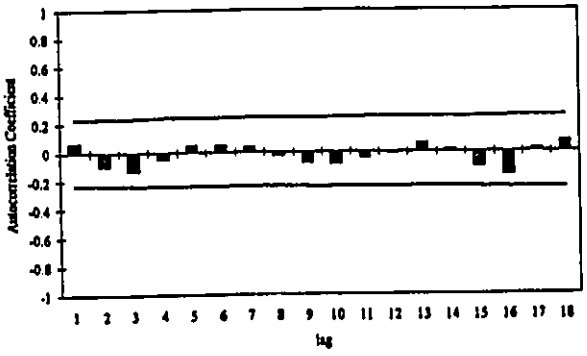

Figure C.4 Autocorrelation Function of the Residuals from the Above Fitted ARIMA Model

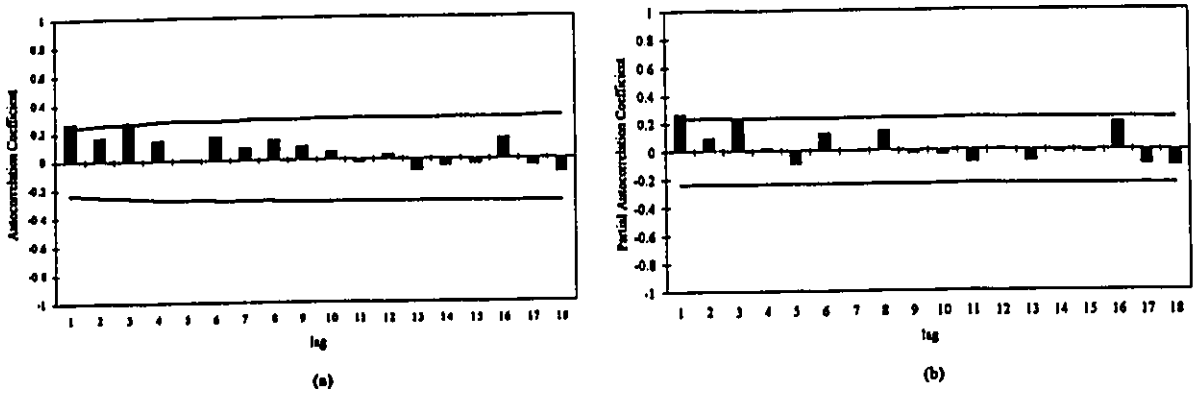

Figure C.5 Coded In-date Cycle Time of the Overall CMOS Process
a) Autocorrelation Function
b) Partial Autocorrelation Function

Table C.3. ARIMA Joint Detection-Estimation Results of the Coded In-date Cycle Time for the CMOS(1.2μm dlm) Process

PARAMETER LABEL	VARIABLE NAME	NUM./ DENOM.	FACTOR	ORDER	CONS-TRAINT	VALUE	STD ERROR	T VALUE
1 CNST1		CNST	1	0	NONE	12.5012	.2890	43.25
2	B6SER	NUM.	1	0	NONE	4.4013	1.1674	3.77
3	B25SER	NUM.	1	0	NONE	-5.0431	1.1484	-4.39
4	B28SER	NUM.	1	0	NONE	-5.5348	1.1365	-4.87
5	B59SER	NUM.	1	0	NONE	6.5247	1.1367	5.74
6 PHI	Zt	D-AR	1	1	NONE	.4775	.0986	4.84

TOTAL NUMBER OF OBSERVATIONS. 72
EFFECTIVE NUMBER OF OBSERVATIONS. 71
RESIDUAL STANDARD ERROR . . . . . .128053E+01

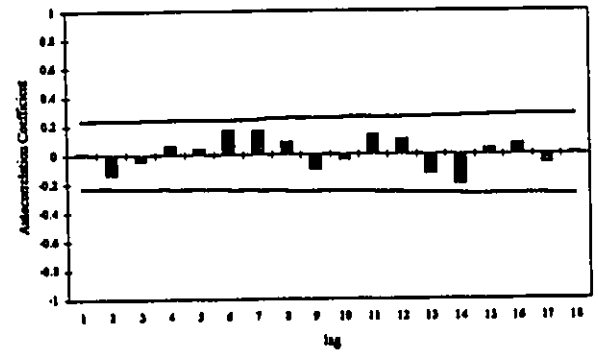

Figure C.6 Autocorrelation Function of the Residuals from the Above Fitted ARIMA Model

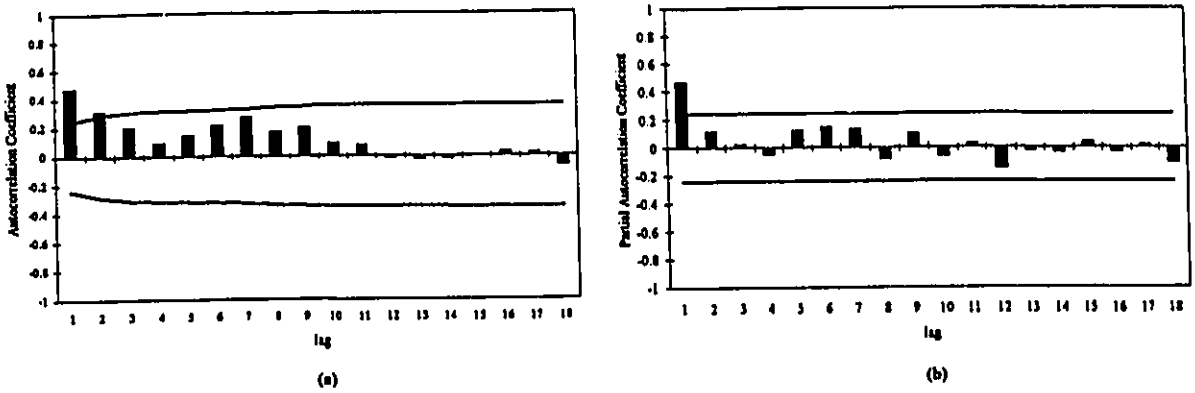

Figure C.7 Coded Out-date Cycle Time for the CMOS(1.2μm dlm) Process
a) Autocorrelation Function
b) Partial Autocorrelation Function

Table C.4 ARIMA Joint Detection-Estimation Results of the Coded Out-date Cycle Time for the CMOS(1.2μm dlm) Process

PARAMETER LABEL	VARIABLE NAME	NUM./ DENOM.	FACTOR	ORDER	CONS-TRAINT	VALUE	STD ERROR	T VALUE
1 CNST1		CNST	1	0	NONE	11.9400	0.3617	32.43
2	B27SER	NUM.	1	0	NONE	-3.0439	0.4598	-6.62
3	B51SER	NUM.	1	0	NONE	4.0873	1.0561	3.87
4	B51SER	DENM	1	1	NONE	.9126	.0425	21.47
5 PHI	Zt	D-AR	1	1	NONE	.5570	.0977	5.70
TOTAL NUMBER OF OBSERVATIONS.							72	
EFFECTIVE NUMBER OF OBSERVATIONS.							71	
RESIDUAL STANDARD ERROR						.129467E+01		

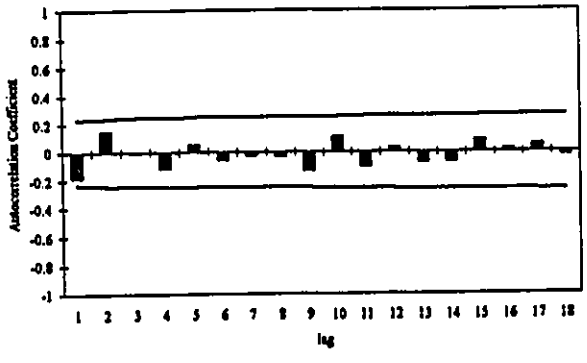

Figure C.8 Autocorrelation Function of the Residuals from the Above Fitted ARIMA Model

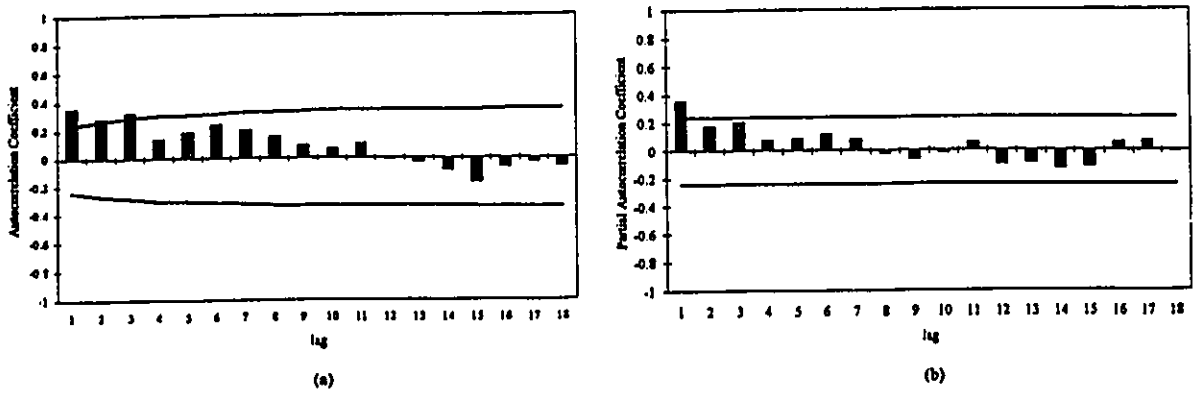

Figure C.9 Coded In-date Cycle Time for the CMOS(1.2μm tlm) Process
a) Autocorrelation Function
b) Partial Autocorrelation Function

Table C.5 ARIMA Joint Detection-Estimation Results of the Coded In-date Cycle Time for the CMOS(1.2μm tlm) Process

	PARAMETER LABEL	VARIABLE NAME	NUM./ DENOM.	FACTOR	ORDER	CONS-TRAINT	VALUE	STD ERROR	T VALUE
1	CNST		CNST	1	0	NONE	15.0243	0.3412	44.03
2		B25SER	NUM.	1	0	NONE	-20.7199	5.0494	-4.10
3	PHI	B25SER	DENM	1	1	NONE	.8190	.0724	3.89
4		B50SER	NUM.	1	0	NONE	-5.1342	1.2491	4.11
5		B58SER	NUM.	1	0	NONE	13.5459	1.4869	9.11
6		B66SER	NUM.	1	1	NONE	4.3940	1.1296	3.89
***	PHI	Zt	D-AR	1	1	EQ 01	.6432	.0724	3.89

TOTAL NUMBER OF OBSERVATIONS. 72
EFFECTIVE NUMBER OF OBSERVATIONS. 71
RESIDUAL STANDARD ERROR . . . . . .157454E+01

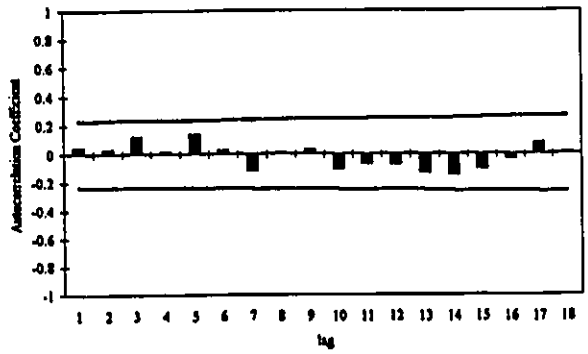

Figure C.10 Autocorrelation Function of the Residuals from the Above Fitted ARIMA Model

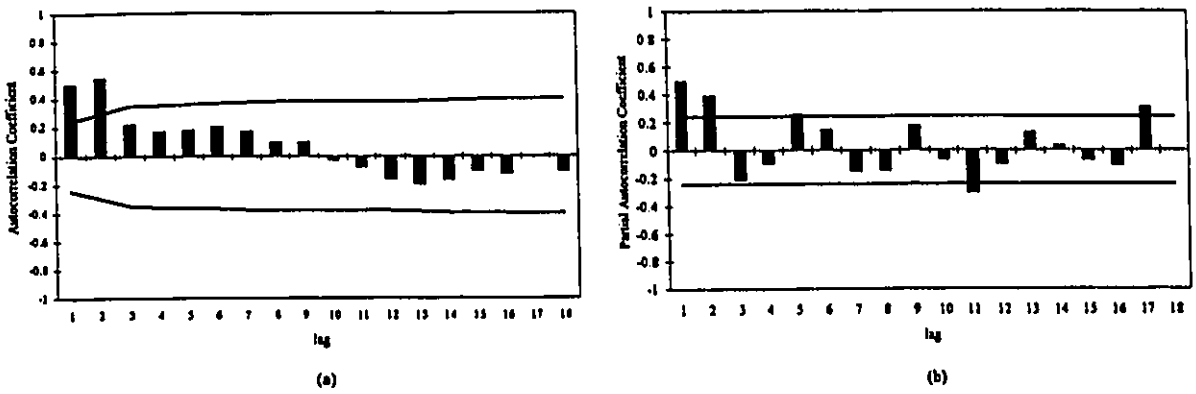

(a) (b)

Figure C.11 Coded Out-date Cycle Time for the CMOS(1.2μm tlm) Process
a) Autocorrelation Function
b) Partial Autocorrelation Function

Table C.6 ARIMA Joint Detection-Estimation Results of the Coded Out-date for the CMOS(1.2μm tlm) Process

PARAMETER LABEL	VARIABLE NAME	NUM./ DENOM.	FACTOR	ORDER	CONS-TRAINT	VALUE	STD ERROR	T VALUE
1 CNST		CNST	1	0	NONE	14.621	0.5538	26.40
2	B19SER	NUM.	1	0	NONE	-3.942	1.2318	-3.20
3	B21SER	NUM.	1	0	NONE	-5.785	1.1903	-4.86
4 PHI	Zt	D-AR	1	1	NONE	.8238	.0857	8.10

TOTAL NUMBER OF OBSERVATIONS. 72
EFFECTIVE NUMBER OF OBSERVATIONS. 71
RESIDUAL STANDARD ERROR . . . . . .15934E+01

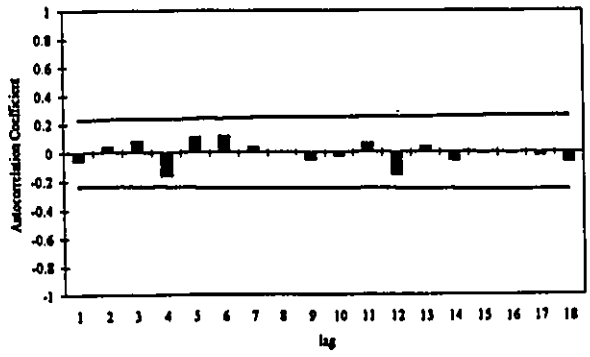

Figure C.12 Autocorrelation Function of the Residuals from the Above Fitted ARIMA Model

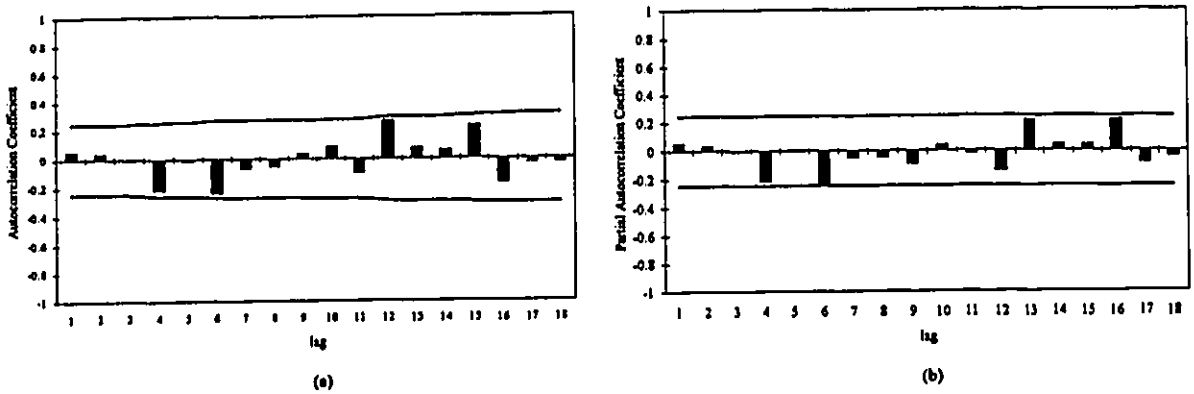

Figure C.13 Coded In-date Yield for the CMOS(1.5μm dlm) Process
a) Autocorrelation Function
b) Partial Autocorrelation Function

Table C.7 ARIMA Joint Detection-Estimation Results of the Coded In-date Yield for the CMOS(1.5μm dlm) Process

PARAMETER LABEL	VARIABLE NAME	NUM./ DENOM.	FACTOR	ORDER	CONS-TRAINT	VALUE	STD ERROR	T VALUE
1 CNST		CNST	1	0	NONE	28.9321	0.3532	81.92
2	B16SER	NUM.	1	0	NONE	-9.6802	2.6593	-3.64
3	B16SER	DENM	1	1	.IONE	.5770	.1577	3.66
4	B30SER	NUM.	1	0	NONE	-9.1014	2.8711	-3.17

TOTAL NUMBER OF OBSERVATIONS. 72
EFFECTIVE NUMBER OF OBSERVATIONS. 72
RESIDUAL STANDARD ERROR . . . . . .298416E+01 .

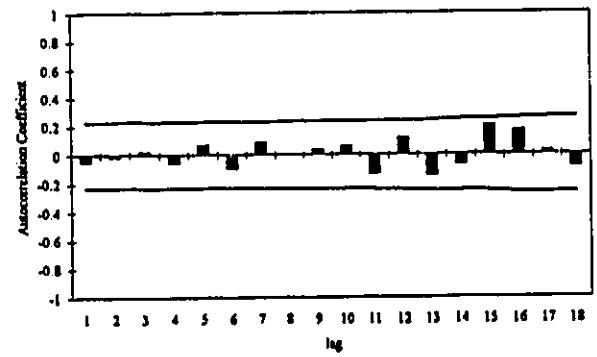

Figure C.14 Autocorrelation Function of the Residuals from the Above Fitted ARIMA Model

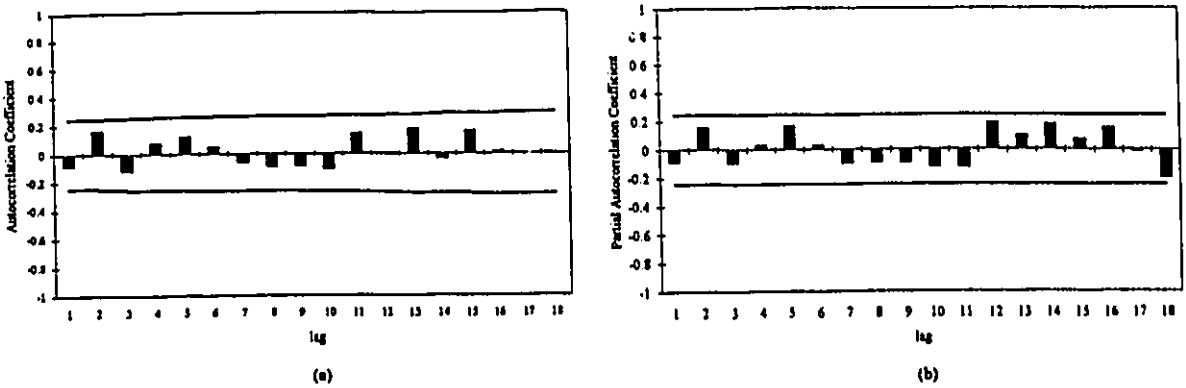

Figure C.15 Coded Out-date Yield for the CMOS(1.5μm dlm) Process
a) Autocorrelation Function
b) Partial Autocorrelation Function

Table C.8 ARIMA Joint Detection-Estimation Results of the Coded Out-date Yield for the CMOS(1.5μm dlm) Process

PARAMETER LABEL	VARIABLE NAME	NUM./ DENOM.	FACTOR	ORDER	CONS-TRAINT	VALUE	STD ERROR	T VALUE
1 CNST		CNST	1	0	NONE	27.6872	0.4005	69.12
2	B13SER	NUM.	1	0	NONE	-17.2382	3.2897	-5.24
3	B25SER	NUM.	1	0	NONE	-15.6941	3.2696	-4.80
4	B46SER	NUM.	1	0	NONE	-13.9845	3.2827	-4.26

TOTAL NUMBER OF OBSERVATIONS. 72
EFFECTIVE NUMBER OF OBSERVATIONS. 72
RESIDUAL STANDARD ERROR . . . . . .349675E+02

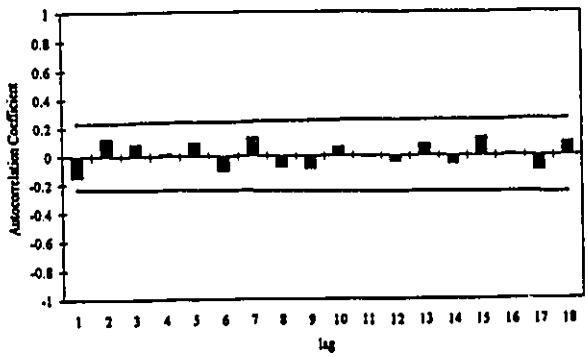

Figure C.16 Autocorrelation Function of the Residuals from the Above Fitted ARIMA Model

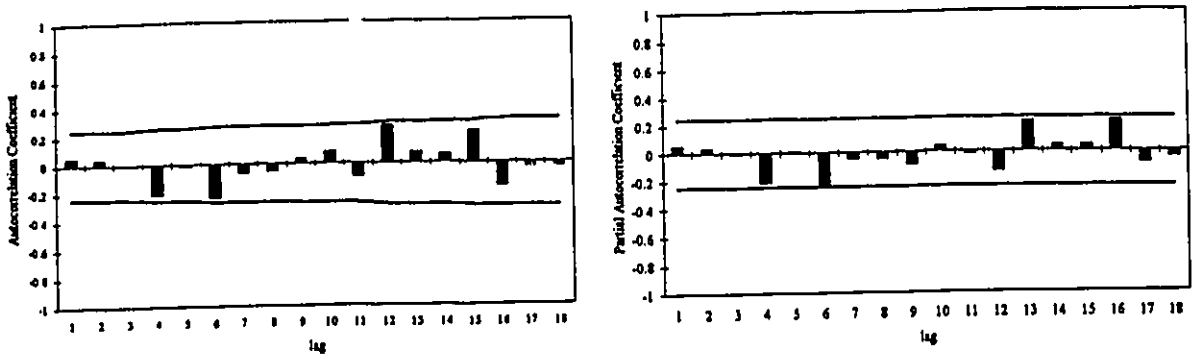

Figure C.17 Coded In-date Yield for the CMOS(1.2μm dlm) Process
a) Autocorrelation Function
b) Partial Autocorrelation Function

Table C.9 ARIMA Joint Detection-Estimation Results of the Coded In-date Yield for the CMOS(1.2μm dlm) Process

PARAMETER LABEL	VARIABLE NAME	NUM./ DENOM.	FACTOR	ORDER	CONS-TRAINT	VALUE	STD ERROR	T VALUE
1 CNST		CNST	1	0	NONE	27.9213	0.3552	78.60
2	B13SER	NUM.	1	0	NONE	-3.1021	1.0093	-3.13
3	B13SER	DENM	1	1	NONE	.7661	.1056	7.25
4	B26SER	NUM.	1	0	NONE	-10.5756	2.4594	-4.30
5	B29SER	NUM.	1	0	NONE	-8.8241	2.4580	-3.59
6	B60SER	NUM.	1	0	NONE	-12.9851	2.2197	-5.82
7	B60SER	DENM	1	1	NONE	.6300	.0975	6.46
8	B62SER	NUM.	1	0	NONE	8.4852	2.8004	3.03
TOTAL NUMBER OF OBSERVATIONS.							72	
EFFECTIVE NUMBER OF OBSERVATIONS.							72	
RESIDUAL STANDARD ERROR						.258353E+01		

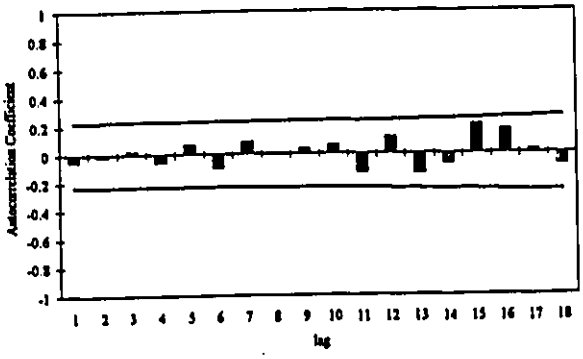

Figure C.18 Autocorrelation Function of the Residuals from the Above Fitted ARIMA Model

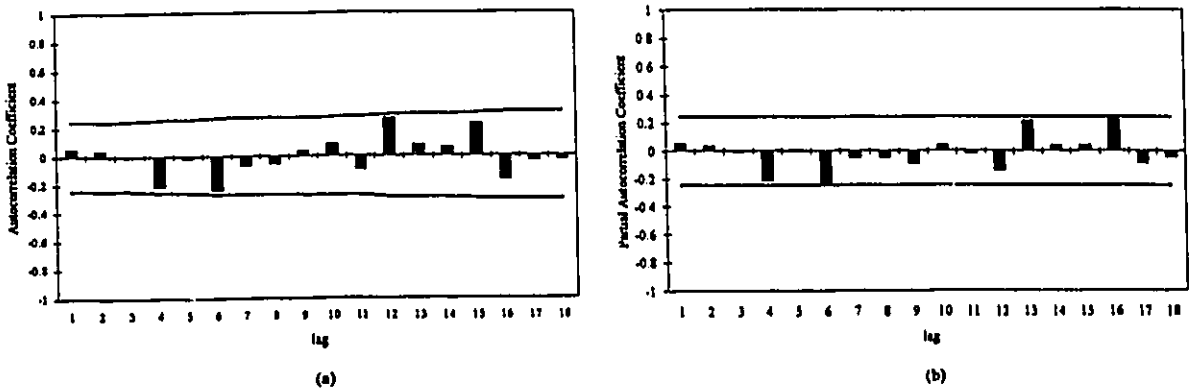

Figure C.19 Coded Out-date Yield for the CMOS(1.2μm dlm) Process
a) Autocorrelation Function
b) Partial Autocorrelation Function

Table C.10 ARIMA Joint Detection-Estimation Results of the Coded Out-date Yield for the CMOS(1.2μm dlm) Process

PARAMETER LABEL	VARIABLE NAME	NUM./ DENOM.	FACTOR	ORDER	CONS-TRAINT	VALUE	STD ERROR	T VALUE
1 CNST		CNST	1	0	NONE	25.8426	.4779	54.07
2	B25SER	NUM.	1	0	NONE	-15.9865	3.9668	-4.03

TOTAL NUMBER OF OBSERVATIONS. 72
EFFECTIVE NUMBER OF OBSERVATIONS. 72
RESIDUAL STANDARD ERROR . . . . . .419246E+02

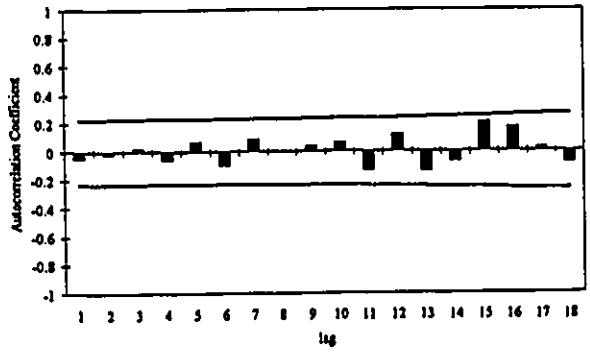

Figure C.20 Autocorrelation Function of the Residuals from the Above Fitted ARIMA Model

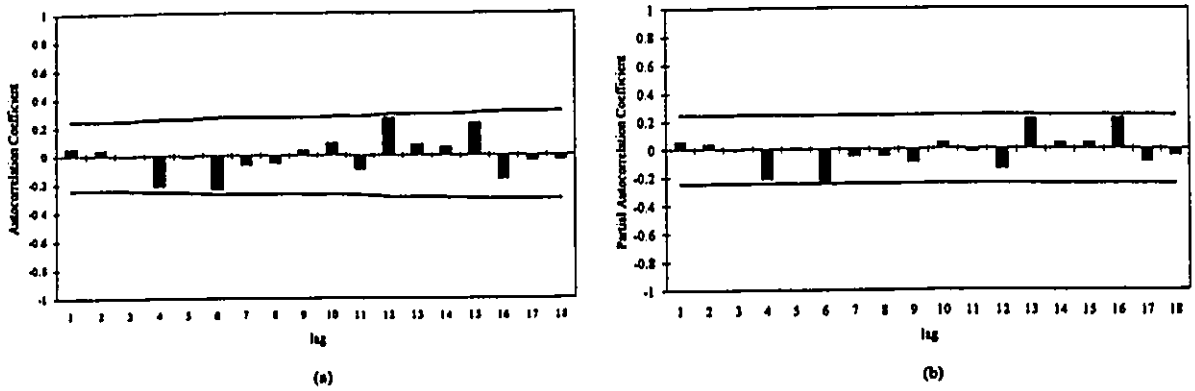

Figure C.21 Coded In-date Yield for the CMOS(1.2μm tlm) Process
a) Autocorrelation Function
b) Partial Autocorrelation Function

Table C.11 ARIMA Joint Detection-Estimation Results of the Coded In-date Yield for the CMOS(1.2μm tlm) Process

	PARAMETER LABEL	VARIABLE NAME	NUM./ DENOM.	FACTOR	ORDER	CONS-TRAINT	VALUE	STD ERROR	T VALUE
1	CYTSI		CNST	1	0	NONE	26.9864	.2635	102.42
2		B7SER	NUM.	1	0	NONE	-10.5683	2.3125	-4.57
3		B34SER	NUM.	1	0	NONE	-1.4254	0.4255	-3.35
4		B44SER	NUM.	1	0	NONE	-8.2137	1.9651	-4.18
5		B54SER	NUM.	1	0	NONE	-9.1868	2.0102	-4.57
6		B59SER	NUM.	1	0	NONE	-11.4274	2.2060	-5.18
7		B60SER	NUM.	1	0	NONE	-8.0318	2.2005	-3.65

TOTAL NUMBER OF OBSERVATIONS. 72
EFFECTIVE NUMBER OF OBSERVATIONS. 72
RESIDUAL STANDARD ERROR . . . . . .233158E+01

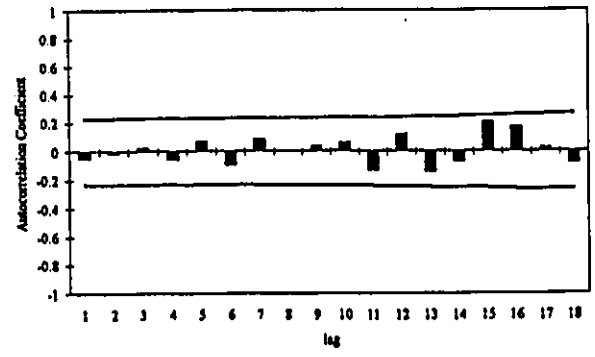

Figure C.22 Autocorrelation Function of the Residuals from the Above Fitted ARIMA Model

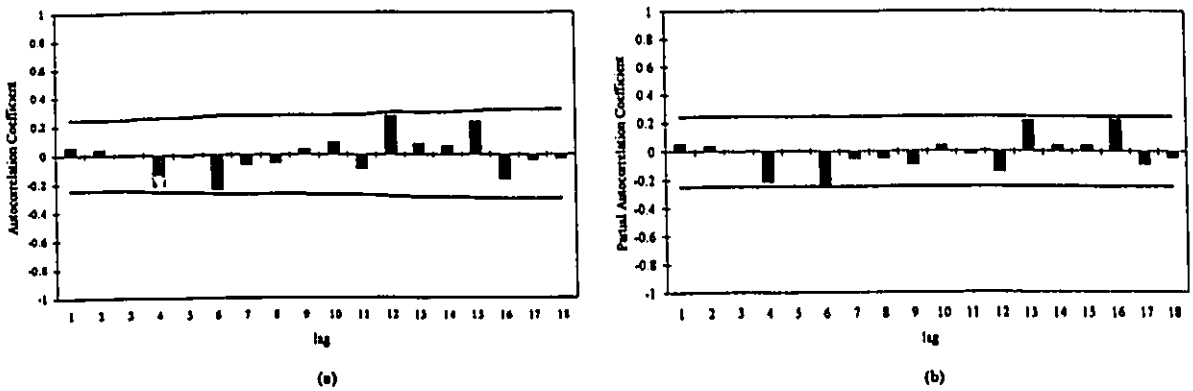

Figure C.23 Coded Out-date Yield for the CMOS(1.2μm tlm) Process
a) Autocorrelation Function
b) Partial Autocorrelation Function

Table C.12 ARIMA Joint Detection-Estimation Results of the Coded Out-date Yield for the CMOS(1.2μm tlm) Process

PARAMETER LABEL	VARIABLE NAME	NUM./ DENOM.	FACTOR	ORDER	CONS-TRAINT	VALUE	STD ERROR	T VALUE
1 CNST		CNST	1	0	NONE	24.1983	0.5318	45.50

TOTAL NUMBER OF OBSERVATIONS. 72
EFFECTIVE NUMBER OF OBSERVATIONS. 72
RESIDUAL STANDARD ERROR . . . . . .467066E+02

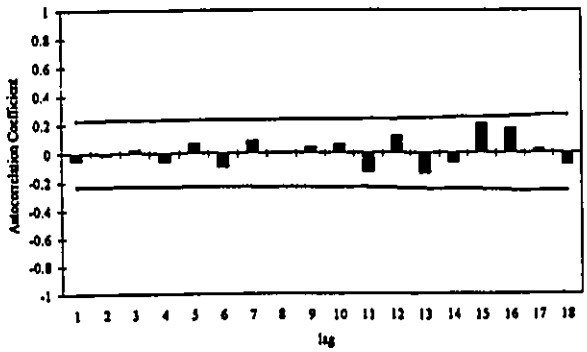

Figure C.24 Autocorrelation Function of the Residuals from the Above Fitted ARIMA Model

Appendix D

JOINT DETECTION-ESTIMATION RESULTS FOR OVERALL PROCESS CAPACITY

This appendix contains complete ARIMA joint detection-estimation results (identification, estimation and diagnostic check) for the overall process capacity.

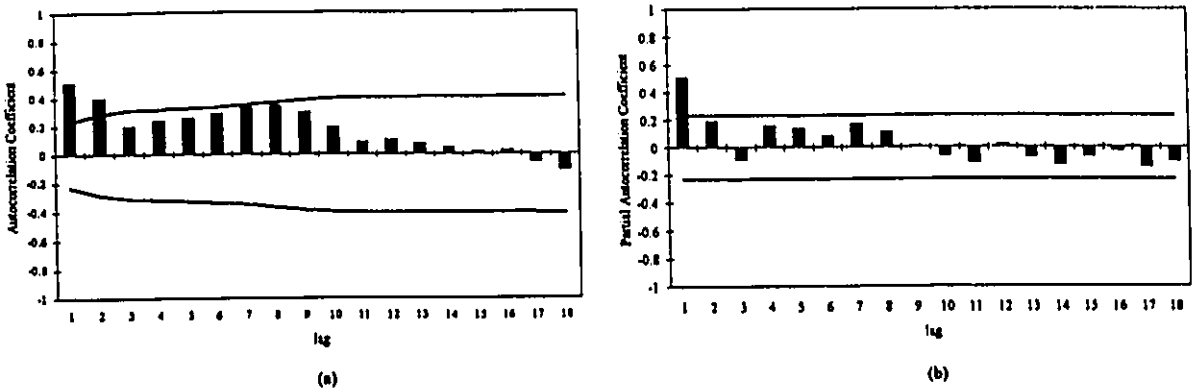

Figure D.1 Coded In-date Capacity for the Overall CMOS Process
a) Autocorrelation Function
b) Partial Autocorrelation Function

Table D.1 ARIMA Joint Detection-Estimation Results for the Coded Out-date Yield for the Overall CMOS Process

VARIABLE NXIALI	TYPE OF VARIABLE RANDOM	ORIGINAL OR CENTERED ORIGINAL	DIFFERENCING NONE

PARAMETER LABEL	VARIABLE NAME	NUM./ DENOM.	FACTOR	ORDER	CONS-TRAINT	VALUE	STD ERROR	T VALUE
1 CNSTX		CNST	1	0	NONE	325.9247	70.6582	4.61
2	Zt	AR	1	1	NONE	.5132	.1019	5.04

TOTAL NUMBER OF OBSERVATIONS. 72
EFFECTIVE NUMBER OF OBSERVATIONS. 71
RESIDUAL STANDARD ERROR (WITHOUT OUTLIER ADJUSTMENT). . .154203E+03
NO OUTLIER IS DETECTED

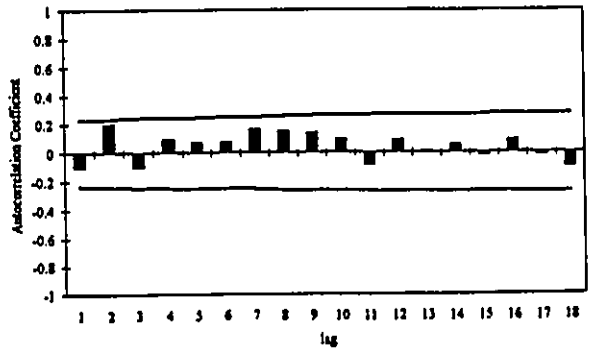

Figure D.2 Autocorrelation Function of the Residuals from the Above Fitted ARIMA Model

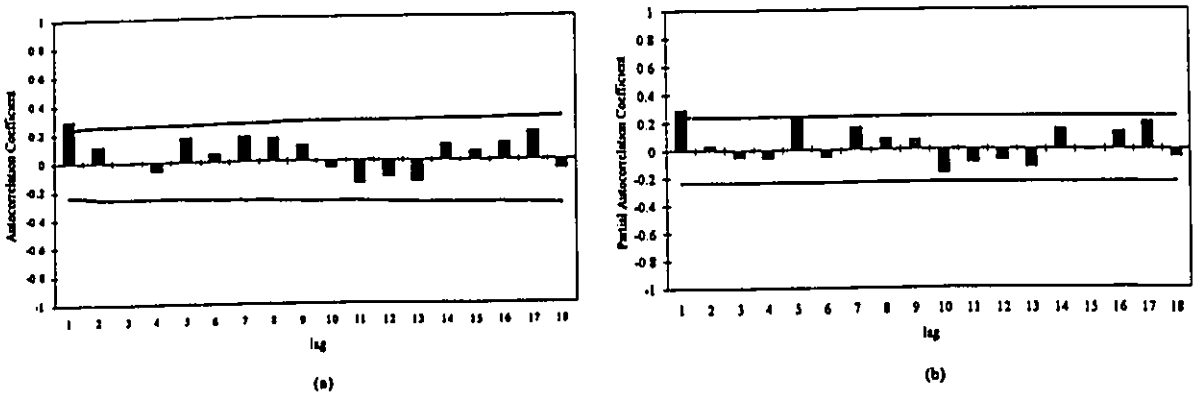

Figure D.3 Coded Out-date Capacity for the Overall CMOS Process
a) Autocorrelation Function
b) Partial Autocorrelation Function

Table D.2 Joint Detection-Estimation Results for the Coded Out-date Capacity for the Overall CMOS Process

VARIABLE	TYPE OF VARIABLE	ORIGINAL OR CENTERED	DIFFERENCING
NWOALO	RANDOM	ORIGINAL	NONE

PARAMETER	LABEL	VARIABLE NAME	NUM./ DENOM.	FACTOR	ORDER	CONS-TRAINT	VALUE	STD ERROR	T VALUE
1	CNST		CNST	1	0	NONE	224.2051	82.1069	2.73
2	PH1	Zt	AR	1	1	NONE	.3035	.0996	3.05
3	PH5	Zt	AR	1	5	NONE	.3002	.0992	3.03

TOTAL NUMBER OF OBSERVATIONS. 85
EFFECTIVE NUMBER OF OBSERVATIONS. 80
RESIDUAL STANDARD ERROR (WITHOUT OUTLIER ADJUSTMENT). . .177076E+03
NO OUTLIER IS DETECTED

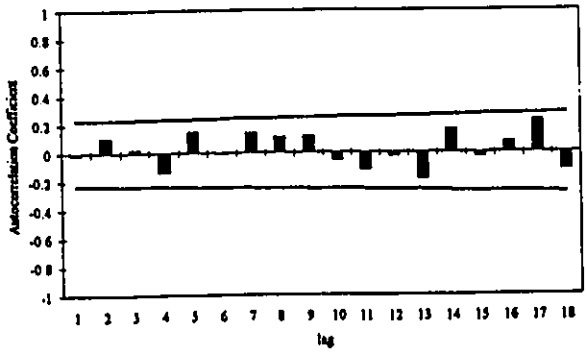

Figure D.4 Autocorrelation Function of the Residuals from the Above Fitted ARIMA Model